

**The Development of some Electrochemical Detection
Systems using Microelectrodes and Their
Application to Biomedical Analysis**



A Thesis Submitted for the Degree of Doctor of Philosophy

by

Michael Malone B.Sc.

under the supervision of Prof. Malcolm R. Smyth

**DUBLIN CITY UNIVERSITY
School of Chemical Sciences**

October 1994

**The Development of some Electrochemical Detection
Systems using Microelectrodes and Their
Application to Biomedical Analysis**



A Thesis Submitted for the Degree of Doctor of Philosophy

by

Michael Malone B.Sc.

under the supervision of Prof. Malcolm R. Smyth

**DUBLIN CITY UNIVERSITY
School of Chemical Sciences**

October 1994

Declaration

I hereby certify that this material, which I now submit for assessment on the programme of study leading to the award of Ph.D. is entirely my own work and has not been taken from the work of others save and to the extent that such work has been cited and acknowledged within the text of my own work.

Signed: Michael Malone Date: 15-9-94
Michael Malone

To my Parents, Carmen, Brian and Maria.

ACKNOWLEDGEMENTS

I am extremely grateful to my Supervisor Prof Malcolm Smyth for his direction throughout this thesis and for giving me the opportunity to work in Spain and the U S A Thanks for all the advice

I would like to thank Prof Paulino Tunon Blanco for accepting me in his laboratory and for all the great times I had there I am also grateful to his staff and research students for making my stay in Spain a very fruitful one

I would like to thank Prof Susan Lunte for welcoming me to the Center for BioAnalytical Research, University of Kansas I would particularly like to thank her for her excellent hospitality and for the opportunities to attend several conferences in the U S A and Europe I also wish to thank her research group for the relationships we enjoyed, both academically and socially I also want to thank Dr Hong Zuo for her expertise in the area of surgical implantation of the microdialysis probes during the rat experiments

I am forever grateful to my Parents who supported me in every conceivable way throughout the years and the rest of my family for their patience I also want to extend my gratitude to Carmen who was always there to support me for the past few years It was this support that made it all possible

CONTENTS

Title Page	1
Declaration	ii
Dedication	iii
Acknowledgements	iv
Table of Contents	v
Abstract	x
1 Theory and Applications of Ultramicroelectrodes	
1 1 Introduction	2
1 1 1 Advantages of Ultramicroelectrodes	2
1 1 2 Diffusion to Ultramicroelectrodes	6
1 2 Applications	9
1 2 1 Chemically Modified Electrodes	11
1 2 2 Liquid Chromatography with Electrochemical Detection	13
1 2 3 Capillary Electrophoresis with Electrochemical Detection	14
1 2 4 <i>In vivo</i> Voltammetry	16
1 2 4 1 Practical Considerations in <i>in vivo</i> Voltammetry	20
1 2 4 2 Recent Applications and Developments of <i>in vivo</i> Voltammetry	22
1 2 5 Other Applications of Ultramicroelectrodes	24
1 3 References	26
2 The Coupling of Electrochemical Detection with Microelectrodes to Capillary Electrophoresis and Microdialysis/Capillary Electrophoresis	
2 1 Introduction	30
2 1 1 Capillary Electrophoresis	30
2 1 2 Microdialysis Sampling	33

2 1 3	Biomedical Importance of Amino Acids	37
2 1 4	Clinical Importance of Mitomycin C	40
2 2	<i>Reductive Electrochemical Detection for Capillary Electrophoresis</i>	43
2 2 1	Introduction	43
2 2 2	Experimental	46
2 2 2 1	Reagents and Materials	46
2 2 2 2	Apparatus	46
2 2 2 3	System Deoxygenation	48
2 2 2 4	Cyclic Voltammetry	50
2 2 2 5	Hydrodynamic Voltammetry	50
2 2 2 6	Sample Preparation	50
2 2 3	Results and Discussion	51
2 2 3 1	Cyclic Voltammetry	51
2 2 3 2	Hydrodynamic Voltammetry	51
2 2 3 3	Analysis of DNP-Amino acids	53
2 2 3 4	Analysis of Anthraquinones	56
2 2 3 5	Determination of Mitomycin C in Human Serum	58
2 2 4	Conclusions	62
2 3	<i>Monitoring of Tryptophan Metabolites in Rat Brain using in vivo Microdialysis and Capillary Electrophoresis/Electrochemistry</i>	63
2 3 1	Introduction	63
2 3 2	Experimental	66
2 3 2 1	Reagents and Materials	66
2 3 2 2	Apparatus	66
2 3 2 3	Cyclic Voltammetry	67
2 3 2 4	Hydrodynamic Voltammetry	67
2 3 2 5	Implantation of the Microdialysis Probe	68

2 3 2 6	Microdialysis Procedures	68
2 3 2 7	Systemic Precursor Loading Studies	68
2 3 3	Results and Discussion	69
2 3 3 1	Cyclic Voltammetry	69
2 3 3 2	Hydrodynamic Voltammetry	69
2 3 3 3	Separation Optimisation	75
2 3 3 4	Analytical Characterisation	76
2 3 3 5	Analysis of Rat Brain Microdialysate using CEEC	80
2 3 4	Conclusions	87
2 4	References	88
3	Development of a Mercury Thin Film Carbon Fibre Ultramicroelectrode for the Adsorptive Stripping Voltammetric Determination of Selected Pteridines	
3 1	Introduction	93
3 1 1	Clinical Importance of the Selected Pteridines	93
3 1 2	Mercury Thin Film Electrodes	100
3 1 3	Phase-Selective Alternating Current Voltammetry	101
3 2	Experimental	105
3 2 1	Reagents and Materials	105
3 2 2	Instrumentation	105
3 2 3	Procedures	106
3 2 3 1	Microelectrode Preparation	106
3 2 3 2	Carbon Fibre Activation	107
3 2 3 3	General Methodology	107
3 2 3 4	Analysis of Biological Fluids	109
3 3	Results and Discussion	111
3 3 1	Electrochemical Behaviour of the Selected Pteridines	111

3 3 2	Optimisation of the Conditions for Mercury Film Formation on Carbon Fibre Electrodes	116
3 3 2 1	Influence of Solution Composition	116
3 3 2 2	Influence of Deposition Potential	117
3 3 2 3	Influence of Deposition Time	120
3 3 2 4	Reproducibility of Film Formation	122
3 3 3	Optimisation of the Phase-Selective AC voltammetric Parameters	125
3 3 3 1	Effect of Phase Angle	125
3 3 3 2	Effect of the Superimposed Alternating Current Amplitude	127
3 3 3 2	Effect of Scan Speed	127
3 3 3 4	Effect of the Frequency of the Superimposed Current	129
3 3 4	Accumulation Behaviour on the Mercury Thin Film Ultramicroelectrode	129
3 3 5	Analytical Characterisation of the Mercury Thin Film Ultramicroelectrode	134
3 3 5 1	Analytical Range/Limit of Detection	134
3 3 5 2	Reproducibility and Stability	137
3 3 6	Analysis of the Selected Pteridines in Biological Fluids	142
3 3 6 1	Direct Analysis of Urine using the Mercury Thin Film Ultramicroelectrode	143
3 3 6 2	Analysis of Human Urine following Solid-Phase Extraction using the Mercury Thin Film Ultramicroelectrode	146
3 3 6 3	Analysis of Human Serum following Solid-Phase Extraction using the Mercury Thin Film Ultramicroelectrode	151
3 3 6 4	Analysis of Human Serum using a Hanging Mercury Drop Electrode	152
3 4	Conclusions	156
3 5	References	157

4	Flow Injection Amperometric Determination of Nitrite using a Carbon Fibre Ultramicroelectrode Modified with the Polymer [Os(bipy)₂(PVP)₂₀Cl]Cl	
4 1	Introduction	160
4 1 1	Chemically Modified Electrodes	163
4 2	Experimental	167
4 2 1	Reagents and Materials	167
4 2 2	Instrumentation	167
4 3	Procedures	168
4 3 1	Construction of the Carbon Fibre Flow Cell	168
4 3 2	Modification of the Working Electrode	170
4 3 3	Meat Sample Analysis	170
4 4	Results and Discussion	171
4 4 1	Cyclic Voltammetry	171
4 4 2	Flow Injection	174
4 4 3	Determination of Nitrite in Meat	178
4 4 4	Interferences	178
4 5	Conclusions	182
4 6	References	183
5	Conclusions	185
	List of Publications	190

Abstract

The main objectives of this doctoral thesis were to develop sensitive and versatile electrochemical detection systems, taking advantage of the unique analytical characteristics of microelectrodes, and apply them to selected biomedical analyses. In order to broaden the applicability of electrochemical detection following capillary electrophoresis (CE), a system was developed which enabled reductive electrochemical detection to be carried out following capillary electrophoresis. This greatly broadens the number of compounds that can be detected electrochemically following separation by CE. The analytical potential of the system was demonstrated for both nitroaromatic compounds and quinones. It was shown to possess major advantages over reductive LCEC, including very short deoxygenation times and low limits of detection. The system was also applied to the analysis of an antitumour compound, mitomycin C, in human serum without the need for prior extraction procedures.

In another project, continuous *in vivo* microdialysis sampling was used in conjunction with capillary electrophoresis and electrochemical detection, to monitor the levels of tryptophan and its metabolites in the extracellular fluid of rat brain. The relative changes in the concentration of these metabolites in the extracellular fluid were monitored following intraperitoneal administration of tryptophan and kynurenine, respectively. The advantages of capillary electrophoresis for sample volume limited analyses were demonstrated, and the high sensitivity of electrochemical detection was shown to be very desirable in this field of research.

In the area of biomedical analysis one of the major objectives is to develop very sensitive techniques for the determination of therapeutic compounds in biological fluids. The advantages of microelectrodes and adsorptive stripping voltammetry were combined by developing a mercury thin film ultramicroelectrode using a carbon fibre substrate. Using phase-selective AC stripping voltammetry, a very sensitive technique was developed for the analysis of methotrexate, aminopterin, and edatrexate, members of the very important pteridine class of chemotherapeutic drugs. These compounds were analysed in human urine and serum, both with and without the employment of prior extraction procedures.

Carbon fibre electrodes were also modified with the polymer $[\text{Os}(\text{bipy})_2(\text{PVP})_{20}\text{Cl}]\text{Cl}$ for the flow amperometric determination of nitrite. This redox polymer greatly enhances the kinetics of nitrite reduction compared with the reaction at bare carbon electrodes. Due to the electrocatalytic effect, a less extreme working potential could be employed which minimised the responses from the commonly present interferents present in real samples. The electrode was applied to the flow amperometric determination of nitrite in processed meat samples. The electrode exhibited excellent selectivity and long term stability.

Chapter 1



Theory and Applications of Ultramicroelectrodes

1.1 Introduction

Since its initiation in the 1970's, research in the area of ultramicroelectrodes has gone from strength to strength and has become, perhaps, the most innovative and exciting area of electroanalytical research today

1.1.1 *Advantages of Ultramicroelectrodes*

Ultramicroelectrodes (UMEs) have several advantageous characteristics compared to conventional size electrodes due to their miniature size and geometry. Many of these advantages have been exploited by electrochemists since the early seventies in an attempt to study phenomena not amenable to conventional size electrodes (macro electrodes), and also to improve the performance of electrochemical detectors. Several informative reviews on UMEs have appeared in the literature [1-4]. When one considers mass transport to UMEs, one is essentially interested in diffusional mass transport. The diffusion of the analyte to the electrode surface is due to a concentration gradient set up when electrolysis occurs. In the case of UMEs, transport due to diffusion is so large that transport due to convection becomes less significant. For this reason, UMEs are generally used in quiescent solutions which in itself is an advantageous feature in several situations, as will be seen later. Due to the small size of UMEs, conditions of semi-infinite diffusion are generally assumed. When one considers a cylindrical UME, radial diffusion must also be taken into account, as opposed to simple planar diffusion in the case of macro electrodes. Due to this superior mass transport, and the fact that the diffusional double layer around the electrode is generally larger than the electrode area, one obtains steady-state voltammograms when using UMEs. These unique

features of UMEs lead to many practical advantages over macro electrodes as will be discussed below

At conventional size electrodes the effect of capacitance (charging) current is often a limiting factor, particularly at short times and low concentrations of analyte. One essentially tries to increase the faradaic-to-charging current ratio (i_F/i_C) in order to obtain a useful analytical signal. The total current in the cell is a combination of charging and faradaic currents. Since the double layer capacitance (charging) current is proportional to the electrode area, one can reduce this by miniaturisation of the electrode. Also, in the case of spherical and disk electrodes at steady-state additional improvements are obtained since the steady state current is proportional to the radius, rather than the area of the electrode. Pulsed voltammetric techniques, with intelligent sampling of the current, have also led to improvements, since after application of a pulse the charging current decays more rapidly (exponentially) compared to the faradaic current ($t^{-1/2}$) under conditions of linear diffusion. The decay of current is much less time dependent at UMEs.

The current flowing (faradaic and charging) through an electrochemical cell generates a potential that opposes the applied potential. This ohmic drop (iR drop) is subtracted from the applied potential difference between the working and reference electrodes. The use of a 3-electrode system, with the working and reference electrodes as close as possible, coupled with electronic compensation, alleviates some of this ohmic drop. This is of particular significance for fast scan voltammetry, and severe distortions of the voltammogram are sometimes observed when conventional size electrodes are used due to the large magnitude of the

charging current. The ohmic drop due to charging current is proportional to the electrode area and can be reduced by miniaturisation of the electrode. The ohmic drop due to faradaic current is independent of electrode geometry. Therefore, an overall diminution of ohmic drop is achieved by miniaturisation of the electrode. This lower iR drop at UMEs leads to a reduced cell time constant, and useful voltammograms can be obtained at scan rates as high as 10^5 Vs^{-1} . In recent years, fast-scan voltammetry (with UMEs) has been used extensively in areas where real time analysis is necessary, such as following *in vivo* neurochemical events. The lower iR drop at UMEs has also led to their use in highly resistive solutions, sometimes without the addition of supporting electrolyte. Under similar conditions conventional electrodes generally yield highly distorted voltammograms. Figure 1.1 illustrates this by comparing the voltammogram of ferrocene in acetonitrile at both an ultramicroelectrode and a conventional size electrode. This is a very important characteristic of UMEs, since they can be employed in such areas as normal phase chromatography.

Perhaps the most obvious advantage of UMEs over conventional electrodes is their small dimensions. This makes them amenable to many applications where conventional electrodes could not be used. This has led to numerous applications of microelectrodes to small volume analysis. An example of this is the ability to insert a UME in the end of a capillary to provide very sensitive detection for capillary electrophoresis techniques and the use of UMEs in microbore chromatography. The use of electrochemical detection in micro-column separations was recently reviewed by Ewing et al. [7]. UMEs can also be used in discrete microscopic locations such as regions of the brain. Several applications of UMEs to *in vivo* electrochemistry

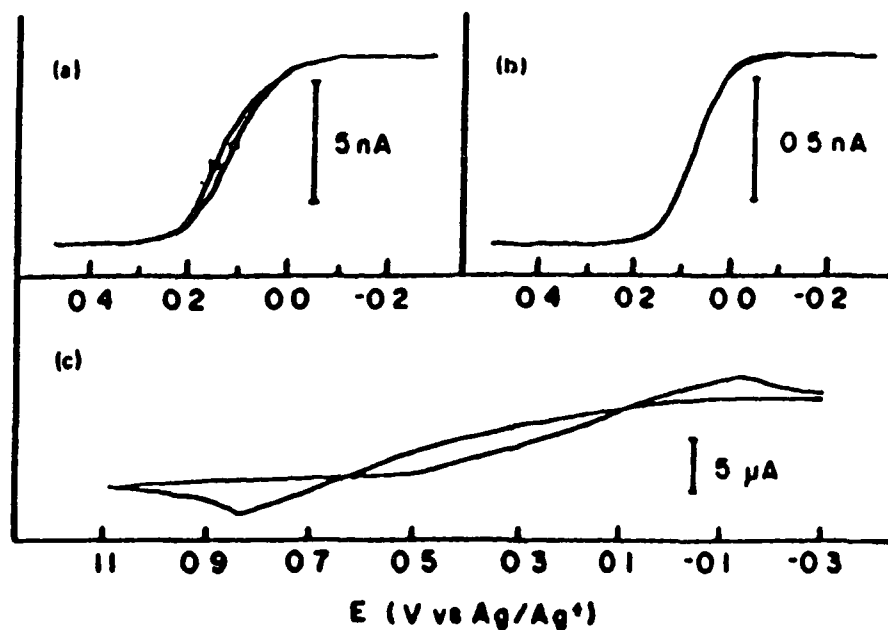


Figure 1

Cyclic voltammograms for oxidation of ferrocene in acetonitrile with various supporting electrolyte concentrations (a) 1.1 mM ferrocene with 0.01 mM TBAP at a 6.5-μm-radius gold microdisk electrode (arrows indicate the scan direction) (b) as (a) but with 0.11 mM ferrocene (c) as (a) but at a 0.4-mm-radius platinum disk electrode (from reference 2)

have been reported in the literature and some examples will be presented later. The insensitivity of UMEs to convective mass transport is of particular importance in these types of *in vivo* applications. A representative cross section of recent applications of ultramicroelectrodes will be presented in section 1.3.

1.1.2 Diffusion to Ultramicroelectrodes

When dealing with diffusion to an ultramicroelectrode, the radial diffusion component must be taken into account. This leads to deviations from planar diffusion and results in the steady-state response often observed at ultramicroelectrodes. Figure 1.2 illustrates the diffusion profile at an ultramicroelectrode.

Thus, the number of electroactive species diffusing to an ultramicroelectrode exceeds that of a conventional sized planar electrode, since the dimensions of the diffusion layer exceed that of the ultramicroelectrode. Figure 1.3 illustrates the different concentration profiles at large and small electrodes after the application of a potential pulse. Thus, when considering the current response at ultramicroelectrodes, the Cottrell equation must be adjusted compared to results obtained at electrodes large enough to be considered planar, by addition of terms that reflect the number of molecules that have access to the ultramicroelectrode. The current is described as follows:

$$i = nFAD_oC_o \left[\frac{1}{(\pi D_o t)^{\frac{1}{2}}} + \frac{1}{r_o} \right]$$

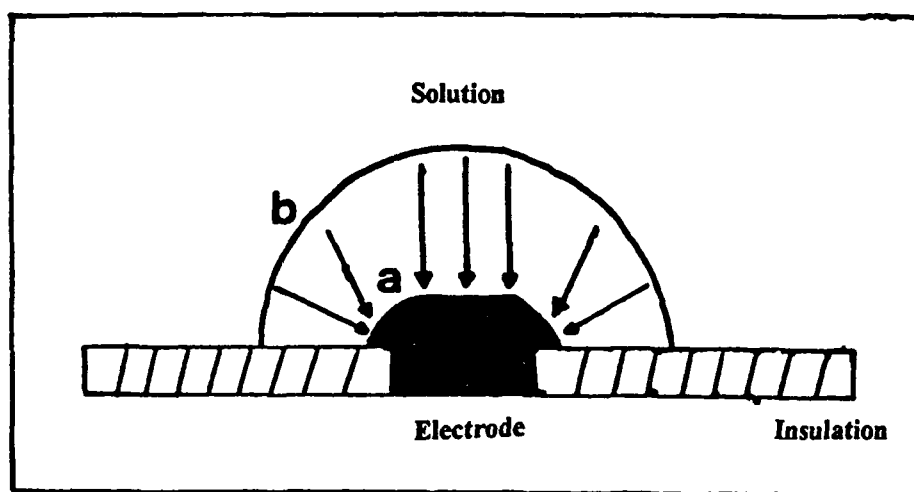


Figure 1.2

The diffusion profile at an ultramicroelectrode at (a) short times as in rapid cyclic voltammetry (100 Vs^{-1}), and (b) long times as in slower scan rate cyclic voltammetry (0.1 Vs^{-1}), (from reference 1)

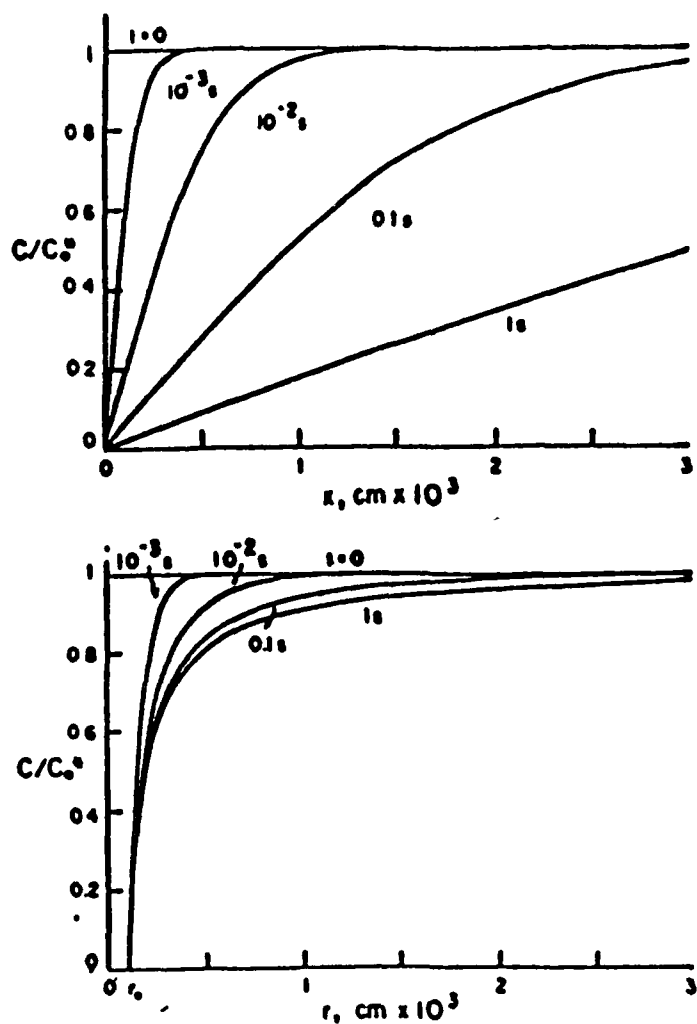


Figure 1 3

Concentration profiles at large ($r_0 \rightarrow \infty$ top) and small ($r_0 = 10^{-1} \text{ cm}$ bottom) electrodes for different times after the application of a potential step of sufficient magnitude to drive the concentration of the electroactive species to zero at the electrode surface. Evaluated for $D_0 = 10^{-6} \text{ cm}^2 \text{ s}^{-1}$ (from reference 2)

where A is given by $4\pi r^2$ for a sphere and $2\pi r^2$ for a hemisphere

i = faradaic current

C_o = bulk concentration of electroactive species

D_o = diffusion coefficient of electroactive species

r_o = radius of electrode

F = Faraday constant

n = number of electrons per molecule oxidised or reduced

t = time

Due to the steady-state diffusion characteristics of these electrodes a wave is seen rather than a peak when linear sweep voltammetry is carried out at normal scan rates. Figure 1.4 outlines the difference between the linear sweep voltammetric response at UMEs and conventional size electrodes at normal scan rates.

1.2 Applications

Because of the novel characteristics of UMEs they have pushed back the boundaries of electrochemistry, and continue to be employed in new areas where conventional electrodes were not found to be very successful. For example, because of the low iR drop exhibited by these electrodes, they can be employed in poorly conductive solutions often in the absence of base electrolyte. Fast establishment of steady-state and rapid charging facilitate the use of rapid-scan voltammetric techniques which are particularly important in the field of *in vivo* electroanalysis. Their small dimensions also make them particularly suitable for detection in micro-column techniques. Some of the recent applications of microelectrodes are reviewed here. Recent reviews by Broderick [5] and Stulik [6] are also useful. These areas of research, where UMEs possess some distinct advantages over conventional sized electrodes, have enjoyed much attention in recent years. The following short review presents some applications of ultramicroelectrodes reported in the literature in recent years.

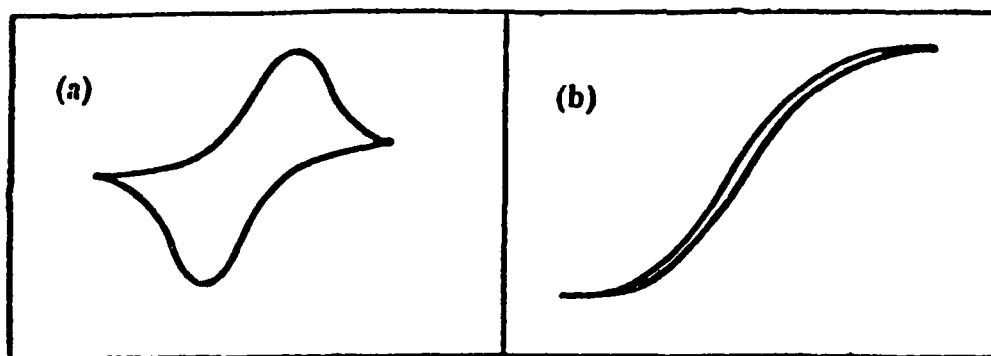


Figure 1.4

Response of (a) a conventional size electrode to linear sweep voltammetry compared with (b) an ultramicroelectrode in the same solution (from reference 2)

The carbon fibre electrode has, perhaps, received more attention in recent years, than any other UME, particularly due to its applications in neuroscience. Metal electrodes such as Au, Ag, Pt and Cu have also been widely used for bioanalysis, particularly in the area of high performance liquid chromatography (HPLC) and flow injection analysis (FIA) with electrochemical detection. However, like conventional electrodes, the responses at these bare electrodes are sometimes sluggish and are prone to surface passivation. Every electrode could be considered a chemically modified electrode (CME) since no electrode substrate is 100 % pure. However, by definition, a CME is deliberately modified to improve one or more characteristics of the electrode. The types of modification have become increasingly varied, and include inorganic salts, redox polymers and permselective films (Nafion and cellulose acetate, for example). Various techniques have been employed for surface modification, including chemical bonding, electrochemical deposition and simple dip coating. The theory and application of modified electrodes was recently discussed elsewhere [8]. Hart and co-workers demonstrated the electrocatalytic effect of cobalt phthalocyanine (CoPC) on screen printed carbon electrodes [9] for the determination of glutathione in human blood. Wang et al [10] also used CoPC modified carbon electrodes, but included a cellulose acetate film to introduce permselectivity. Base hydrolysis was used to control the permeability of the two domain (CoPC/CA) structure in a manner similar to that common at single domain cellulosic films. Selectivity is of major importance for the analysis of biological fluids, and several types of membranes have been evaluated. Nafion is widely used for *in vivo* voltammetric analysis in order to increase the selectivity of the electrode.

towards parent neurochemicals over certain metabolites and ascorbic acid

Wightman et al [11] recently studied pH-dependent processes at Nafion-coated carbon fibres, and concluded that the surface waves for oxidation of dopamine and reduction of benzoquinone shifted linearly with pH and could be used to diagnose alterations in the pH of the solution

Wilson et al [12] employed a set of membranes made of Nafion and collagen over a gold working electrode to improve the selectivity of the system

Using pulsed amperometric detection (PAD), the non-enzymatic sensor yielded a limit of detection of 4-5 μg of glucose injected

Another objective of modified electrodes is to develop electrodes that are capable of analyses in the absence of supporting electrolyte

This would allow electrochemical detection in supercritical fluids and in the gas phase

Wightman and co-workers [13] studied the use of microelectrodes coated with ionically conducting polymer membranes for voltammetric detection in flowing supercritical carbon dioxide

The 5 μm platinum electrode was coated with 0.5 μL of 0.5 % Nafion (H^+ form) and ferrocene was tested as the model analyte

Another group [14] investigated the use of a film of poly-(ethylene oxide) containing LiCF_3SO_3 (PEO Li) for analysis in supercritical carbon dioxide and in CO_2 modified with water or acetonitrile

Biosensors can also be considered chemically modified electrodes

The development and application of biosensors have been extensively reported in the literature

The use of a Nafion-Crown ether carbon fibre microbiosensor was reported recently [15] for the detection of neurotransmitters

The authors reported improved sensitivities for dopamine caused by enrichment of the compound in the polymembrane by interaction of oxygen atoms of the crown ether and the positively charged amino group of the catecholamine

Platinised carbon (8 μm diameter)

ultramicroelectrodes were used [16] as glucose biosensors. After platinisation, glucose oxidase was immobilised and an electropolymerised film of poly-(1,3-diaminobenzene) was used to prevent interfering species. The sensor gave a linear response to glucose over the range of 3-7 mM with a response time of 15-45 seconds.

1.2.2 Liquid Chromatography with Electrochemical Detection (LCEC)

Since its first application in 1973 [17] for the determination of catecholamines, LC with electrochemical detection (LCEC) has taken a high priority position in bioanalytical research. The merger of these two analytical techniques combines the well recognised resolution of LC with the high sensitivity of electrochemical detection. Reviews by Kissinger [18] and Stulik [6], respectively, have discussed the present status of LCEC and trends for the future. Traditionally, macro electrodes such as glassy carbon were generally used due to their robustness and ease of use. However, the use of microelectrodes introduces obvious advantages in terms of sensitivity and feasibility of use in microcolumn techniques. For instance, a micro-electrochemical flow cell [19] has been developed using carbon or gold fibres for voltammetric and amperometric detection. This flow cell was used for the anodic and adsorptive stripping determination of Se(VI) and Cr(VI). It was also used for the amperometric detection of terbutaline in human plasma [20] following column-switching. Stulik and co-workers [21] also used a carbon fibre electrode following LC separation for the determination of phenazone and 4-aminophenazone in urine. The electrode was used in the amperometric mode, and limits of detection of 8.6 ng and 5.0 ng were obtained, respectively. Even though amperometric

detection continues to be the most widely used mode of electrochemical detection following LC, some workers are concentrating on more complex waveforms for specific applications. For example, pulsed electrochemical detection (PED) is one such technique used with gold or platinum electrodes for the detection of sulphur-containing compounds and carbohydrates that are otherwise difficult to oxidise. A recent review by Johnson et al [22] has dealt with the theoretical concepts of PED and various applications in ion chromatography. Vandeberg and Johnson [23] used PED with a gold electrode for the detection of thiols and disulphides following LC separation. The PED waveform utilised current integration throughout the period of a fast cyclic potential scan to eliminate the large background current normally observed for the conventional three-step PED waveform as a consequence of surface oxide formation which is required by the detection mechanism. Both the reduced and oxidised forms of some thiols were detected simultaneously and limits of detection at the picomolar level were reported.

1.2.3 Capillary Electrophoresis with Electrochemical Detection (CEEC)

Capillary electrophoresis is another example of the trend towards miniaturisation in the field of biomedical analysis. In biomedical analysis the sample is frequently concentration and volume limited. Thus, the use of capillary electrophoresis with electrochemical detection provides a very sensitive technique that is capable of handling very small volumes (usually nL injection volumes). Some of the concepts involved in CEEC will be discussed in chapter 2 of this thesis. Figure 1.5 shows a schematic diagram of the CEEC system developed by O'Shea et al [24]. Ewing et al [7] recently reviewed the use of electrochemical detection in microcolumn

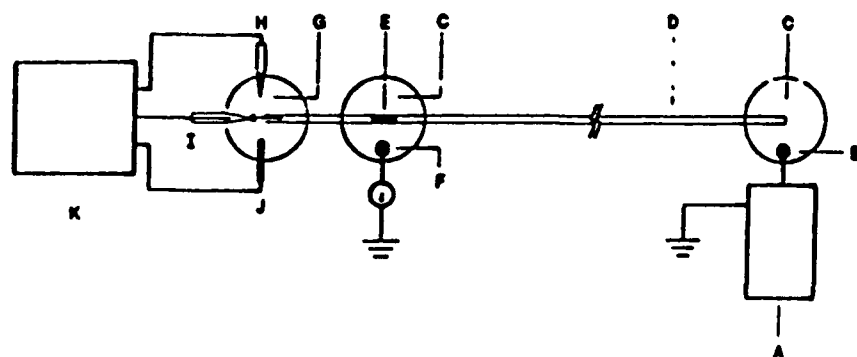


Figure 1 5

Schematic diagram of a CEEC system A High-voltage power supply B anode, C buffer reservoir D capillary column E Nafion joint F cathode G detection cell H reference electrode, I carbon fibre microelectrode J auxiliary electrode K amperometric detector (from reference 24)

separation, and stated that electrochemical detection is ideally suited for the miniaturisation of LC and CE. In recent years more groups have become interested in CEEC due to its advantageous features. As in LCEC, generally oxidative amperometric detection is used. However, some groups have tried to broaden the range of applications of CEEC in biomedical analysis. Cassidy et al. [25] looked at both constant potential and pulsed voltammetric conditions for the detection of metal ions separated by CE. O' Shea et al. used PAD detection at a gold electrode for the detection of carbohydrates following capillary electrophoresis and applied the system to the determination of glucose in blood and reported a limit of detection of 9×10^{-7} M glucose in standard solutions. CEEC has also been used to monitor the pharmacokinetics of L-dopa [27] in the rat by inserting a microdialysis probe in a vein and collecting samples at regular intervals. This area of research has gained a lot of interest in recent years since it provides very useful information and the probe can be used to sample essentially any part of the anatomy. Electrochemical detection will play a major role in its development due to its high sensitivity and selectivity.

1.2.4 *In vivo Voltammetry*

Since the initial report by Adams' group [28] in the early seventies, voltammetry in neuroscience has grown to become, perhaps, one of the most innovative and exciting areas of electroanalytical chemistry. The main area of interest is in the study of biogenic amines (catecholamines and indolamines), which are important neurochemicals. These neuronal substances have action times of milliseconds, so a technique with good temporal resolution is required. The catecholamines of interest include epinephrine (E), norepinephrine (NE) and their precursor dopamine (DA),

along with its metabolites 5-hydroxyphenylacetic acid (DOPAC) and homovanillic acid (HVA). The indolamines include serotonin (5-HT) and its metabolite 5-hydroxyindoleacetic acid (5-HIAA). All these neurochemicals undergo a $2\text{H}^+/2\text{e}^-$ electrochemical oxidation according to the reaction illustrated in Figure 1.6 [29]. One can begin to understand the complexity of *in vivo* neurovoltammetry when one considers that all these compounds co-exist in the extracellular fluid (ECF) of the brain along with high concentrations of ascorbic acid, and that their oxidation potentials all lie within a narrow potential window ranging approximately between 0 V and +0.4 V versus Ag/AgCl. Figure 1.7 represents the approximate oxidation potentials of the various neurotransmitters and the potential interferents at a carbon-based electrode. Ultramicroelectrodes are obviously very attractive for *in vivo* voltammetry due to their small size, reduced ohmic drop and low capacitive currents. These characteristics allow for the implementation of fast voltammetric techniques which are often used to distinguish between several neurochemicals present in the ECF. Carbon fibres have been used most widely and have been modified both electrochemically and chemically. However, other substrates have also seen some use although quite limited. Cylindrical carbon fibre electrodes have been produced for *in vivo* analysis with effective diameters as low as 1 μm . Several reviews have appeared in the literature [5,30,31] dealing with *in vivo* electrodes. These electrodes exhibit diffusional characteristics of a spherical electrode and their advantages are numerous, including higher sensitivity, lower charging currents, less perturbation of the neural environment and faster measurement times. Another advantage of these ultramicroelectrodes is that chemical reactions that may follow

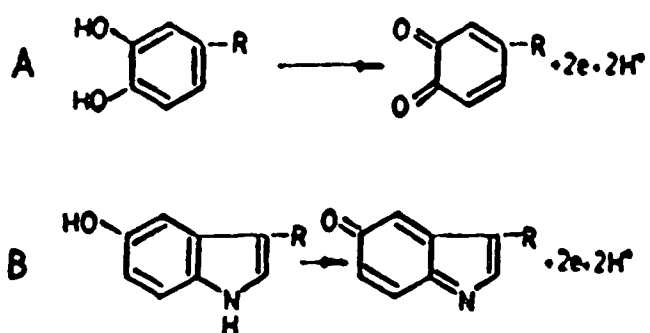


Figure 1 6

Oxidation of catechol and indole derivatives (A) Catechol derivatives where $R=CH_2CH_2NH_2$ =dopamine (DA) $R=CH(OH)CH_2NH_2$ =noradrenaline (NA) $R=CH_2COOH$ =dihydroxyphenylacetic acid (DOPAC), $R=CH(OH)CH_2OH$ =dihydroxyphenylethylene glycol (DOPEG) (B) Indole derivatives where $R=CH_2CH_2NH_2$ =serotonin (5-HT) $R=CH_2COOH$ =5-hydroxyindoleacetic acid (5-HIAA) (from reference 29)

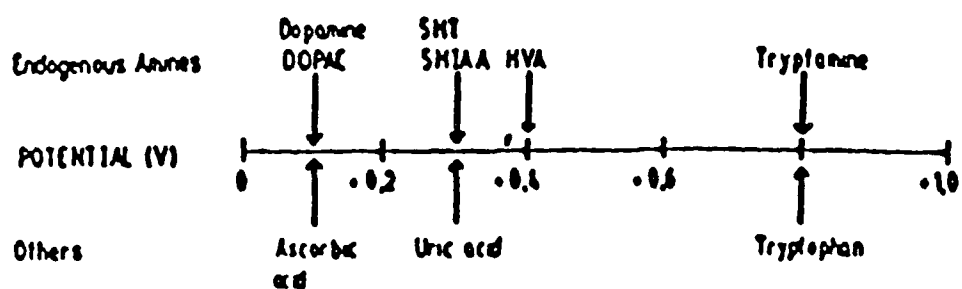


Figure 1.7

Schematic representation of the oxidation potentials of some biogenic amines. The list is not comprehensive and precise oxidation potentials are not given since they vary with the type of electrode used (from reference 29)

the initial oxidation, such as reduction of the oxidised neurotransmitter in the presence of ascorbic acid, will have less of an effect on the current than at conventional electrodes since the average distance the neurotransmitter diffuses before reacting with the ascorbic acid in solution is larger than the diameter of the electrode

1 2 4 1 *Practical Considerations in in vivo Voltammetry*

When dealing with *in vivo* neurovoltammetry there are many practical considerations to be kept in mind, some of which are unique to this field. Reviews referred to earlier [5,31] deal with the types of electrodes used in this field. A recent review by Wightman et al [34] gives a comprehensive overview of the concepts involved in *in vivo* voltammetry. It is outside the scope of the present introduction to deal with all the practical considerations involved, but the major ones will be dealt with briefly. Due to the presence of a large number of electroactive compounds in the brain it is of paramount importance that unambiguous identification of the compounds responsible for the signal is achieved. Marsden et al [32] and O' Neill et al [33] have summarised some important criteria for peak identification and these include complete characterisation of the compound behaviour *in vitro* before *in vivo* studies. The electrode must be shown to be capable of measuring the compound of interest in the presence of normal *in vivo* concentrations of typical interferents. The *in vivo* signal should then show voltammetric identity with the compound considered to be responsible for the *in vitro* signal. Specific local stimulation or inhibition (chemical or enzymatic) of a particular signal can sometimes be useful in peak identification.

Electrode calibration is a major problem for *in vivo* voltammetry, and a fully reliable *in situ* calibration method has not yet been reported. The most widely used technique involves the pre- or post-calibration of the electrode *in vitro*, typically in pH 7.4 phosphate buffered saline (PBS) containing 200 μ M ascorbic acid (AA), 10 μ M DOPAC and any other basal level components deemed necessary for the particular system. It has been reported that the sensitivity of carbon fibre electrodes drops sharply within the first 2.5 h after implantation [35]. Hence post-calibration is most reliable and the results best represent the actual sensitivity of the electrode from 2.5 h until termination of the experiment. Adam's group [36,37] have considered the problems associated with *in vitro* calibrations of *in vivo* electrodes and have suggested that *in vivo* voltammetric measurements have a relative uncertainty of ± 20 -40 %. Morgan and Freed [38] recommended the use of acetaminophen as an internal standard for calibrating *in vivo* electrodes by comparing the peak current yielded by the oxidation of a certain concentration of acetaminophen.

1.2.4.2 Recent Applications and Developments of *in vivo* Voltammetry

Applications of voltammetry to neuroscience cover a wide spectrum, ranging from attempts at the analysis of basal levels of neurotransmitter and their metabolites in the ECF to post-stimulation analyses, and applications in behavioural studies. Recent reviews [32,36] have dealt with *in vivo* methodology and applications. Carbon electrodes, on the whole, have found wider application, although noble ultramicroelectrodes such as platinum [39,40] have also been employed. O' Neill and Lyne [41] utilised a stearate modified carbon paste electrode for the detection of dopamine *in vivo*, but found that the lipophilic nature of the brain tissue destroyed the selectivity of the electrode by removing the hydrophobic elements from the electrode surface. The most widely used chemical modification used is the application of a Nafion film which discriminates against anionic compounds such as ascorbic acid and DOPAC [35,42,43]. Pretreatment generally slows down the electrode response, sometimes making them unsatisfactory for monitoring short duration pulsed release of neurotransmitters. Adams et al. [37] have reported on the use of electrochemically pretreated, Nafion-coated carbon fibre electrodes for monitoring the ventrobasal complex of the thalamus in awake rats for the presence of NE overflow following manipulations and physiological stimulation. Complex electrochemical waveforms are frequently employed both to reduce surface fouling and to increase the faradaic signal. Crespi et al. [44] employed differential pulse voltammetry (DPV) with a carbon fibre electrode for the selective detection of dopamine and serotonin metabolites in the striatum of two inbred strains of mice. A triangular voltage waveform [45] was employed in PBS for the electrochemical pretreatment of a carbon fibre electrode before it was employed for the PAD

detection of dopamine metabolites Reverse differential pulse voltammetry (RDPV) was used [46] with electrochemically pretreated carbon fibre electrodes for the successful voltammetric discrimination between different catechols Before use, the 8 μm carbon fibre electrodes were subjected to a triangular potential waveform between 0.0 and 3.0 V at 200 Vs^{-1} for 20 s in PBS (pH 7.4) containing 0.15 NaCl Subsequently, the electrode was kept at -0.8 V for 5 s and at +1.5 V for 5 s

Fast scan cyclic voltammetry ($>100 \text{ Vs}^{-1}$) has also gained considerable attention in recent years since its introduction by Millar [47] This technique allows high temporal resolution that is necessary to observe rapid concentration changes The technique has been employed extensively [48-50] for *in vivo* voltammetric studies The inherent high background current experienced in cyclic voltammetry, particularly at high scan rates, can be digitally subtracted [51] to yield analytically useful data and high sensitivity

Numerous applications of *in vivo* voltammetry have been reported relating to the study of the effect of administration of various compounds [52,53], and electrical stimulation [54,55] on the release and uptake of several neurotransmitters The effects of several physical manipulations such as tail pinching, forced locomotion, shaking and exposure to high noise levels have also been studied [56,57]

The wide range of *in vivo* applications of voltammetry can be appreciated from the examples cited above The inevitable continued growth in this area of research will undoubtedly strive towards the development of improved systems in terms of selectivity and sensitivity, new electrode substrates, unambiguous peak identification and reliable *in situ* calibration techniques

Arrays of microelectrodes have been of interest because of their advantages such as high current density and fast response while the same magnitude is maintained as with conventional electrodes. Microarrays have been fabricated using such techniques as photolithography, electrodeposition, and mechanical assembly using metal substrates such as Pt, Au and Cr, various forms of carbon, semiconductor materials, and oxides. Various geometries have been reported including microdisks, microbands and interdigitated arrays (IDA). Carbon film based IDA microelectrodes were reported recently [58] for the voltammetric measurements of reversible and quasi-reversible redox species. Since each of the two electrodes were connected to separate potentiostats an electroactive species generated at one electrode (generator) could diffuse to the second electrode (collector). As a result, a large current was obtained with a high S/N ratio. Wang et al [59] reported on the use of screen-printed ultramicroelectrode arrays for on-site stripping measurements of trace metals. The carbon-based microdisks were coated using mercury electrodeposition. Stripping performance of the micro-array was not compromised by placing non-deaerated quiescent sample drops on the strip when square-wave voltammetry was employed. This is very advantageous for field monitoring of trace metals. The micro-array was applied to the analysis of drinking water and wine and the workers concluded that the array was ideally suited as a throw away device. Kounaves et al [60] have fabricated iridium-based microelectrode arrays by microlithography. The microdisk array was coated with mercury by electrodeposition and was applied to the analysis of trace metals in spring water using square-wave voltammetry.

The use of microarrays will undoubtedly be extended to the development of miniature detection systems for microcolumn techniques such as microbore chromatography and capillary electrophoresis. They could provide such advantages as increased currents and the ability to carry out voltammetric characterisation of the eluting components since each electrode could be individually monitored.

1.3 References

- 1 R M Wightman, *Anal Chem* , **53** (1981) 1125A
- 2 R M Wightman, D O Wipf, in A J Bard, Ed , *Electroanalytical Chemistry*, Marcel Dekker, 1989, pp 267
- 3 S Pons and M Fleischman, *Anal Chem* , **59** (1987) 1391A
- 4 K Aoki, *Electroanalysis*, **5** (1993) 627
- 5 P A Broderick, *Electroanalysis*, **2** (1990) 241
- 6 K Stulik, *Anal Chim Acta*, **273** (1993) 435
- 7 A G Ewing, J M Mesaros and P G Gavin, *Anal Chem* , **66** (1994) 527A
- 8 R J Forster and J G Vos, in M R Smyth and J G Vos (Eds), *Analytical Voltammetry*, Elsevier, 1992
- 9 S A Wring and J P Hart, *Anal Chim Acta*, **231** (1990) 203
- 10 J Wang, T Golden, and R Li, *Anal Chem* , **60** (1988) 1642
- 11 K T Kawogoe, P A Garris and R M Wightman, *J Electroanal Chem* , **359** (1993) 193
- 12 D S Bindra and G S Wilson, *Anal Chem* , **61** (1989) 2566
- 13 A C Michael and R M Wightman, *Anal Chem* , **61** (1989) 270
- 14 E F Sullenberger and A G Michael, *Anal Chem* , **65** (1993) 2304
- 15 T Baumeyer, J Dittrich and F Crespi, *Electroanalysis*, **5** (1993) 565
- 16 E R Reynolds and A M Yacynych, *Electroanalysis*, **5** (1993) 405
- 17 P T Kissinger, C Refshange, R Dreiling and R N Adams, *Anal Lett* , **6** (1973) 465
- 18 P T Kissinger, *Electroanalysis*, **4** (1992) 359
- 19 C Hua, K Sagar, K McLaughlin, M Jorge, M P Meaney and M R Smyth, *Analyst*, **116** (1991) 1117
- 20 K A Sagar M T Kelly and M R Smyth, *J Chrom Biomed Appl* , **577** (1992) 481
- 21 A Burcinova, M Tichy, V Pacakova and K Stulik, *J Chromatography*, **455** (1988) 420

- 22 D C Johnson, D Dobberpuhl, R Roberts and P J Vandeberg, J Chromatogr , **640** (1993) 79
- 23 P J Vandeberg and D C Johnson, Anal Chem , **65** (1993) 2713
- 24 T J O' Shea, R D Greenhagen, S M Lunte, C E Lunte, M R Smyth, D M Radzik and N Watanabe, J Chromatogr , **593** (1992) 305
- 25 W Lu and R M Cassidy, Anal Chem , **65** (1993) 1649
- 26 T J O' Shea, W R LaCourse and S M Lunte, Anal Chem , **65** (1993) 948
- 27 T J O' Shea, M W Telting-Diaz, S M Lunte, C E Lunte and M R Smyth, Electroanalysis, **4** (1992) 463
- 28 P T Kissinger, J B Hart and R N Adams, Brain Res , **55** (1973) 209
- 29 K F Martin, C A Marsden and F Crespi, TrAC, **7** (1988) 334
- 30 T G Stein, J Electrochem Soc , **138** (1991) 254C
- 31 J M Sequaris, in M R Smyth and J G Vos, Eds , Analytical Voltammetry, Elsevier, 1992
- 32 C A Marsden, M H Joseph, Z L Kruk, N T Maidment, R D O' Neill, J O Schenk and J A Stamford, Neuroscience, **25** (1988) 389
- 33 R D O' Neill and M Fillenz, in J B Justice, Jr , (Ed), Voltammetry in Neurosciences, Principles, Methods and Applications, Humana Press, New Jersey, 1987
- 34 K T Kawagoe, J B Zimmerman and R M Wightman, J Neuroscience Methods, **48** (1993) 225
- 35 P Capella, P Ghasemzadeh, B Mitchell and R N Adams, Electroanalysis, **2** (1990) 175
- 36 R N Adams, Progress in Neurobiology, **35** (1990) 297
- 37 K J Renner, L Pazos and R N Adams, Brain Res , **577** (1992) 49
- 38 M E Morgan and C R Freed, Pharmacol Exp Ther , **219** (1981) 49
- 39 T K Chen, Y Y Lau, D K Y Wong and A G Ewing, Anal Chem , **64** (1992) 1264
- 40 Y Y Lau, T Abe and A G Ewing, Anal Chem , **64** (1992) 1702
- 41 P D Lyne and R D O' Neill, Anal Chem , **62** (1990) 2347

- 42 D J Wiedeman, A Basse-Tomusk, R L Wilson, G V Rebec and R M Wightman, *J Neurosci Methods*, **35** (1990) 9
- 43 M B Ghasemzadeh, P Capella, K Mitchell and R N Adams, *J Neurochemistry*, **60** (1993) 442
- 44 F Crespi, K F Martin, D J Heal, C A Marsden, W R Buckett and M K Sanghera, *Brain Res*, **500** (1989) 241
- 45 M K Sanghera, F Crespi, K F Martin, D J Heal, W R Buckett and C A Marsden, *Neuroscience*, **39** (1990) 649
- 46 F M Matysik, G Nagy and E Pungor, *Anal Chim Acta*, **264** (1992) 177
- 47 J Millar, J M Armstrong and Z L Kruk, *Brain Res*, **205** (1981) 419
- 48 J A Stamford, Z L Kruk and J Millar, *Brain Res*, **381** (1986) 351
- 49 J E Baur, E W Kristtensen, L J May, D J Wiedemann and R M Wightman, *Anal Chem*, **60** (1988) 1268
- 50 P A Garriss and R M Wightman, *J Neuroscience*, **14** (1994) 442
- 51 J Millar, J A Stamford, Z L Kruk and R M Wightman, *Eur J Pharmacol*, **109** (1989) 341
- 52 J P Ng, G W Hubert and J B Justice, Jr, *J Neurochem*, **56** (1991) 1485
- 53 P A Broderick, *Pharmacol Biochem Behav*, **40** (1991) 969
- 54 L J Lay, W G Kuhr and R M Wightman, *J Neurochem*, **51** (1988) 1060
- 55 F Crespi, K F Martin and C A Marsden, *Neuroscience Letters*, **90** (1988) 285
- 56 M Bertolucci, A Serrano and B Scatton, *J Neurosci Methods*, **34** (1990) 135
- 57 M H Joseph and H Hodges, *J Neurosci Methods*, **34** (1990) 143
- 58 O Niwa and H Tabei, *Anal Chem*, **66** (1994) 285
- 59 J Wang, J Lu, B Tian and C Yarnitsky, *J Electroanal Chem*, **361** (1993) 77
- 60 S P Kounaves, W Deng, P R Hallock, G T A Kovacs and C W Stormont, *Anal Chem*, **66** (1994) 418

CHAPTER 2

The Coupling of Electrochemical Detection with Microelectrodes to Capillary Electrophoresis and Microdialysis/Capillary Electrophoresis

2.1 Introduction

The main objective of this work was to integrate microelectrode detection systems with microvolume techniques such as capillary electrophoresis and microdialysis. The chapter is divided into two main sections. In the first section work is presented regarding the development of a system suitable for reductive electrochemical detection with capillary electrophoresis. The second section deals with the use of capillary electrophoresis with electrochemical detection (CEEC) for monitoring *in vivo* microdialysates of rat brain for tryptophan metabolites. Prior to describing the experimental work carried out this introduction will describe some of the concepts involved in these techniques.

2.1.1 *Capillary Electrophoresis*

Capillary electrophoresis is a highly efficient separation technique that has been defined as the differential movement of charged species by attraction or repulsion in an electric field. Since the introduction of capillary electrophoresis, as we know it today, by Jorgenson and Lukacs [1] the technique has been shown to possess several advantages over both classical electrophoretic techniques and liquid chromatographic techniques. The major advantages this technique holds over liquid chromatography include greater efficiency (theoretical plates), very low volume sample volume requirement (usually 1-10 nL, but sometimes lower), and lower mass detection limits. The major advantages it holds over classical slab electrophoresis include the inherent anticonvective properties of the capillary which reduces convective broadening, and also the high surface area-to-volume ratio of the capillary wall which facilitates more efficient dissipation of joule heating (the heat generated by the passage of electrical currents), which traditionally limited electrophoretic techniques. In high performance capillary electrophoresis (HPCE), electrophoresis is performed in narrow-bore capillaries, typically 25 to 75 μm inner diameter which are usually filled only with buffer. In its basic design the ends of the

fused silica capillary (polyimide coated) are placed in anodic and cathodic buffer reservoirs, the contents of which are identical. These reservoirs also contain the electrodes (usually platinum) used to make the electrical contact between the high voltage supply (0 to 30 kV) and the capillary. Sample is loaded ("injected") onto the capillary by replacing one of the reservoirs (usually the anode) with a sample reservoir and applying either an electric field or an external pressure. After replacing the buffer reservoir the electric field is applied and the separation is performed.

Capillary zone electrophoresis (CZE)(also known as free-solution electrophoresis) is the most widely used mode of HPCE. Resolution of components is generally achieved by careful selection of the pH of the electrolyte which affects both the electroosmotic flow and the electrophoretic mobilities of the analyte components (according to their pI values). However, other modes of HPCE are also used including, micellar electrokinetic chromatography (MEKC), capillary gel electrophoresis, capillary isoelectric focusing (CIEF) and isotachopheresis (ITP). Each one of these modes has its own principle of separation. Extensive literature is available regarding these techniques [1-5]. Figure 2.1 illustrates the principles involved in some of these techniques.

The most popular mode of detection to date has been UV detection, where a detection cell is made by burning a detection window in the polyimide coating, allowing direct on-column detection. The path-length dependency of this technique is a sensitivity limiting factor. Fluorescence detectors are more sensitive, but are limited to certain wavelengths. Electrochemical detection offers potentially more sensitive detection and in fact has been shown to offer advantages over the more popular modes of detection. Some modifications to the HPCE system are necessary, however, for electrochemical detection.

When performing electrochemical detection, generally amperometric in nature, the electrochemical cell must be isolated from the high separating voltage applied

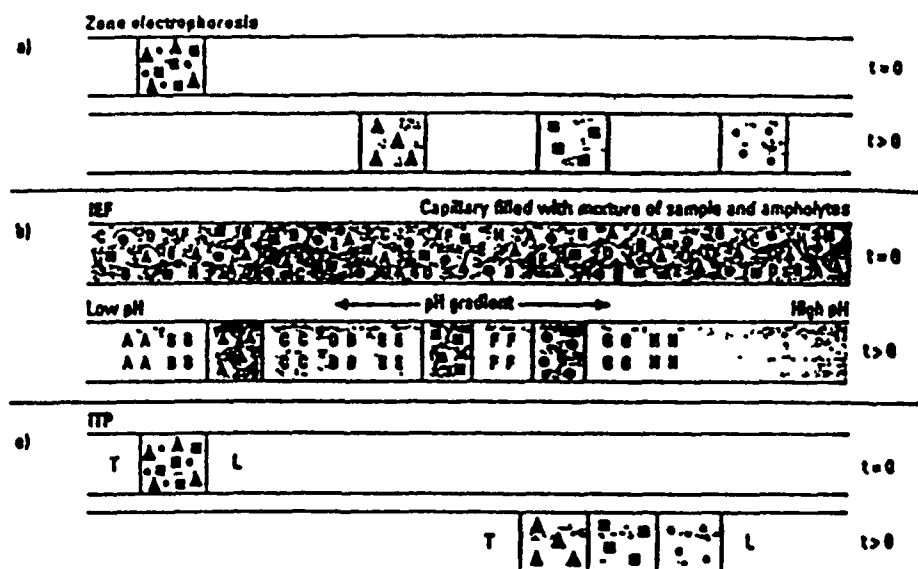


Figure 2.1

Illustration of zonal, IEF and ITP electrophoresis. (copied from 'High performance capillary electrophoresis', Hewlett Packard, 1992)

across the capillary. Some workers have used end-column detection with small internal diameter capillaries [2] where the electrophoretic current through the capillary is small (1-15 nA) and therefore the electrical interference is minimised. Whilst this technique works well for small internal diameter capillaries, the electrical interference is more problematic when using larger capillaries. Several workers have reported the use of on-column joints (decouplers) to ground the high separating voltage before it reaches the detection cell. This allows for so called "off-column" detection where the electrode is inserted in the end of the capillary leading to improved sensitivity and reduced band broadening compared to end-column detection. Various designs have been reported ranging from a porous glass decoupler [2] to an on-column frit [3], Nafion tubing [4], and recently cellulose acetate [5]. Each system grounds the high separating voltage to a greater or lesser extent. One of the major driving forces today in this area of research is to develop a decoupler that can be fabricated easily and reliably and that may allow post-column additions to facilitate pH changes and derivatisation reactions before detection. This is an area of major importance since there is often a large discrepancy between the optimum separating pH and the optimum pH required for electrochemical detection. A Nafion decoupler was employed throughout the studies presented in this thesis and will be described in more detail in the experimental section of this chapter.

2.1.2 *Microdialysis Sampling*

Microdialysis was originally introduced in the 1970's by Ungerstedt et al [6]. In recent years it has enjoyed steadily growing interest due to its ability to sample substances from and/or deliver substances to the extracellular fluid of essentially any tissue in the body with minimal perturbation to the tissue. The dialysis fibre is slowly perfused with a medium, which should closely match the composition of the fluid being sampled. Small molecules diffuse through the semi-permeable membrane, driven by a concentration gradient. Several useful reviews have

appeared in the literature recently [7-10] which give a more comprehensive overview of this field of research than is possible here

The microdialysis probe generally consists of a stainless steel or fused silica shaft, 20-100 mm in length and approximately 0.6 mm in diameter. The most common microdialysis membrane materials used are polyacrylonitrile, polycarbonate, and regenerated cellulose acetate and the dimensions vary depending on the intended application. Generally, the membranes are 1 to 5 mm long and approximately 0.3-0.5 mm in diameter. The membrane material used should be semi-permeable and inert so as to allow diffusion of the small molecules with minimal interactions. Figure 2.2 shows some of the designs currently used for microdialysis probes, the most popular of which is the concentric probe design. The probe is implanted in the tissue of interest and is slowly perfused with a physiological salt solution. Substances diffusing across the membrane into the perfusate are carried away continuously, and are either analysed on-line or collected at appropriate intervals and analysed off-line. The membrane materials used generally have molecular cut-offs of 5000 to 20000 daltons which means that the dialysate analysed is free of proteins. This is of major analytical significance since further sample preparation regimes are usually not required.

Usually metabolic processes and pharmacokinetic studies are carried out by removing blood samples at regular intervals. These samples are then analysed to derive a concentration-time profile. Infrequent sampling results in poor temporal resolution while frequent removal of blood causes a decrease in total blood volume which may alter the observed distribution and elimination of the drug. Protein removal is also generally necessary prior to analysis. The measurement of total drug concentration (after protein precipitation) in the blood gives an average picture of the result of the metabolism taking place. However, using microdialysis, the free drug concentration can be monitored in any specific organ of interest with minimal perturbation, leading to an ultimately more detailed map of the function of each

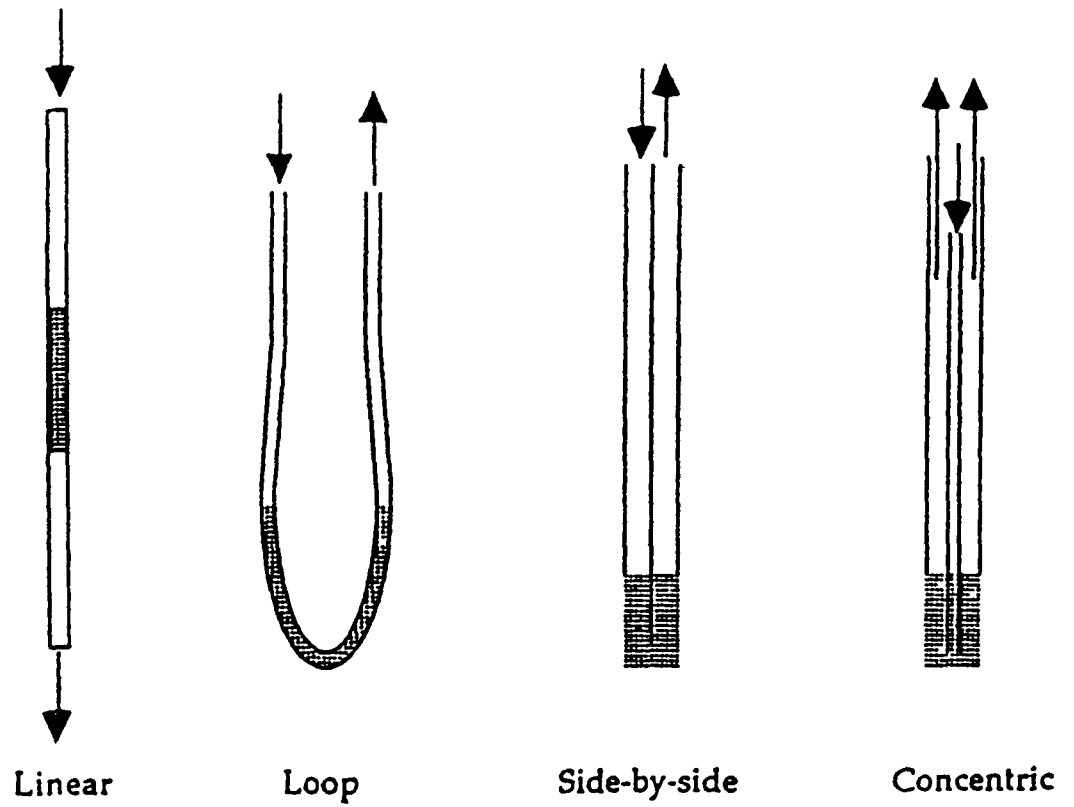


Figure 2.2

Illustration of the four types of microdialysis probes. The arrows indicate direction of flow of the perfusion medium. (copied from reference 11)

particular organ with regards to the process of interest. Also due to the molecular weight cut-off of the membrane material, enzymes responsible for metabolism cannot diffuse across to the perfusate so that the collected sample does not undergo further metabolism.

Several factors affect the recovery of a particular compound by a given probe, including the initial concentration of the substance of interest in the perfusion medium, the membrane surface area, perfusion flow rate and the tissue temperature. The parameter of most practical importance is the perfusion flow rate. The 'relative recovery' of a compound by microdialysis is the final concentration of this compound in the perfusion medium related to the concentration of the compound in the extracellular fluid, and is usually expressed as a percent value. The term 'absolute recovery' refers to the absolute amount of the substance that is removed by the perfusion medium per unit time. By increasing the perfusate flow rate, one increases the absolute recovery but decreases the relative recovery. It must be kept in mind that the more material removed per unit time, the greater the perturbation to the system and this may lead to depletion of the compound in the extracellular fluid of interest. The flux across the membrane does not increase significantly at flow rates above approximately $3 \mu\text{Lmin}^{-1}$ due to ultrafiltration of the perfusate across the membrane. High relative recoveries (slow perfusion flow rates) are generally favoured since they increase the reliability of the physiological experiment and also provide samples of higher concentration which is desirable for their ultimate detection.

Much of the work to date has concentrated on the study of relative changes in concentrations of neurochemicals with respect to various stimuli. However, the determination of absolute concentrations of compounds in the body is of obvious biomedical importance. This demands a reliable calibration of the microdialysis probe in terms of the recovery of each compound of interest under the normal experimental conditions. In vitro probe calibration is often employed as an

approximation of the *in vivo* behaviour of the probe. However, the development of *in vivo* calibration procedures is of major importance in this area of research. Several *in vivo* calibration techniques have been used, including retrodialysis [12], extrapolation to zero flow [13], external calibration [14] and zero net flux [15]. The zero net flux (or concentration equilibrium) technique appears to be the most reliable *in vivo* calibration available to date. In this technique the probe is perfused with a series of known concentrations of the compound at a very low flow rate. The concentrations are selected to be both below and above the expected extracellular concentration. The difference in the amount of compound in the perfusion medium before and after dialysis is plotted against the initial concentration in the perfusate. The 'true' extracellular concentration is then extrapolated from the point of zero deviation (i.e. the point at which no compound is lost or gained from the probe).

Many practical considerations must be kept in mind when performing microdialysis sampling, both to maximise the relative recovery of the probe and to minimise perturbation to the tissue under investigation. The most common analytical technique applied to microdialysates to date has been HPLC with UV, fluorescence or electrochemical detection. The objective of the work presented in the second main section of this chapter was to demonstrate the use of capillary electrophoresis with electrochemical detection (CEEC) for monitoring tryptophan metabolites in *in vivo* rat brain microdialysate samples. The advantages that this technique holds over LC techniques will be demonstrated and discussed.

2.1.3 *Biomedical Importance of Amino Acids*

Amino acids are essential biological building blocks. Every protein molecule can be viewed as a polymer of amino acids, all consisting of a tetrahedral carbon called the (α) carbon which is covalently bonded on one side to an amino group and on the other side to a carboxyl group. A third bond is always hydrogen and the fourth bond is to a variable side chain (R). In addition to the twenty commonly occurring α

-amino acids, a variety of other amino acids are found in minor amounts in proteins and non-protein compounds, normally resulting from the modification of the common amino acids. In neutral solution the amino acid exists as a zwitterion, since the carboxyl group loses one proton and the amino group gains one. Some amino acid side chain (R) groups are ionisable and introduce a further variable charge depending on the pH of the solution. Thus, capillary electrophoresis is a very useful technique for the separation of amino acids since resolution is based on the size/charge ratio of the compounds. The analysis of amino acids has long been an important issue due to the importance of determining the composition and sequence of amino acids in proteins. However, certain amino acids are of major interest as individual entities due to their important roles in biological processes, particularly in the area of neurotransmission. The best documented examples of chemical neuromessengers other than acetylcholine are the catecholamines, certain amino acids and their derivatives, and a variety of peptides. The catecholamines are all biosynthesised in the adrenal gland from an amino acid called tyrosine, by hydroxylation which is catalysed by tyrosine hydroxylase. The hydroxylation of this amino acid yields 3,4-dihydroxyphenyl-alanine (L-Dopa) from which dopamine is derived by a decarboxylation reaction. Norepinephrine and epinephrine are, in turn, derived from dopamine. All these related amines have been shown to serve as neurotransmitters in a number of nerve pathways in the brain. Amino acids that are believed to have roles as neurotransmitters include GABA and glycine (inhibitory role), and glutamate and aspartate (excitatory role). Another key amino acid that is biochemically metabolised to produce compounds of neurochemical importance is tryptophan. The hydroxylation of tryptophan (Trp) yields 5-hydroxytryptophan (5-HTP). Decarboxylation of 5-HTP then yields 5-hydroxytryptamine (serotonin, 5-HT) which is a very important neurochemical. Following another biochemical pathway, known as the kynurenine pathway (Figure 2.3) tryptophan is metabolised

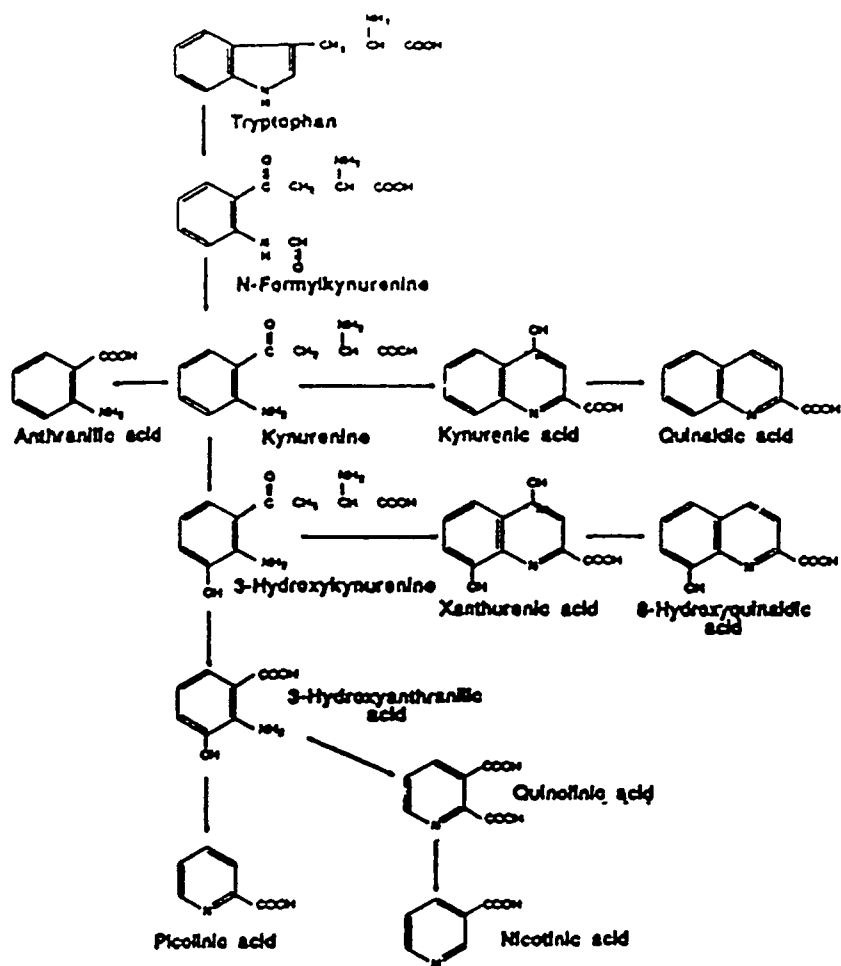


Figure 2.3

Tryptophan ('kynurenine pathway') metabolic pathway (from J Chromatogr , 534 (1990) 13)

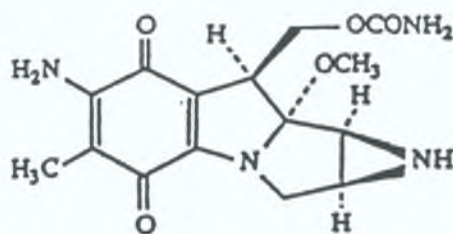
to a number of important neurochemicals including kynurenic acid and quinolinic acid, which are also known to function as neuromessengers

Amino acids, in general, possess few notable analytically useful features. The aromatic amino acids, namely phenylalanine, tyrosine, and tryptophan possess absorption maxima in the near-ultraviolet arising from interaction of radiation with electrons in the aromatic ring. However UV detection techniques are path length dependent which often leads to limited sensitivity. Some amino acids and their metabolites are electroactive. Many investigators have concentrated on derivatisation techniques to yield fluorescent and/or electroactive products. In the first main section of this chapter some dinitrophenyl derivatised amino acids were separated using CE and detected by reductive electrochemical detection to demonstrate the efficacy of the system for nitroaromatic compounds.

In the second main section of this chapter tryptophan and some of its metabolites were directly detected in rat brain dialysate, and the levels of the compounds were monitored over extended periods of time as a function of various loading experiments.

2.1.4 *Clinical Importance of Mitomycin C*

Mitomycin C (I) is an antitumour antibiotic isolated from *Streptomyces caespitosus* in 1958 [16]. Initial clinical trials in the United States employed a series of dosage schedules, and were characterised by serious myelosuppression and responses of very brief duration. However, it wasn't until 1974, that the potential for mitomycin C to induce delayed cumulative myelosuppression was recognised, from when more rational dose schedules were developed [17]. Subsequently, although still highly toxic, and capable of inducing only short-term remissions, mitomycin C proved to be of increasing value in the treatment of various malignant diseases.



I

Mitomycin C is an alkylating agent and possesses three potentially active groups, namely a quinone, a urethane, and an azinidine, group but requires activation by reduction of the quinone and subsequent loss of the methoxy group. The proposed *in vivo* activation is rapid and is NADPH dependent. Many structural analogues of mitomycin C have been synthesised in an effort to improve the therapeutic ratio. However, mitomycin C is still considered the most effective member of the group.

The most significant effect of the interactions of mitomycin C is the inhibition of the *de novo* DNA synthesis. However, the repair DNA synthesis is apparently not inhibited by mitomycin C. Studies in humans have shown that mitomycin C is absorbed erratically after oral administration. It is also absorbed after intraperitoneal and intrapleural administration. Very little information is available concerning the distribution, metabolism and elimination of mitomycin C in humans [18], mainly due to the lack of a sensitive, reproducible assay.

Initial clinical trials used daily dose schedules, but it was subsequently found that intermittent therapy was more effective, at equivalent levels of toxicity, than daily administration. Today, the preferred regimen for mitomycin C when given as a single agent is 20-50 mg/m² i.v. every 6-8 weeks. It has demonstrated activity against several solid tumours including; breast, stomach, head and neck, and lung, and has also shown activity against the leukemias. This drug has also been used in combination with other chemotherapeutic compounds such as adriamycin and 5-

flourouracil The most significant toxicity associated with mitomycin C is delayed, cumulative myelosuppression, the incidence and severity of which is dose related

In the work presented here, mitomycin C was taken as an example of a class of therapeutic compounds that are readily reducible, to demonstrate the analytical potential of the CEEC system developed

2.2 Reductive Electrochemical Detection for Capillary Electrophoresis

2.2.1 Introduction

The majority of electrochemical investigations since the advent of polarography have dealt with reducible compounds. This is primarily due to the early use of classical mercury electrodes. However, liquid chromatography/electrochemistry (LCEC) has been very popular because of its applicability to oxidisable compounds. The use of reductive electrochemical detection in LC, although quite extensively investigated, has been compromised by the high background currents which occur due to dissolved oxygen and trace metals in the system. In 1978, MacCrehan and Durst [19] used a gold/mercury amalgam electrode with differential pulse reductive electrochemical detection for the determination of organomercury cations in biological samples after liquid chromatographic separation. Reductive LCEC was further advanced by Bratin and Kissinger [20] who evaluated various electrode substrates, including carbon and gold/mercury amalgams. They applied their system to the determination of several electrochemically reducible compounds, including explosives [21,22] and nitro-containing pharmaceuticals [23]. Reductive LCEC was later investigated for the detection of nitroaromatic compounds [24-26] and for the determination of polynuclear aromatic hydrocarbons in diesel exhausts [27]. All of these papers reported the need for lengthy deoxygenation procedures, including overnight heating of the mobile phase with nitrogen sparging. In addition, the chromatographic system needed to be plumbed completely with stainless steel tubing to prevent diffusion of oxygen into the system. Despite these drawbacks, reductive LCEC has been employed for the analysis of various types of compounds, including antitumour agents [28,29], antirheumatic compounds [30], benzodiazepines [31] and vitamins [32]. Electrode substrates employed included mercury [28,29,31], gold/mercury amalgam [30] and glassy carbon [32].

Two other techniques used to circumvent the high background characteristic of reductive LCEC include reverse pulsed amperometric detection [33] and dual electrode detection [34]. Reversed pulse amperometry is based on the application of an unsymmetrical square wave with a large negative deposition potential followed by a positive potential pulse. Dual electrode detection involves the employment of a generator electrode poised at a potential more negative than the half-wave potential of the analyte of interest, and a detector electrode at a potential suitable for the oxidation of the product generated by the first electrode. Because the actual detection occurs in the oxidative mode, there is no interference from oxygen and trace metals. However, this approach is applicable only to chemically electrochemically reversible compounds [20,24,35-37].

Capillary electrophoresis has several advantages over LC, particularly in terms of its high efficiency and low volume requirements. Electrochemical detection is ideally suited to CE, due to the fact that it can be miniaturized without loss of sensitivity or selectivity. The utility of capillary electrophoresis/electrochemistry (CEEC) has been demonstrated in the past [38-43]. However, the majority of applications have dealt with oxidative detection. The exception to this is the work of Cassidy et al [41,42] who investigated the use of gold/mercury electrodes for the reductive end-column detection of metal ions. However, in this case, the system was not deoxygenated, and there was a significant background current due to reduction of oxygen. The authors reported limited stability of the gold/mercury disc electrode in their paper, which could be due to the oxidation of Hg by oxygen present in the run buffer.

The main aim of this study was to demonstrate the feasibility of reductive CEEC for organic compounds, including nitroaromatics and quinones. It has been shown that the system possesses major advantages over reductive LCEC, including very short deoxygenation times and the fact that stainless steel plumbing is not necessary. The system has been applied to the separation and detection of dinitrophenyl derivatised

amino acids and a series of anthraquinones. Finally, the system was applied to the determination of an antitumor compound, mitomycin C, in human serum demonstrating its high selectivity as compared to CE with UV detection.

2.2.2 Experimental

2.2.2.1 Reagents and Materials

The dinitrophenyl-L-amino acid derivatives, mitomycin C, MES (2-[N-morpholine]ethanesulfonic acid) and human serum were all purchased from Sigma (St Louis, MO). Anthraquinone-2-carboxylic acid and anthraquinone-2-sulfonic acid were obtained from Aldrich (Milwaukee, WI). Sulfobutylether- β -cyclodextrin was supplied by the Center for Drug Delivery Research (CDDR), University of Kansas, Lawrence, KS. All other chemicals were analytical reagent grade. All chemicals were used as received. Solutions were prepared in NANOpure water (Sybron-Barnstead, Boston, MA) and passed through a membrane filter (0.2 μ m pore size) before use. The separation buffer consisted of 10 mM MES containing 1 mM Na₂EDTA, which was adjusted to pH 7.0 with sodium hydroxide. This was used as the electrolyte throughout the study. All stock solutions of the DNP-amino acids, anthraquinones and mitomycin C were prepared daily in run buffer and stored at 4°C. Ultrahigh purity nitrogen was used for all deoxygenation throughout the study.

2.2.2.2 Apparatus

The basic CEEC system has been described previously [43]. Electrophoresis in the capillary was driven by a high-voltage supply (Spellman Electronics Corp., Plainview, NY). Polyimide-coated fused silica capillary columns (360 μ m o.d., 50 μ m i.d.) were obtained from Polymicro Technologies (Phoenix, AZ), and capillary lengths between 60 and 80 cm were used. Sample introduction was accomplished using a laboratory-built pressure injection system. The injection volume was calculated to be 9.8 nL using the continuous fill mode by recording the time required for the sample to reach the detector.

When performing capillary electrophoresis with electrochemical detection, the detection end of the capillary column must be isolated from the high applied separating voltage. In this work a Nafion joint decoupler was employed. The construction of this joint is described here. A capillary cutter (Supelco, Bellefonte, PA, USA) was used to score the polyimide coating approximately 2 cm from the detection end of the capillary column. A 1 cm length of Nafion tubing (ID 360 μ M, OD 510 μ M) (Perma Pure Products, Tom's River, NJ, USA) was then carefully threaded over the score mark. Both ends of the Nafion tubing were sealed to the capillary using UV-cure-glue (UVEXS, Sunnyvale, CA). This was mounted on a piece of glass microslide using deposits of UV-cure-glue and the whole assembly was cured for approximately 20 minutes. Once cured, gentle pressure was applied to the Nafion tubing, causing the capillary to fracture at the score. The Nafion tubing holds the capillary joint in place and insures correct alignment. The Nafion polymer prevents sample loss but allows the separating current to be grounded. The Nafion joint assembly was then placed in a small plastic tube which serves as the cathodic buffer reservoir. The detection end of the capillary was then inserted in the electrochemical detection cell. The cathodic buffer reservoir (approximately 2 ml volume) was filled with deoxygenated buffer and sealed with a rubber septum, through which the cathodic platinum electrode was introduced. Once all this procedure has been completed, the working electrode was inserted in the detection end of the capillary using an X-Y-Z micromanipulator, with the aid of a microscope for visualisation.

Cylindrical carbon fiber microelectrodes were constructed using 33 μ m diameter fibers (AVCO Specialty Products, Lowell, MA). The fiber was bonded to a length of copper wire using silver epoxy (Ted Pella, Inc., Redding, CA). Capillary tubes were pulled to a narrow tip with a Liste-Medical (Greenvale, NY) model 3A vertical pipette puller. The carbon fiber was then inserted through the capillary until it protruded approximately 0.5 cm from the tip. UV-cure-glue (UVEXS, Sunnyvale,

CA) was applied to the tip at the junction of the capillary and the carbon fiber. The fiber was then drawn back until the desired length (150–300 μm) protruded, and the glue was cured under an ultraviolet light source. The opposite end of the capillary was then sealed with thermogrip glue (Black & Decker) to fix the copper connecting wire in place.

2.2.2.3 *System Deoxygenation*

Some modifications of the CEEC system were necessary for the reductive electrochemical detection (Figure 2.4). A laboratory-built system was employed which consisted of one nitrogen inlet tube and pressure adjuster leading to a set of four adjustable valves, each of which could be controlled separately to regulate the flow through its respective nitrogen delivery tube. Complete deoxygenation of the anodic buffer, cathodic buffer and the electrolyte was carried out off-line for 15 min at ambient temperature. The cathodic buffer was filled with deoxygenated buffer and sealed with a rubber septum through which the cathodic platinum electrode was introduced. The microelectrode was then inserted in the end of the capillary, and the electrochemical cell was filled with deoxygenated electrolyte (buffer). Both the cathodic reservoir and the electrochemical cell were housed in a box which could be loosely sealed. This box was lined with a series of nitrogen delivery tubes derived from inlet tube 1 (see Figure 2.4). Once the cathodic reservoir and the electrochemical cell were filled with deoxygenated buffer, the box was closed and the nitrogen inlet tubes were switched on. This created a nitrogen atmosphere and a positive pressure inside the box, ensuring the expulsion of any atmospheric oxygen present. This positive pressure was maintained throughout the experiment, thus preventing the entry of oxygen. The anodic reservoir was then filled with deoxygenated buffer and sealed in position. Using an 18-gauge needle, a nitrogen delivery tube (Tube 2, Figure 2.4) was introduced through the rubber septum which was used to seal the reservoir. A second needle inserted in the septum allowed a continuous outward flow of nitrogen. In this way a nitrogen blanket was

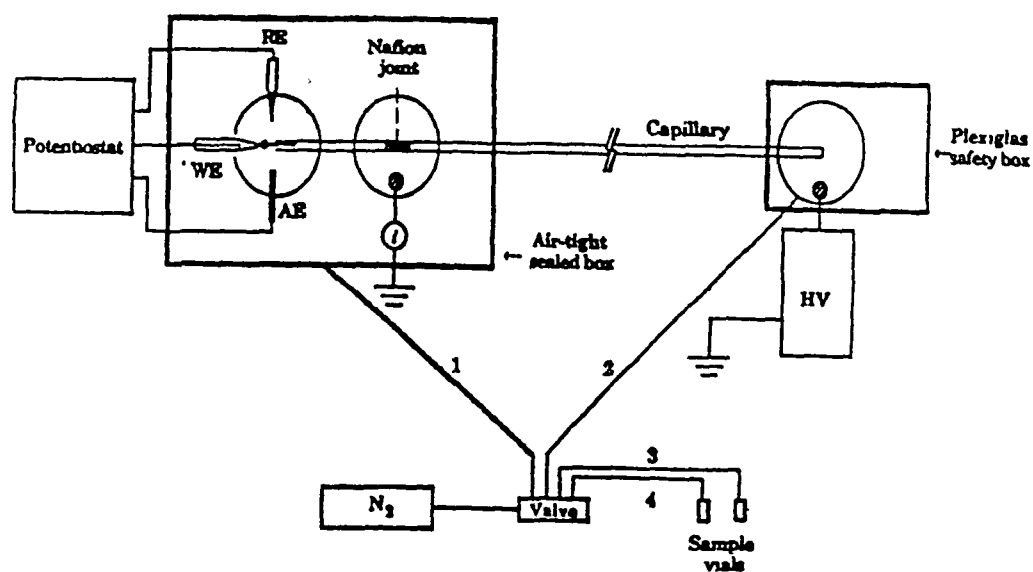


Figure 2.4

A schematic representation of the reductive CEEC system 1-4 are nitrogen delivery tubes, as described in the text.

maintained over the anodic buffer throughout the experiment. Once the high voltage source was switched on, the system stabilized within ca. 5 min at negative applied potentials. Samples were deoxygenated using nitrogen lines 3 and/or 4 for 10 min prior to analysis. The whole procedure of deoxygenation and set-up took no more than 30 min, and once operational, the system could be used for 24 hr.

2.2.2.4 *Cyclic Voltammetry*

All cyclic voltammetry experiments were carried out on deoxygenated solutions using a model CySy-1 computerized electrochemical analyser (Cypress Systems, Lawrence, KS). A three-electrode cell was used which consisted of a carbon fiber working electrode, a Ag/AgCl reference electrode and a platinum auxiliary electrode. All cyclic voltammograms were carried out in 10 mM MES pH 7 buffer using a scan rate of 100 mV/s.

2.2.2.5 *Hydrodynamic Voltammetry*

Hydrodynamic voltammograms were obtained by repeated injections of standards while varying the working potential between -200 and -1000 mV and measuring the resultant peak currents at 100 mV intervals. The separation was performed in 10 mM MES buffer, pH 7.0 with an applied voltage of 25 kV. The effective capillary length was 60 cm.

2.2.2.6 *Sample Preparation*

One mL aliquots of serum were spiked with the appropriate amount of mitomycin C stock solution to achieve the desired final concentration. Dilution (1:4) of the serum was carried out using 10 mM sodium borate (pH 9.0) buffer. Final solutions were filtered through a membrane filter (0.2 μ m pore size) before analysis. It was necessary to deoxygenate the sample very slowly to avoid excessive frothing of the serum. Complete deoxygenation was not essential since the analyte peak was resolved from the oxygen response.

2.2.3 Results and Discussion

2.2.3.1 Cyclic Voltammetry

The initial study involved a cyclic voltammetric investigation of the behavior of the DNP-amino acid derivatives at carbon fiber electrodes. Voltammograms were run in MES buffer at pH 7.0 since good separation of the amino acid derivatives could be obtained at this pH using CE. The use of low pH electrolytes is advantageous for reductive electrochemical processes, since the half-wave potential of proton-dependent reductions will move to less negative potentials, introducing an improvement in selectivity. However, since the initial reduction of each nitro group is a $4\text{H}^+/4\text{e}^-$ process, there should be only a 15 mV/pH shift in reduction potential. Therefore, for this particular class of analytes, a substantial drop in pH would be necessary to have any significant effect on the half-wave potential. This presents a problem in CE since electroosmotic flow is much lower at pH values below 7.0, resulting in excessively long migration times for the analytes. For this reason, a pH 7.0 buffer was used throughout. Figure 2.5 shows the cyclic voltammetric behavior of DNP-glycine at a bare carbon fiber electrode before and after electrochemical pretreatment. It is obvious from these voltammograms that electrode activation is necessary. Therefore, for all further analysis the electrode was electrochemically activated before each injection using a 50 Hz square-wave waveform of 2 V amplitude for 30 seconds. The DNP-glycine shows two reduction processes at ca. -650 and -800 mV versus Ag/AgCl, respectively, which is in agreement with the cyclic voltammetric behavior reported for polynitroaromatic compounds using macroelectrodes [24,25].

2.2.3.2 Hydrodynamic Voltammetry

Hydrodynamic voltammograms (HDV) were constructed using capillary electrophoresis and reductive electrochemical detection for several DNP-amino acids and anthraquinones, and for the pH 7.0 MES background electrolyte.

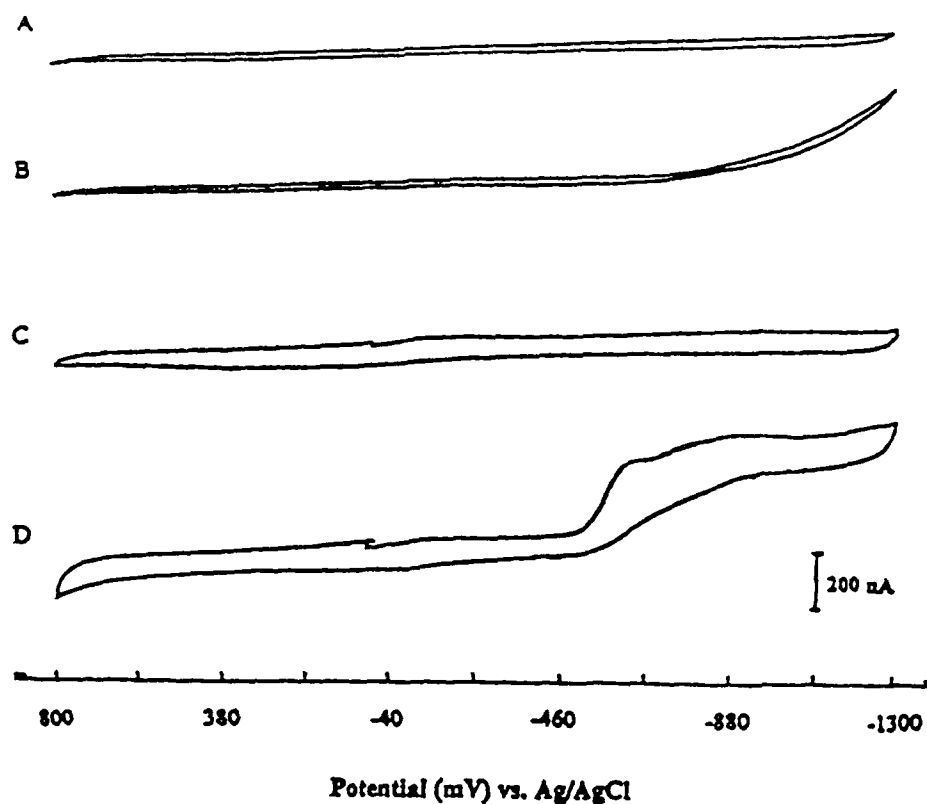


Figure 2.5

Cyclic voltammograms on a bare carbon fiber electrode of 2×10^{-4} M DNP-glycine in 10 mM MES buffer (pH 7). Curves (A) and (C) are voltammograms of the blank buffer before and after electrochemical pretreatment of the carbon fiber electrode, respectively. Curves (B) and (D) show voltammograms of 2×10^{-4} M DNP-glycine before and after electrochemical pretreatment of the carbon fiber.

Figure 2.6 represents a plot of the normalized currents (normalized against the maximum current response in each HDV) versus the applied potential, for (A) background electrolyte and anthraquinone-2-COOH, respectively; and (B) DNP-glycine. The HDV behavior of the DNP glycine was in excellent agreement with the data obtained using CV. It can be seen from Figure 2.6A that at potentials lower than -600 mV there is a dramatic increase in the background current due to the reduction of residual oxygen. The maximum background current measured (11.10 nA) was observed at an applied potential of -1000 mV. At the potentials chosen as the working potentials for anthraquinones (-700 mV) and DNP-amino acids (-800 mV), the background currents were 2.7 and 5.9 nA, respectively. The substantial decrease in background current due to deoxygenation is evident when these values are compared to the background currents measured in a non-deoxygenated buffer at the same potentials (72 and 100 nA). Carbon fiber electrodes possess advantages over conventional size glassy carbon for CE due to their miniature size leading to much lower background currents. A carbon fiber was chosen over a gold/mercury amalgam electrode for this work because it is more rugged and easier to insert in the capillary.

Figure 2.6A shows the HDV of the anthraquinone. The $2\text{H}^+/2\text{e}^-$ reduction occurs at a potential less extreme than that of the derivatised amino acids. On the basis of these studies, working potentials of -800 and -700 mV were used for subsequent reductive CEEC studies of the DNP-amino acids and anthraquinones, respectively.

2.2.3.3 *Analysis of DNP-Amino acids*

The separation and reductive detection of DNP-amino acids was carried out to demonstrate the utility of the system. Figure 2.7 shows the separation of a mixture of 20 μM each of DNP derivatives of glycine, GABA, serine, phenylalanine and tyrosine. It is evident that even at -800 mV a reasonable baseline is obtained, enabling the detection of these compounds. The linearity of this method was evaluated for a series of standards ranging from 1–10 μM (equivalent to 9.8 to 98

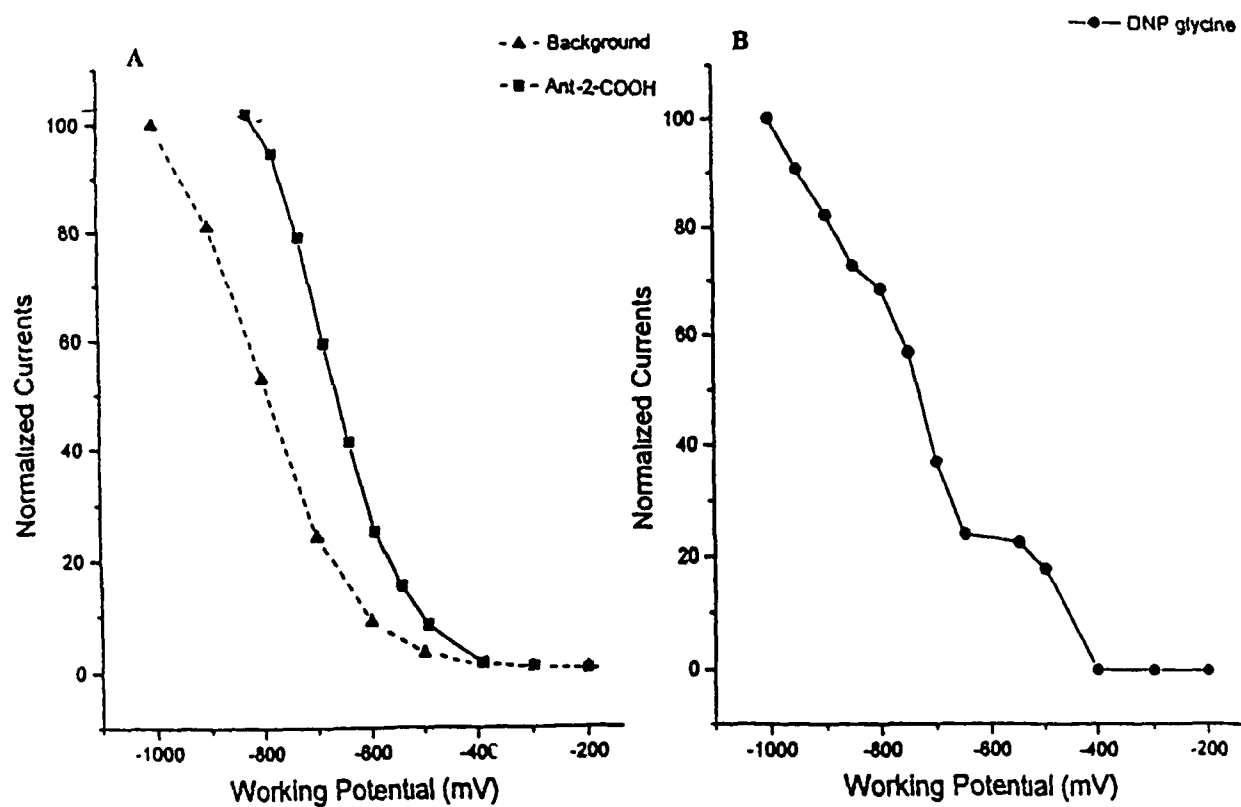


Figure 2.6

Normalized hydrodynamic voltammograms using reductive CEEC of; (A) background buffer, 10 mM MES (pH 7), and 10 μ M anthraquinone-2-carboxylic acid respectively, and (B) 50 μ M DNP-glycine. Separation voltage = 25 kV See text for procedures

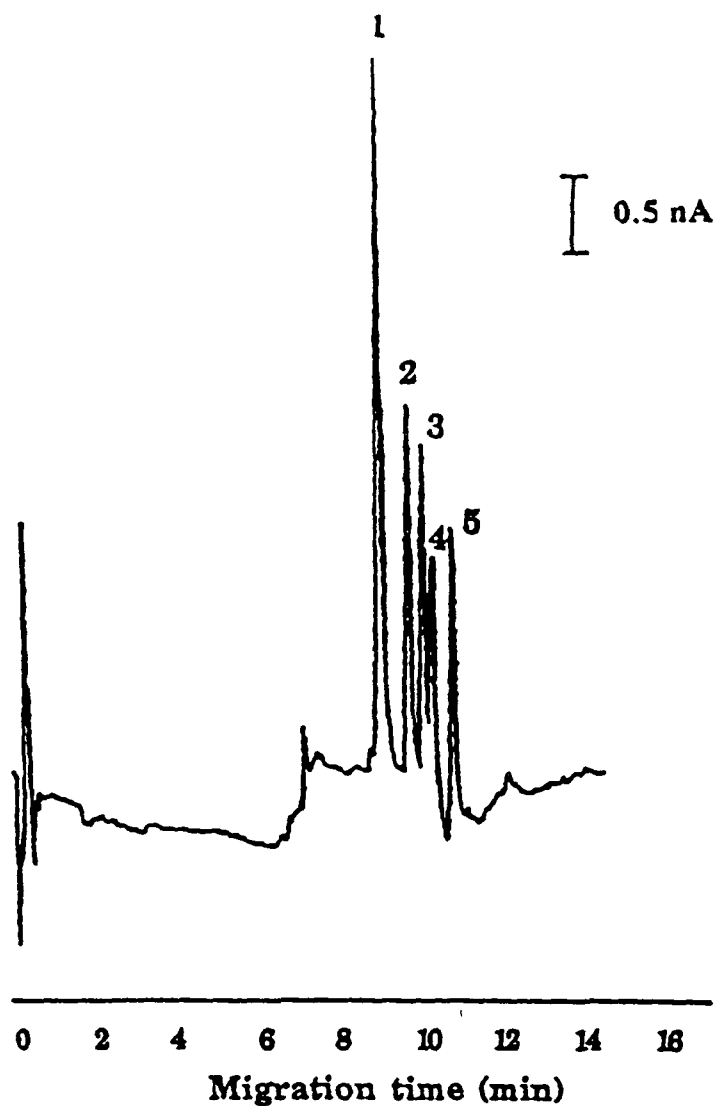


Figure 2.7

Electropherogram of a mixture of 10 μ M each of five DNP-amino acids in 10 mM MES (pH 7) buffer. Peak identities, (1) tyrosine; (2) phenylalanine, (3) serine, (4) GABA, and (5) glycine. Separation voltage = 20 kV. An applied working potential of -800 mV was used.

fmol injected) DNP-GABA. The slope (sensitivity) was $0.41 \mu\text{M/nA}$ with a regression coefficient $r = 0.998$ ($n = 5$). The limit of detection was calculated to be 1.6 fmol at a $S/N = 2$ and is three orders of magnitude lower than that reported by Jacobs and Kissinger using reductive LCEC [24].

The reproducibility of the detector was studied by making several injections of a 196 fmol DNP-GABA standard and measuring the corresponding peak height of the reduction response. This yielded a relative standard deviation of 3.87% ($n=7$). The reproducibility could be further improved by employing an internal standard to minimize variation in injection volume, which is recognized as one of the precision limiting factors in CE [44].

2.2.3.4 Analysis of Anthraquinones

The reduction of the quinone moiety to hydroquinone occurs more readily than that of the reduction of the nitro group, so that the less extreme potential of -700 mV was employed for their detection. More stable baselines were obtained at this working potential. Figure 2.8 shows the reductive electrochemical detection of a mixture of $10 \mu\text{M}$ anthraquinone-2-carboxylic acid and anthraquinone-2-sulfonic acid. The electropherogram demonstrates good resolution and a stable baseline, reinforcing the effectiveness of the system for reductive detection without interference from oxygen. The linearity of response was evaluated for a concentration range of 1 to $10 \mu\text{M}$ (equivalent to 9.8 to 98 fmol injected) anthraquinone-2-carboxylic acid and yielded a slope of $0.293 \mu\text{M/nA}$ with a regression coefficient $r = 0.999$ ($n = 6$). The linearity was also evaluated over a wider concentration range by injecting anthraquinone-2-sulfonic acid standards ranging between 5 and $200 \mu\text{M}$ (equivalent to 0.05 to 1.2 pmol injected). In this case, the regression coefficient was $r = 0.995$ ($n = 10$). The limit of detection was determined to be 1.3 fmol anthraquinone-2-carboxylic acid based on a $S/N = 2$.

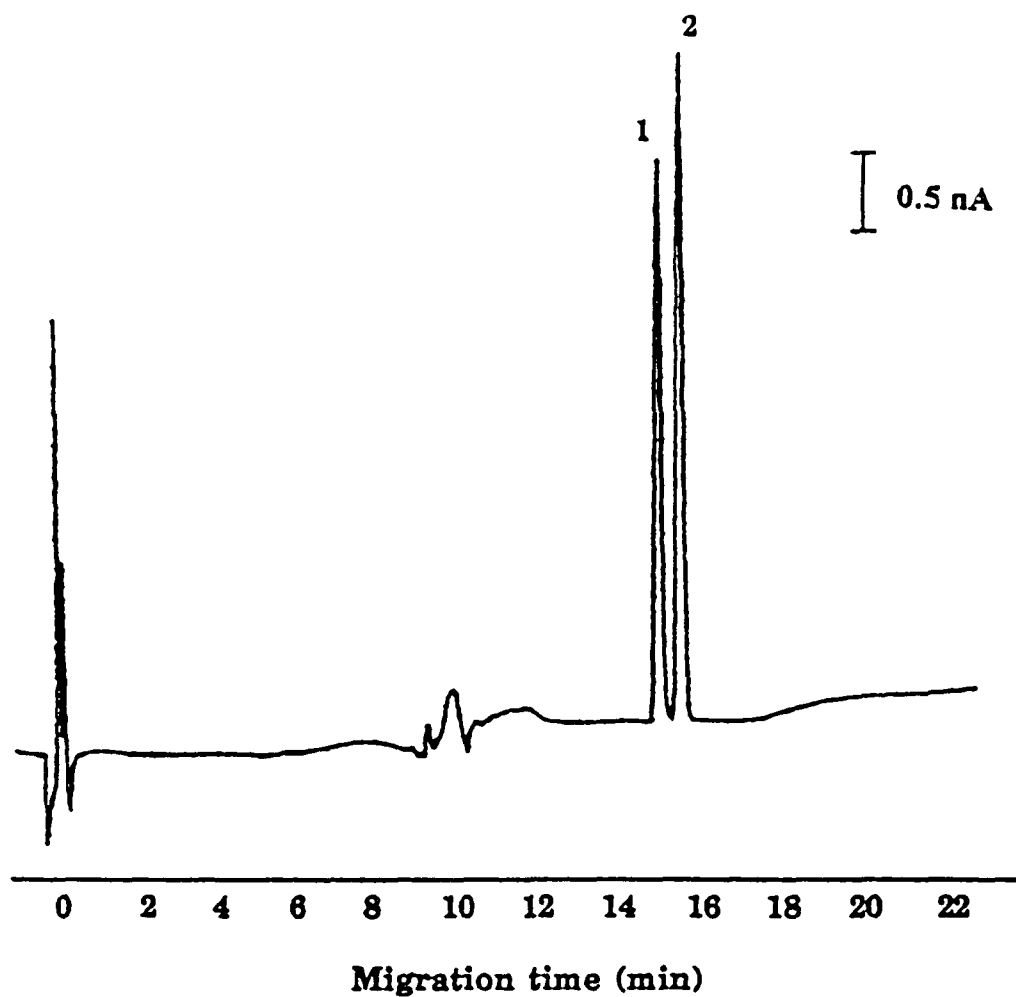


Figure 2.8

Electropherogram of 10 μM (98 fmol injected) each of (1) anthraquinone-2-carboxylic acid, and (2) anthraquinone-2-sulfonic acid. Separation voltage = 15 kV. An applied working potential of -700 mV was used.

These results demonstrate that the precision and sensitivity of this system are as good or better than those of reductive LCEC

2.2.3.5 Determination of Mitomycin C in Human Serum

Mitomycin C, an antineoplastic agent produced by *Streptomyces caespitosus*, contains the quinone moiety within its structure. A good response was obtained for this compound using CEEC at an applied potential of -700 mV. The response was linear between 9.8 and 98 fmol injected with a regression coefficient of $r = 0.999$ ($n = 5$) and a sensitivity of 0.223 $\mu\text{M/nA}$. The limit of detection under the same conditions was found to be 0.77 fmol based on a $S/N = 2$. For this compound, the concentration LOD is about one order of magnitude lower than those obtained using reductive LCEC with a static mercury drop electrode [28]. However, the mass detection limits are three orders of magnitude lower. In initial studies using pH 7.0 buffer, mitomycin C eluted around the same time as the system peak due to oxygen. This peak is more pronounced in serum because of the difficulty of sample deoxygenation. To enhance the separation, sulfobutylether- β -cyclodextrin was added to the run buffer in order to increase the migration time of mitomycin C relative to the system peak. This highly soluble form of cyclodextrin has been shown previously to complex with aromatic compounds [45]. The final separation was achieved using a sodium borate (pH 9) buffer containing 5 mM sulfobutylether- β -cyclodextrin.

Figure 2.9 compares the selectivity of (A) reductive electrochemical detection at an applied working potential of -700 mV with (B) UV detection at a wavelength of 216 nm under the same conditions for a blank serum sample. It is obvious that the strong absorbance of serum compounds at 216 nm makes it impossible to detect mitomycin C. In contrast, the blank serum shows little response when reductive electrochemical detection is employed. The two negative peaks seen in Figure 2.9A at migration times of approximately 12 and 13 min are caused by the discrepancy in

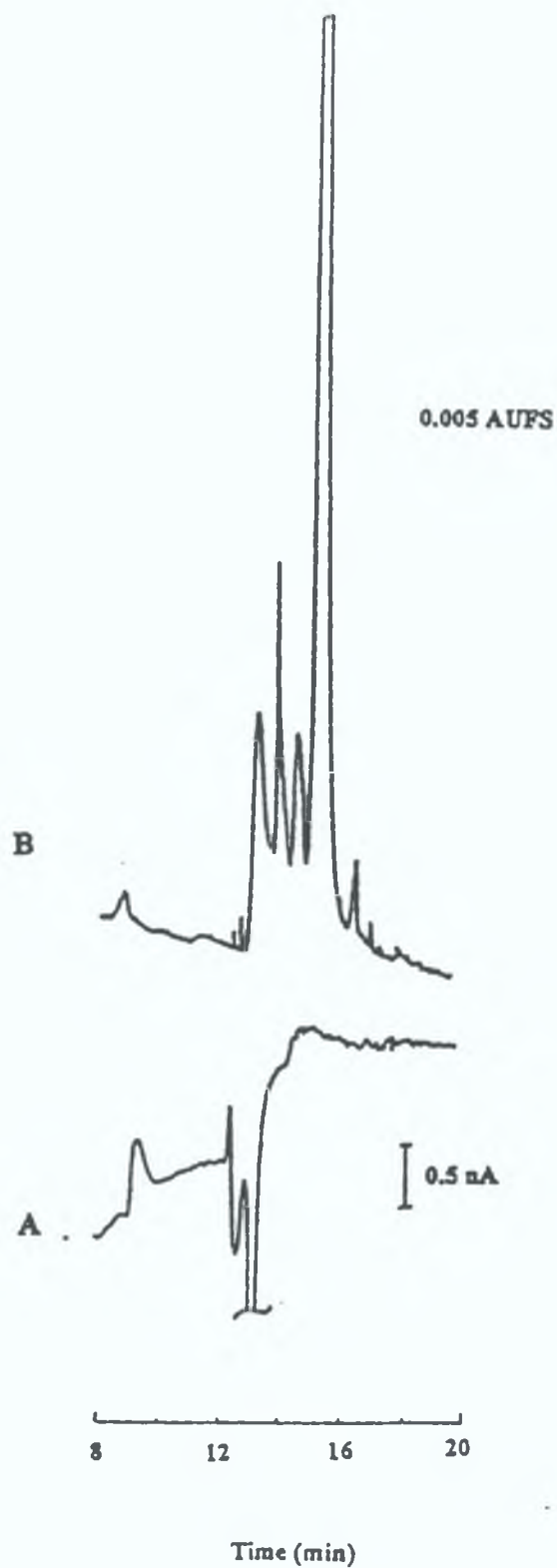


Figure 2.9

Electropherograms of blank serum using (A) reductive electrochemical detection at an applied working potential of -700 mV and (B) UV detection at a wavelength of 216 nm. A sodium borate buffer (pH 9) containing 5 mM sulfobutylether- β -cyclodextrin was used. Separation voltage = 15 kV.

the amount of residual oxygen present in the run buffer and that in the sample. These peaks are also seen with the buffer blank. Figure 2.10 shows an electropherogram of a human serum sample containing 10 $\mu\text{g/mL}$ of mitomycin C, which is readily detected without interference from endogenous compounds by CEEC. The same level could not be detected by CE using UV detection at 216 nm because of endogenous interferences. Spectroscopic detection of 10 $\mu\text{g/mL}$ of mitomycin C at 360 nm was also attempted because this approach has been shown to be more selective than detection at 216 nm. However, due to the low molar absorptivity of the compound at that wavelength and the small path length characteristics of the fused silica capillary, it could not be detected at that level. The selectivity and sensitivity of reductive electrochemical detection in biological samples is convincingly demonstrated by this example.

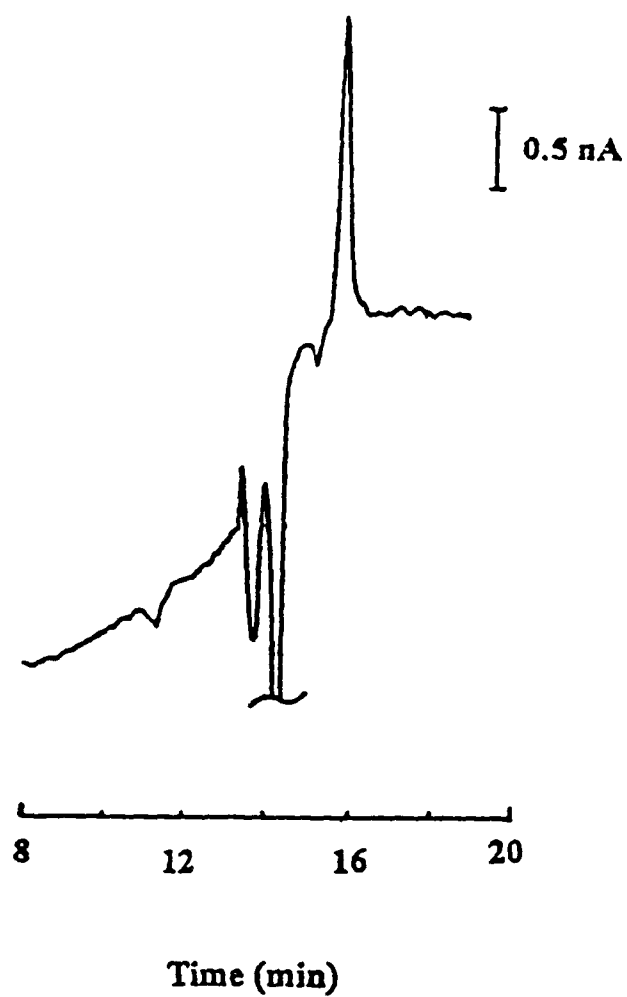


Figure 2.10

Electropherogram of human serum containing 10 $\mu\text{g/mL}$ mitomycin C using electrochemical detection at an applied working potential of -700 mV . A sodium borate buffer (pH 9) containing 5 mM sulfobutylether- β -cyclodextrin was used. Separation voltage = 15 kV

2.2.4 Conclusions

The study has shown the utility of CE with reductive electrochemical detection, and its major advantages over LC with reductive detection have been outlined particularly in terms of rapid and simple set-up and ease of operation. The deoxygenation time is substantially shorter for CEEC (15 min) compared to LCEC (8 hr), and there is no need to replumb the system with stainless steel or to reflux the mobile phase. In addition, the concentration detection limits are very close to those obtainable by LCEC, making it an extremely sensitive and selective technique. CEEC provides additional advantages in those cases where one is sample-limited, such as microdialysis sampling [46,47] or analysis of single cells [48,49]. The utility of CEEC for the analysis of microdialysis samples will be demonstrated in the next section of this chapter. With CE it is also possible to analyze a single 1 μ L sample several times by CE using different separation and detection conditions without a noticeable loss of sample volume. This is in contrast to LC, where typically sample volumes of 1–20 μ L are required for a single analysis. Through a comparison of reductive electrochemical detection with ultraviolet spectrometric detection, the superior sensitivity and selectivity of this system have been demonstrated. This technique could be applied to many other compounds of biological or environmental interest in the future.

2.3 Monitoring of Tryptophan Metabolites in Rat Brain using *in vivo* Microdialysis and Capillary Electrophoresis/Electrochemistry

2.3.1 Introduction

Capillary electrophoresis is a highly efficient separation technique capable of analysing very small volumes. Since the development of modern capillary electrophoresis by Jorgenson and Lukacs [1] the technique has been shown to possess several advantages over both classical electrophoresis and liquid chromatography. The integration of microelectrode detection systems with capillary electrophoresis results in highly efficient and highly sensitive systems capable of analysing very small sample volumes. The utility of capillary electrophoresis/electrochemistry (CEEC) has been demonstrated in the past for easily oxidisable compounds [40,50,51] and more recently for easily reducible compounds [52]. The latest advances in this field were recently reviewed by Ewing et al. [53].

Microdialysis is a bioanalytical sampling technique which has increased in popularity in recent years [54,55] due to its ability to monitor substances from the extracellular space of tissue and organs without significant removal of liquid. It is also possible to introduce substances into the extracellular space without injecting fluid, thus minimising perturbation to the body. The technique allows for continuous sampling and provides protein free samples due to the low molecular weight cut-off of the microdialysis membrane. Most frequently, liquid chromatography has been

employed for the analysis of microdialysis samples. In order to obtain adequate sensitivity, either fluorescence or electrochemical detectors are usually employed.

More recently, CE has been employed for the separation of analytes following microdialysis sampling. Both laser induced fluorescence (LIF) and electrochemical detectors have been employed. CEEC has several significant advantages over liquid chromatography/electrochemical detection (LCEC) for the analysis of microdialysates. These include the ability of CE to handle very small volumes (typically nL injection volumes) and electrochemical detectors to detect very low concentrations of various analytes with a high degree of selectivity. Because of the low sample volume requirement of CE as compared to LCEC, lower microdialysis perfusion rates can be employed to obtain higher recovery and/or samples analysed more frequently resulting in higher temporal resolution. The advantages of CEEC for the analysis of microdialysis samples have been demonstrated for example in the investigation of the pharmacokinetics of L-Dopa [47], and the release of excitatory amino acids from the frontoparietal cortex of the rat brain [46]. Microdialysis has been used extensively for the monitoring of neurochemical events. In particular, the role of certain amino acids and their metabolites as neuromessengers has been extensively studied using microdialysis. LCEC or LC with laser induced fluorescence (LIF) have generally been employed for the detection of the amino acids. In recent years there has been a surge in interest in the neurological role of the metabolites of tryptophan. Tryptophan (Trp) is hydroxylated *in vivo* to yield 5-hydroxytryptophan (5-HTP). Subsequent decarboxylation of 5-HTP yields the widely studied neurotransmitter, serotonin [56,57]. Another biochemical pathway, known as the 'kynurenine pathway', gives rise to another set of metabolites

collectively known as 'kynurenines', and accounts for approximately 90 % of tryptophan metabolism in mammals. The most widely investigated metabolites are kynurenic acid (KA) and quinolinic acid (QA). Kynurenic acid is believed to act as a non-selective antagonist of excitatory amino acid receptors and to attenuate the neuronal excitation induced by agonists of N-methyl-D- aspartate (NMDA), including quinolinic acid. The basal levels of KA and QA have been reported to be in the low nM range in the ECF of rats and slightly higher in humans [58,59]. Most reports on the metabolism of these compounds employ microdialysis and LC with fluorescence or electrochemical detection. Typical experiments investigate the effect of administration of metabolic precursors including tryptophan itself [57,63], 5-hydroxytryptophan [56], kynurenine [59-61], and an analogue of kynurenine called nicotynylalanine [58,62]. In a recent report by Hasiguti et al [64], the relationship of 5-HTP and L-Dopa levels was investigated by looking at the effects of one upon the other. All studies involving tryptophan metabolism mentioned above employed microdialysis and liquid chromatography with electrochemical or fluorescence detection.

It was the purpose of this study to evaluate the use of CEEC for the analysis of microdialysis samples for tryptophan metabolites. The use of CEEC for the analysis of microdialysis samples offers several advantages, including high sensitivity and selectivity, improved temporal resolution over LCEC techniques, and the ability to analyse samples several times due to the small sample volume requirements of the technique.

2.3.2 Experimental

2.3.2.1 *Reagents and materials*

Tryptophan and its metabolites were all purchased from Sigma (St. Louis, MO). All other chemicals were used as received. Solutions were prepared in NANOpure water (Sybron-Barnstead, Boston, MA) and passed through a membrane filter (0.2 μm pore size) before use. The separation buffer consisted of 20 mM sodium borate (pH 9.0). This was used as the electrolyte throughout most of the study. When a higher pH was required, the solution was adjusted to the appropriate pH using sodium hydroxide. All stock solutions of tryptophan and its metabolites were prepared daily in water and stored at 4°C.

2.3.2.2 *Apparatus*

The CEEC system and the Nafion joint construction have been described in detail in Section 2.2.2 of this chapter. In this study, the non-modified system was employed, which excludes the necessity for nitrogen lines and complete sealing of the system. Apart from these differences, the system was identical to that described in Section 2.2.2. Polyimide-coated fused silica capillary columns (360 μm o.d., 50 μm i.d.) were obtained from Polymicro Technologies (Phoenix, AZ), and capillary lengths of between 70 and 90 cm were used. Sample introduction was accomplished using a laboratory-built pressure injection system. The injection volume was calculated to be 9.8 nL using the continuous fill mode by recording the time required for the sample to reach the detector. During the analysis of the rat brain microdialysates, a

Spectra-Physics (Data Jet) integrator was employed to measure peak heights for the various components

Cylindrical carbon fibre microelectrodes were constructed as outlined in Section 2.2.2 of this chapter using 33 μm diameter fibres (AVCO Specialty Products, Lowell, MA)

2.3.2.3 *Cyclic Voltammetry*

All cyclic voltammetry experiments were carried out using a model CySy-1 computerised electrochemical analyser (Cypress Systems, Lawrence, KS). A three-electrode cell was used which consisted of a carbon fibre or glassy carbon working electrode, a Ag/AgCl reference electrode and a platinum counter electrode. All cyclic voltammograms were carried out in 20 mM sodium borate (pH 9.0) buffer using a scan rate of 100 mVs^{-1} .

2.3.2.4 *Hydrodynamic Voltammetry*

Hydrodynamic voltammograms were obtained by repeated injections of standards while varying the working potential and measuring the resultant peak currents at 100 mV intervals. Normalised currents (normalised as a percentage of the highest current reading recorded) were then plotted versus the working potential. The separation was performed in a 20 mM sodium borate buffer, pH 9.0 with an applied separating voltage of 20 kV. The effective capillary length was approximately 80 cm.

2 3 2 5 *Implantation of the Microdialysis Probe*

Male Sprague-Dawley rats (290-400 g) were anaesthetised with urethane (1.5 g/Kg i.p.) and maintained under anaesthesia during the whole experiment. Anaesthetised rats were placed in a stereotaxic frame and placed on a heating pad at 37 °C. CMA/12, 3 mm dialysis probes were implanted into the hippocampus of the rat brain at the coordinates 4.8 mm posterior to the bregma, 4.8 mm lateral to the midline and 5.8 mm ventral to the skull surface.

2 3 2 6 *Microdialysis Procedures*

The microdialysis probes were perfused with artificial cerebrospinal fluid (ACSF) (120 mM NaCl, 20 mM NaHCO₃, 3 mM KCl, 1.2 mM CaCl₂, 1.0 mM MgCl₂, and 0.25 mM NaH₂PO₄) at a flow rate of 0.25 µl/min. Microdialysate samples were collected at 15 minute intervals. Probes were calibrated *in vitro* by placing them in a standard mixture of the tryptophan metabolites. The dialysates were collected and analysed every 15 minutes and the relative recovery calculated for each compound. All dialysates were injected into the CEEC system directly.

2 3 2 7 *Systemic Precursor Loading Studies*

Two groups of rats were systemically administered tryptophan (100 mg/Kg i.p.) or kynurenine (450 mg/Kg i.p.). Baseline fractions were collected beginning approximately three hours after probe implantation. At least four 15-minute fractions were collected before any manipulation was attempted. Microdialysates were collected up to eight hours in the case of tryptophan loading experiments and up to five hours in the case of kynurenine loading experiments.

2.3.3 Results and Discussion

2.3.3.1 *Cyclic Voltammetry*

Cyclic voltammograms of tryptophan and the metabolites of interest were run on both glassy carbon and carbon fibre electrodes using a 20 mM borate buffer, pH 9.0. This was also the optimal CE running buffer. The tryptophan metabolites exhibited a wide range of half-wave potentials. These are summarised in Table 2.1. The wide potential window presents difficulties when attempting to choose an optimum working potential for the subsequent CEEC studies. In particular the detection of kynurenic acid is problematic due to its very high half-wave potential. In fact, kynurenic acid was previously stated to be non electroactive [65]. Figure 2.11 compares the voltammetry of tryptophan and kynurenic acid on a glassy carbon electrode. All cyclic voltammograms were also carried out at carbon fibre electrodes for comparative purposes, and they showed similar behaviour to that obtained at glassy carbon. From Table 2.1 it can be seen that compounds such as 3-hydroxykynurenine, 3-hydroxyanthranilic acid, and 5-hydroxyanthranilic acid exhibit very low detection potentials (as low as +150 mV) while a potential of at least +1100 mV is required to yield a useful response for kynurenic acid. Hydrodynamic voltammograms were carried out using CEEC to optimise the working potential for further studies.

2.3.3.2 *Hydrodynamic Voltammetry*

Since there is normally some discrepancy between the half-wave potential measured from the cyclic voltammograms and the optimum amperometric working potential in a flowing stream, mainly due to differences in mass transport, it is very important

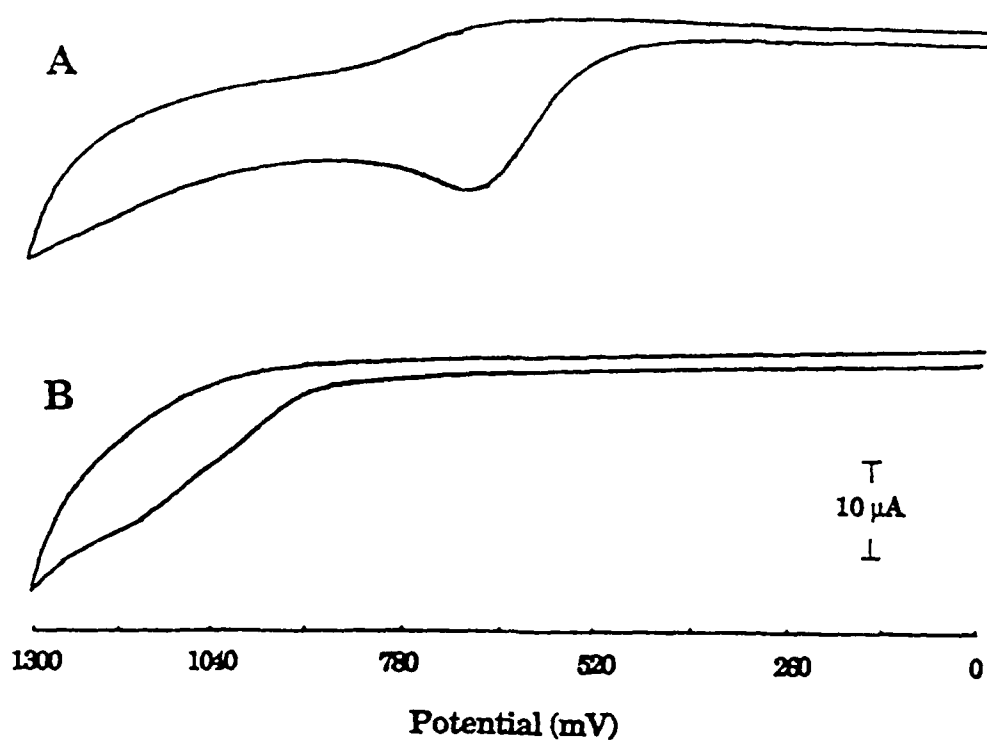


Figure 2.11

Cyclic voltammograms of 1 mM (A) tryptophan and, (B) kynurenic acid at a glassy carbon electrode. A 20 mM sodium borate pH 9.0 buffer was used. Scan rate = 100 mV/s

<i>Compound</i>	<i>Half-wave Potential(s), mV</i>
Tryptophan	590 mV
Kynurenine	760 mV
3-Hydroxykynurenine	100 mV
Anthranilic acid	690 mV
3-Hydroxyanthranilic acid	160 and 830 mV
5-Hydroxyanthranilic acid	95 mV
Kynurenic acid	1015 mV
Xanthurenic acid	460 mV

Table 2.1

The half-wave potentials of the tryptophan metabolites vs Ag/AgCl using a glassy carbon electrode
Experimental conditions as in Figure 2.11

to optimise the working potential under hydrodynamic conditions. This is particularly true of CEEC since one must consider the effect the high voltage applied across the capillary has on the working electrode, especially for on-column electrochemical detection. Therefore, hydrodynamic voltammograms were recorded as outlined earlier. Figure 2.12 shows the results obtained for (A) 20 μ M tryptophan and (B) 20 μ M kynurenic acid. It is clearly evident that a useful analytical signal can be obtained for tryptophan at potentials above +600 mV and the HDV reaches a plateau for potentials above +850 mV. However, no response for kynurenic acid was obtained until a potential of +850 mV was reached. At this potential the ratio of current response for tryptophan (20 μ M) and kynurenic acid (20 μ M) is 17:1 in favour of tryptophan. To obtain a useful signal for kynurenic acid it is necessary to employ a working potential of +1100 mV. However, at potentials above +950 mV the background current increases significantly due to oxidation of the aqueous buffer components and activation of the electrode substrate leading to higher current densities, resulting in noisy baselines and a degree of baseline drift. Figure 2.13 demonstrates that at a working potential of +900 mV no response was obtained for KA (Figure 2.13A). At a potential of +1000 mV (Figure 2.13B) a response is seen for the KA present. However, appreciable change in the quality of the baseline at the more extreme potential is also evident, which is even more evident at higher potentials necessary to produce a sensitive response for KA. Therefore, a working potential of +900 mV was used for most subsequent studies except for studies where kynurenic acid was the sole analyte of interest and in that case higher potentials were employed.

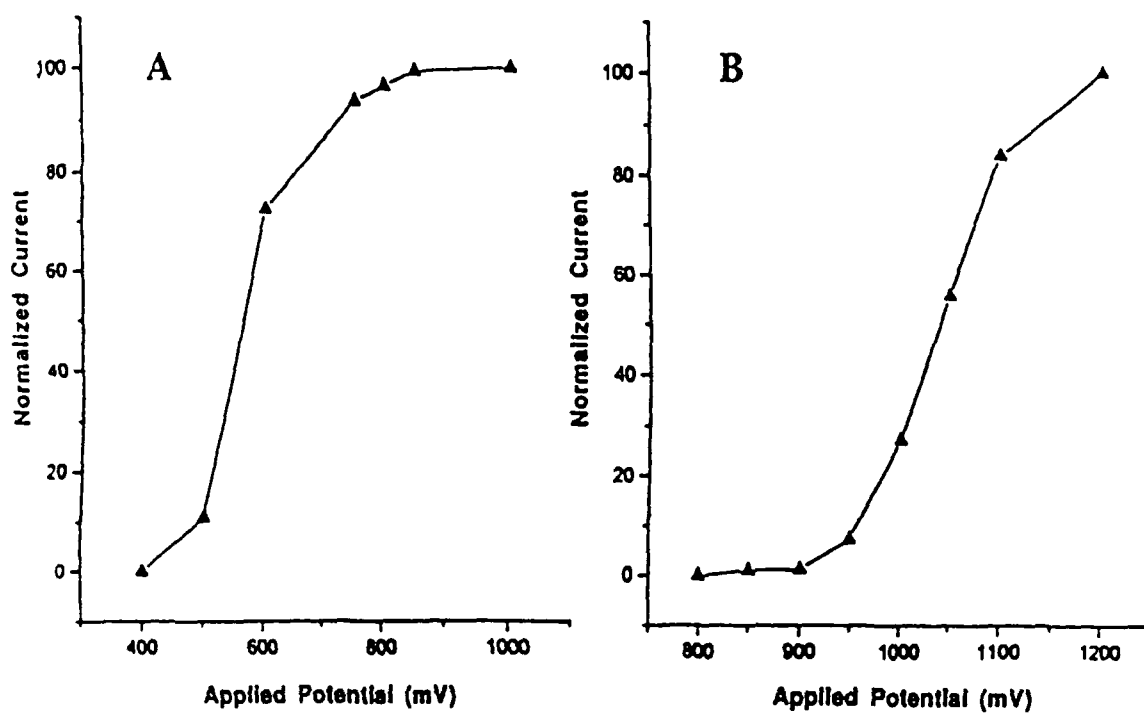


Figure 2.12

Hydrodynamic voltammograms of 20 μM (A) tryptophan and, (B) kynurenic acid, using CEEC. A 20mM sodium borate buffer pH 9.0 was used. Effective capillary length = 80 cm. Capillary diameter = 50 μm . Separating voltage = 20 kV.

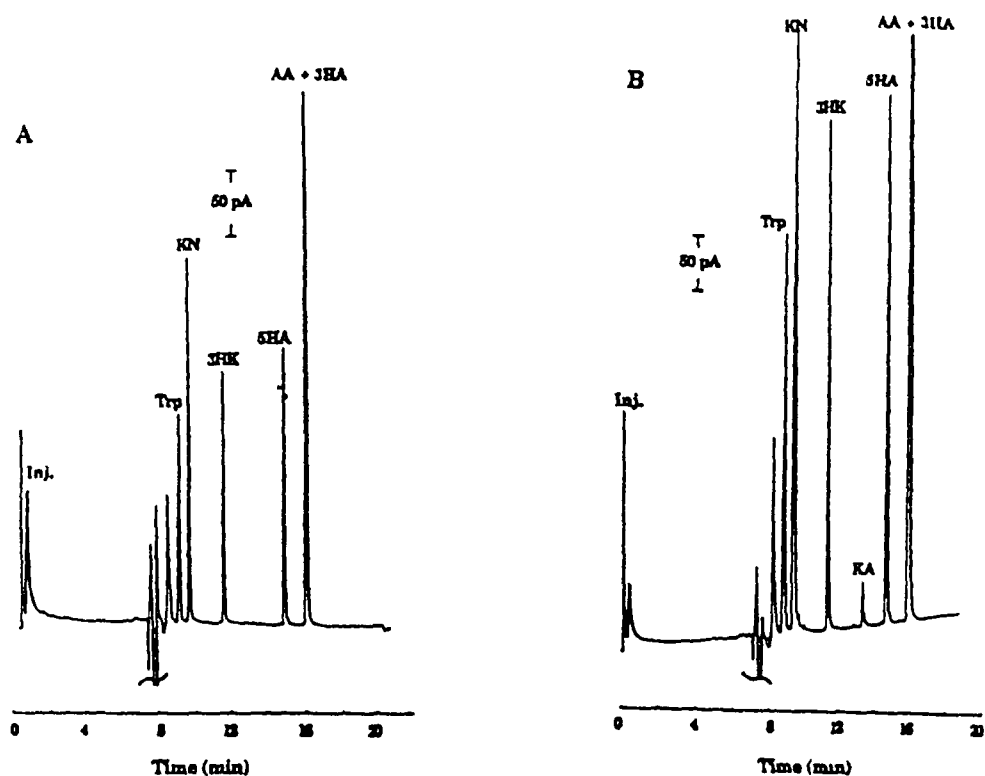


Figure 2.13

Electropherograms of a standard mixture of tryptophan metabolites containing $1\ \mu\text{M}$ each of tryptophan (TRP), kynurenine (KN), 3-hydroxykynurenine (3HK), anthranilic acid (AA), 3-hydroxyanthranilic acid (3HA), and 5-hydroxyanthranilic acid (5HA) and $2\ \mu\text{M}$ kynurenic acid (KA). Working potential of (A) $+900\ \text{mV}$ and (B) $+1000\ \text{mV}$ were applied. Other conditions as in Figure 2.12

The effect of pH on the separation of the tryptophan metabolites was investigated. Most of the more slowly migrating compounds (higher negative charge/mass ratio) were resolved using a 10 mM MES buffer, pH 7.0. However, both tryptophan and kynurenine eluted with the system (neutral) peak. However, by using a 10 mM sodium borate buffer at a pH of 9.0 tryptophan and kynurenine possessed a net negative charge and resolution was further improved by raising the ionic strength of the borate buffer to 20 mM which suppressed the capillary wall zeta potential and therefore the electroosmotic flow. This study demonstrates the high sensitivity of capillary electrophoresis to changes in pH, and the importance of these parameters when trying to resolve closely related compounds. The separation of kynurenine and tryptophan from the system peak is crucial for the analysis of rat brain microdialysates, since several endogenous compounds, including high concentrations of various salts, commonly elute with the system peak during the analysis of microdialysates. Inadequate resolution of analytes from the system peak would undoubtedly render their identification and quantification impossible.

Raising the ionic strength and/or the pH of the running buffer had a detrimental effect on the efficiency of the xanthurenic acid peak. This metabolite contains an aromatic carboxyl group and two phenolic groups. At high pH it will have a large net negative charge and consequently a very negative electrophoretic mobility. The loss in efficiency is suspected to be due to a combination of its long migration time and on-column chemical oxidation. Therefore, for subsequent analyses, a 20 mM sodium borate buffer, pH 9.0, was employed. Under these conditions anthranilic

acid and 3-hydroxyanthranilic acid were found to coelute. If the pH was increased to pH 9.6 the two peaks could be resolved. However, there was an apparent loss in separation efficiency and as much as a 30 % loss in peak height. Figure 2.14 illustrates this effect by comparing electropherograms of the same tryptophan metabolite mixture run at (A) pH 9.0 and (B) pH 9.6, respectively. For this reason the pH 9.0 buffer was used in subsequent studies. Better resolution of these compounds was observed for the analysis of microdialysate samples due to the inherently high salt concentration of the dialysate which suppresses the capillary wall zeta potential and consequently the electroosmotic flow.

2.3.3.4 *Analytical Characterisation*

The analysis of microdialysates is a very demanding area of analytical chemistry due to the inherent sample limitations both in terms of volume and concentration. A highly sensitive technique that is capable of handling ultrasmall sample volumes is required. CEEC is ideally suited to these challenges since CE is capable of high efficiency separations of ultrasmall volumes, typically nL, and microelectrochemical detection has long been recognised as one of the most sensitive modes of detection available to the analytical chemist and is also easily miniaturised without a loss in sensitivity. However, even under optimised conditions, some CEEC systems fail to reach the limits of detection necessary for the determination of analytes in microdialysates. Therefore, the system reported here was characterised under the optimum CEEC conditions outlined above, in an effort to assess its potential for analysis of tryptophan metabolites in rat brain microdialysate.

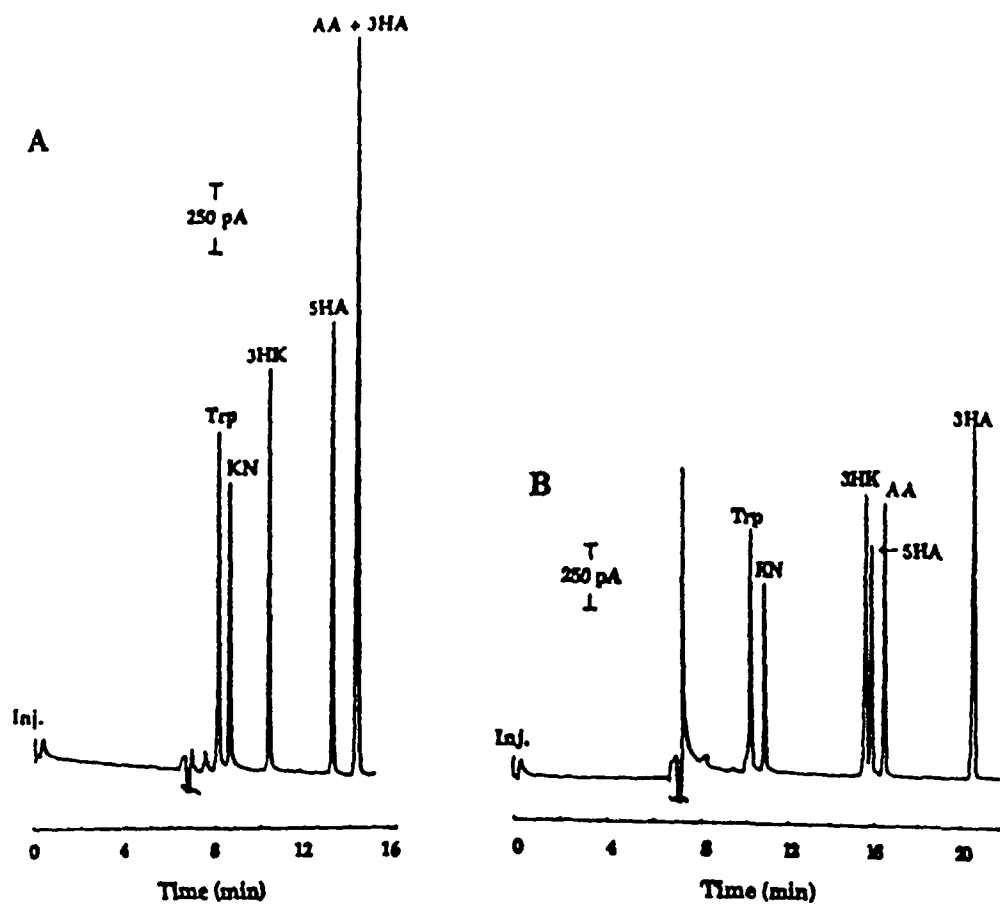


Figure 2.14

Electropherograms of a standard mixture of tryptophan metabolites containing $5 \mu\text{M}$ each of Trp, KN, 3HK, AA, 3HA, 5HA, and $10 \mu\text{M}$ KA. The electropherograms were run in a 20 mM sodium borate buffer at a pH of (A) 9.0 , and (B) 9.6 . A working potential of $+900 \text{ mV}$ was used. All other conditions as in Figure 2.12.

The system exhibited excellent linearity over a wide concentration range. For a series of kynurenine standards ranging from 0.5 to 100 μM (equivalent to 4.9 to 980 fmol injected) a slope of 0.22 $\mu\text{M}/\text{nA}$ and a regression coefficient, $r = 0.9992$ ($n=12$) was obtained. The reproducibility of the signal was evaluated by making repetitive injections of a 10 μM (98 fmol injected) kynurenine standard and measuring the resultant peak height of the oxidative response. This yielded a relative standard deviation of 4.54 % ($n=11$). No electrochemical activation of the carbon fibre between injections was performed, since no passivation of the carbon fibre was evident following continuous use over a period of several hours. However, electrochemical activation of the carbon fibre was necessary before its initial use. Failure to do so resulted in slower electrode kinetics which was evident during cyclic voltammetric studies.

The limits of detection for tryptophan metabolites was evaluated for each compound at a $S/N=2$ using a working potential of +900 mV in all cases except for kynurenic acid for which the higher potential of +1100 mV was used. A summary of the results obtained is presented in Table 2.2. Very low limits of detection, generally in the low attomole region, were obtained for most of the metabolites. The higher LOD exhibited by kynurenic acid is attributed to the higher baseline noise and higher oxidation potential. It is apparent from these results that the system may be sensitive enough for the analysis of tryptophan metabolites in rat brain microdialysates.

<i>Compound</i>	<i>Concentration Limit of Detection, nM</i>	<i>Mass Limit of Detection, amol</i>
Tryptophan	4.8 nM	46 amol
Kynurenine	3.1 nM	30 amol
3-Hydroxykynurenine	0.4 nM	4 amol
Anthranilic acid	3.3 nM	33 amol
3-Hydroxyanthranilic acid	6.0 nM	59 amol
5-Hydroxyanthranilic acid	0.2 nM	2 amol
Kynurenic acid	22.2 nM	218 amol
Xanthurenic acid	0.6 nM	6 amol

Table 2.2

Concentration and mass limits of detection of the tryptophan metabolites using CEEC. A working potential of + 900 mV was used for all compounds except for kynurenic acid where + 1100 mV was employed. All other conditions as in Figure 2.12.

2 3 3 5 *Analysis of Rat Brain Microdialysate using CEEC*

In this study the utility of CEEC for monitoring tryptophan metabolites *in vivo* was demonstrated. The effect of intraperitoneal administration of tryptophan and kynurenine, respectively, on the concentration of related metabolites in the extracellular fluid of the rat brain hippocampus was studied. Capillary electrophoresis is ideally suited to microvolume analyses since very low injection volumes are required. Therefore very slow perfusion flow rates were employed (0.25 $\mu\text{L}/\text{min}$) resulting in high relative recovery values in contrast to previous reports where LC was used to analyse the microdialysis samples. Using this very slow perfusion flow rate, the relative recovery of tryptophan was calculated to be 72.5 % ($n=5$), in contrast to a previously reported recovery of 19 % using a perfusion flow rate of 2 $\mu\text{L}/\text{min}$ [66]. Similarly, percentage recovery values for kynurenine (83.8 %), 3-hydroxykynurenine (43.2 %), 5-hydroxykynurenine (34.8 %), and anthranilic acid (62.4 %), were higher than those reported previously.

In agreement with previous reports, it was found that immediately on implantation of the microdialysis probe, the level of endogenous substances in the perfusate was high. For this reason, the probe was perfused for a period of at least three hours before sampling was commenced, after which time baseline fractions were collected at 15 minute intervals for at least a one hour period before any manipulation was carried out. Tryptophan (100 mg/Kg) was administered to the animal intraperitoneally and the resultant changes in extracellular concentrations of its metabolites were monitored over a six hour period. Figure 2.15 shows an electropherogram of microdialysates collected before Trp loading and also near the

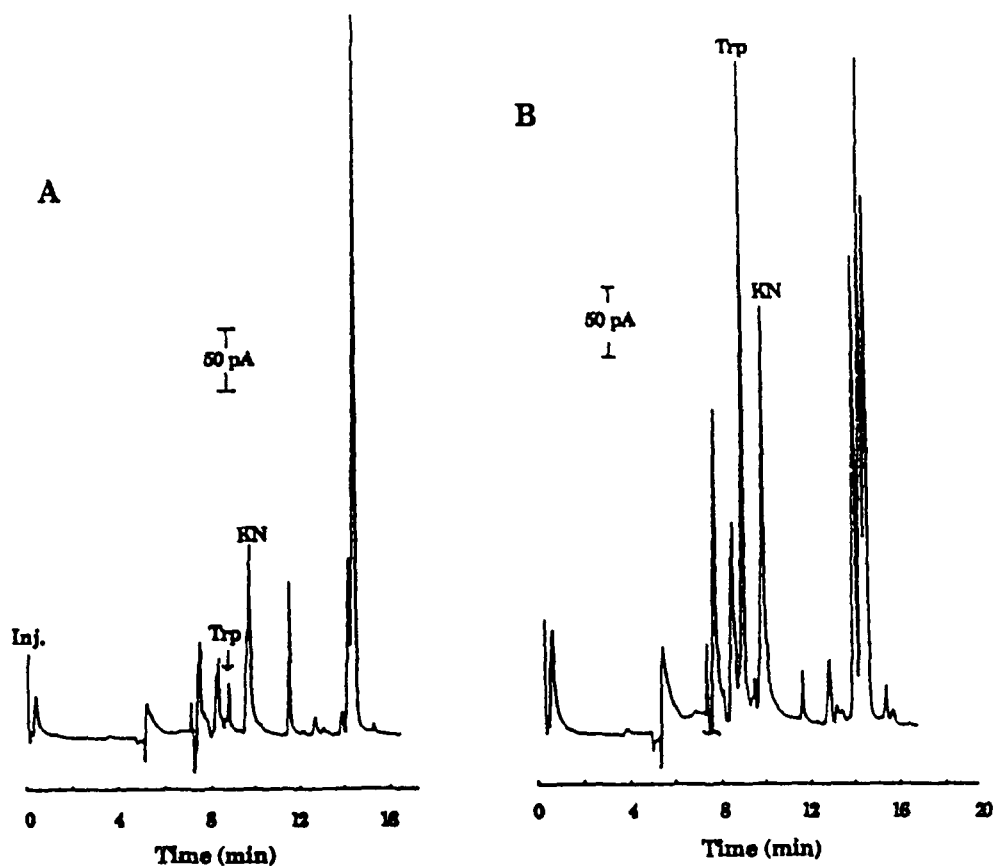


Figure 2.15

Electropherograms of *in vivo* microdialysis samples taken from the hippocampus region of the brain of an anaesthetised rat. (A) Microdialysate taken before tryptophan administration and (B) microdialysate taken after Trp administration (100 mg/kg i.p.) near the maximum ECF concentration of Trp. The figure demonstrates the increase in both Trp and KN concentrations. Working potential = +900 mV. Other conditions as in Figure 2.12.

maximum ECF concentration of Trp. This clearly illustrates the increase in tryptophan concentration and subsequently kynurenine, in the ECF of the hippocampus region. In each experiment it was observed that the tryptophan concentration increased 3-4 fold reaching a maximum concentration of 2-3 μM ($n=3$). This maximum concentration was reached approximately 90 minutes after the systemic administration. This can be seen from Figure 2.16A. The tryptophan metabolite, kynurenine (KN), reached a maximum concentration (1.3 μM , $n=3$) approximately 60 minutes after the tryptophan maximum was reached as can be seen in Figure 2.16B. Other tryptophan metabolites were present in such low concentrations that it was difficult to unambiguously monitor their behaviour. However, by carefully optimising the system for any given metabolite, it may be possible to monitor its behaviour using this system. Kynurenic acid (KA) could not be detected due to reasons discussed earlier. According to previous reports, a maximum KA concentration should be obtained in the brain ECF approximately 6 hours after tryptophan administration.

Administration of kynurenine, the bioprecursor of kynurenic acid has previously been reported to increase the ECF kynurenic acid levels [61-63] and reach a maximum concentration approximately 2 hours after administration. Kynurenine loading experiments were also carried out in this study to demonstrate the transport of this compound across the blood-brain barrier. Kynurenine (450 mg/Kg) was administered intraperitoneally. This caused a more than 30-fold increase in the kynurenine ECF concentration. Figure 2.17 shows electropherograms of microdialysates collected 30 minutes after KN loading, and also near the maximum

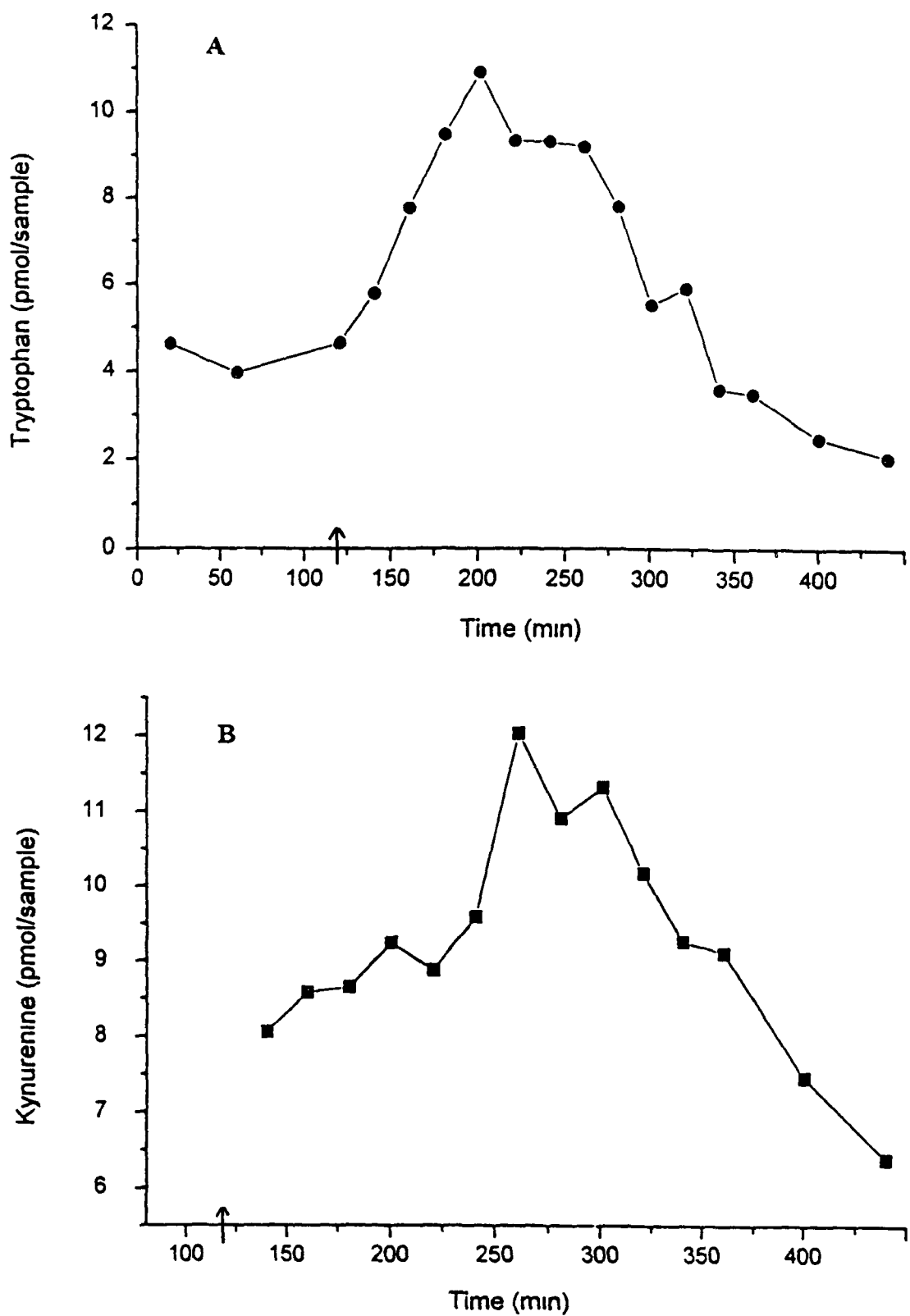


Figure 2.16

A plot of ECF concentration against time for (A) tryptophan and, (B) kynurenine, for a tryptophan loading experiment (100 mg/kg i.p). The arrows indicate the time of Trp administration. Working potential = +900 mV. All other conditions as in Figure 2.12

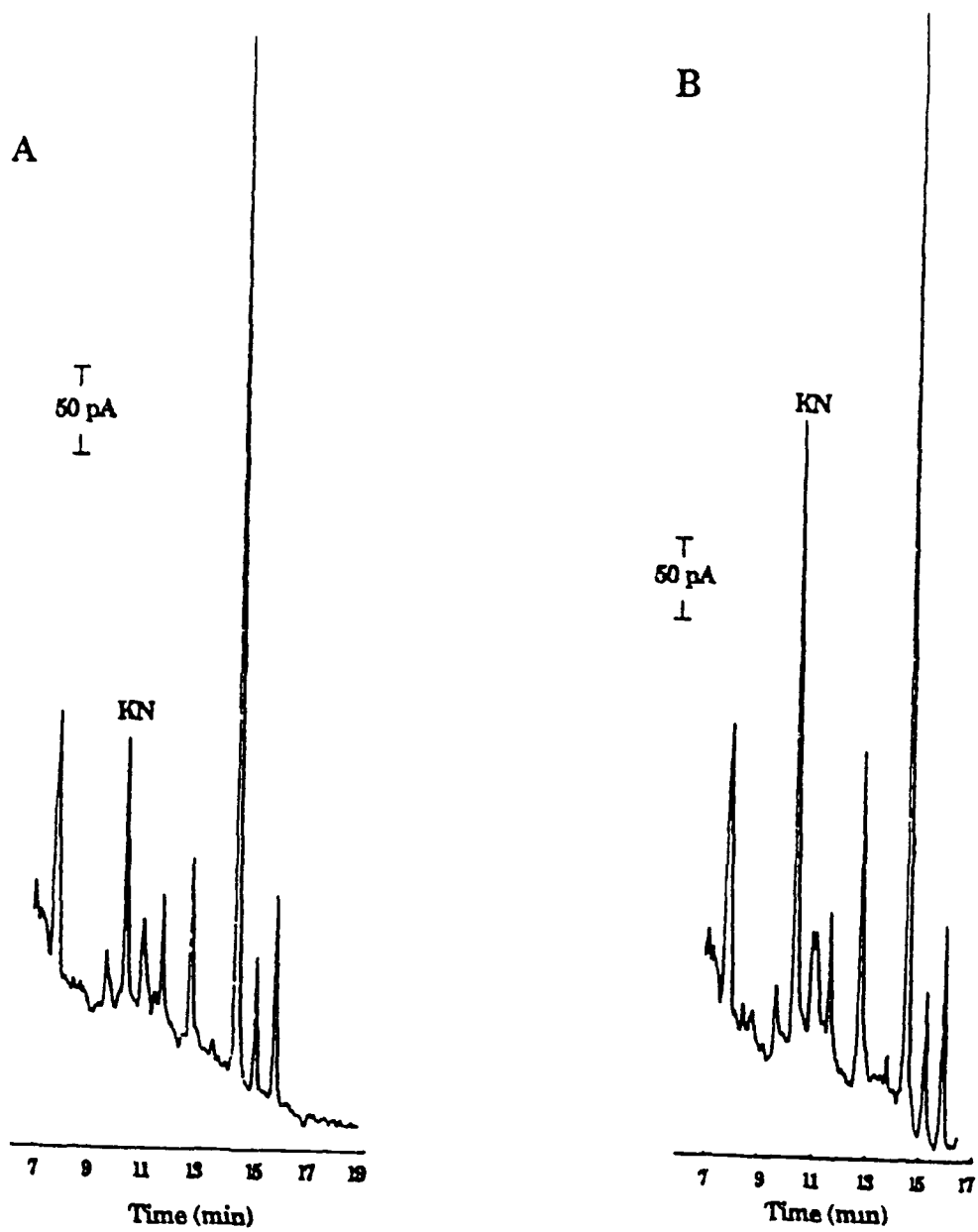


Figure 2.17

Electropherograms of *in vivo* microdialysis samples taken from the hippocampus region of the brain of an anaesthetised rat (A) 30 minutes after i.p. administration of 450 mg/kg KN and (B) near the maximum ECF concentration of KN. Working potential = + 900 mV. Other conditions as in Figure 2.12.

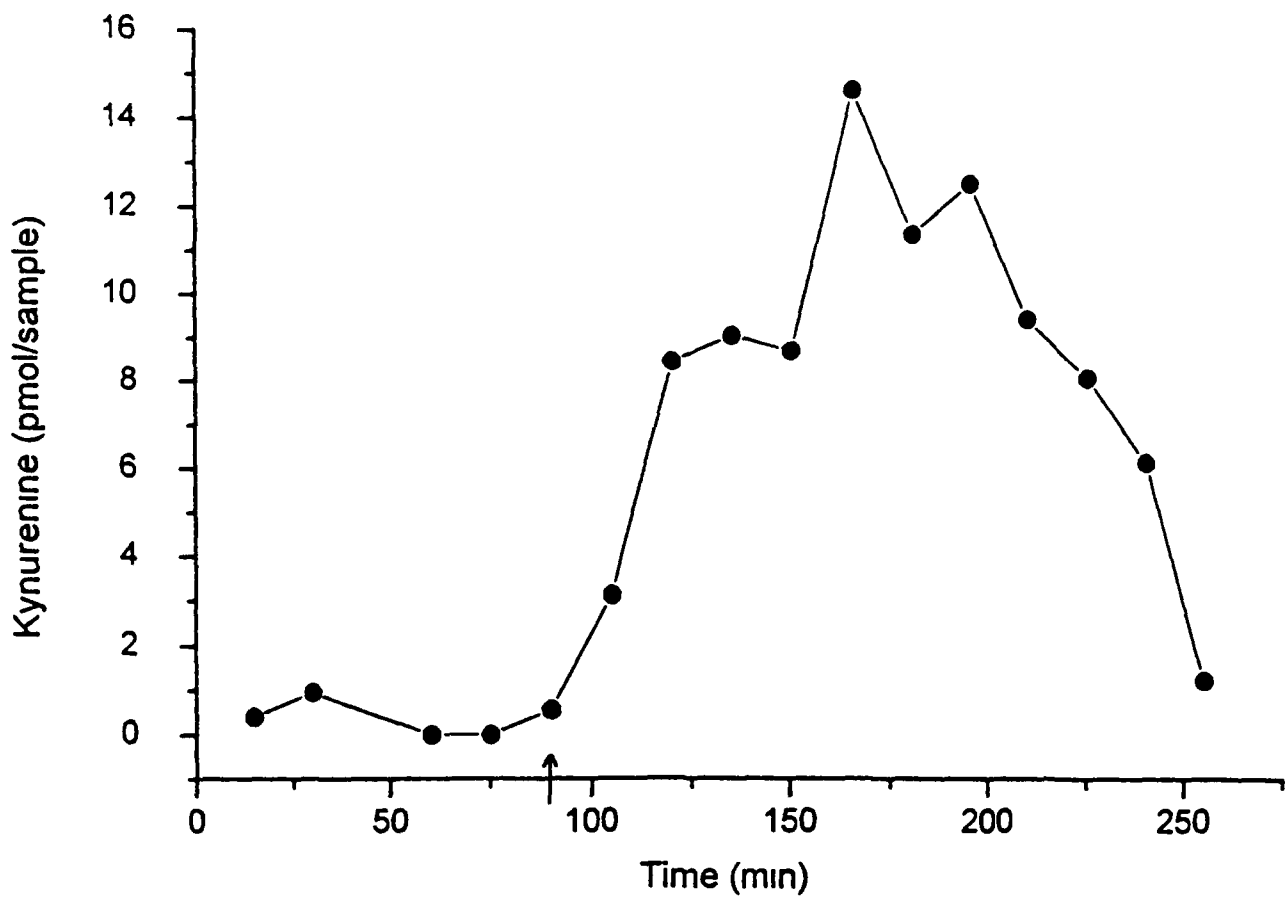


Figure 2.18

A plot of the ECF KN concentration against time for a KN loading (450 mg/kg i.p.) experiment. The arrow indicates the time of KN i.p. administration. Working potential = +900 mV. Other conditions as in Figure 2.

KN concentration The maximum concentration of approximately 4 μM was reached 75 minutes after administration, as can be seen from Figure 2.18

Each peak was identified on the basis of migration time comparisons and standard addition experiments. Voltammetric characterisation was also used to verify the identity of the kynurenine peak. This was done by calculating the current ratios for 900/950 mV and 800/850 mV, respectively, for both the microdialysate and a kynurenine standard. The current ratios for 900/950 mV were calculated to be 0.95 and 0.98 for the microdialysate and standard, respectively. Similarly, the ratios calculated for 800/850 mV were 0.65 and 0.62 for the sample and standard, respectively. This helped to verify the identity of the peak along with the other criteria used including migration time, the electropherogram profile, and standard spiking.

2.3.4 Conclusions

In this study, the use of CEEC for monitoring *in vivo* microdialysis samples for tryptophan metabolites has been demonstrated. Some of the advantages it has over LCEC in terms of lower sample volume requirements allowing for greater temporal resolution have also been discussed. The high sensitivity (attomole detection limits) of the technique is essential for monitoring *in vivo* microdialysis samples since they are generally both volume and concentration limited. It is foreseen that this technique will be used extensively in the future for monitoring microdialysis samples taken from various tissues and organs.

2.4 References

- 1 J W Jorgenson and K D Lukacs, *Anal Chem* , **53** (1981) 1298
- 2 R A Wallingford and A G Ewing, *Anal Chem* , **59** (1987) 1762
- 3 X Huang and R N Zare, *Anal Chem* , **61** (1989) 98
- 4 T J O' Shea, R D Greenhagen, S M Lunte, C E Lunte, M R Smyth, D M Radzik and N Watanabe, *J Chromatogr* , **593** (1992) 305
- 5 I Chih and C W Whang , *J Chromatogr* , **644** (1993) 208
- 6 U Ungerstedt and C Pycock, *Bull Schweiz Akad Med Wiss* , **1278** (1974) 1
- 7 B H C Westerlink, *Trends Anal Chem* , **11** (1992) 176
- 8 U Ungerstedt, *J Intern Med* , **230** (1991) 365
- 9 C E Lunte, D O Scott and P T Kissinger, *Anal Chem* , **63** (1991) 773A
- 10 P Lonnroth and U Smith, *J Intern Med* , **227** (1990) 295
- 11 C M Riley, J M Ault and C E Lunte, in 'Liquid Chromatography in Biopharmaceutical and Biomedical Analysis', Elsevier, 1994
- 12 C I Larsson, *Life Sci* , **49** (1991) PL73
- 13 I Jacobson, M Sandberg and A Hamberger, *J Neurosci Meth* , **15** (1985) 263
- 14 R A Yokel, D D Allen, D E Burgio and P J M^cNamara, *J Pharmacol Toxicol Methods*, **27** (1992) 135
- 15 P Lonnroth, P A Janson, B B Fredholm and U Smith, *Am J Physiol* , **256** (1987) E250
- 16 S Wakaki, H Marumo, T Tamioka, G Shimizu, E Kato, H Kamada, S Kudo and Y Fujimoto, *Antibiot Chemother* , **8** (1958) 228
- 17 L H Baker, F M Caoli, R M Izbicki, M I Opirari and V F Vaitkevicius, *Proc Amer Assoc Cancer Research*, **15** (1974) 182
- 18 S T Crooke and A W Prestayko, Eds , in *Cancer and Chemotherapy-Antineoplastic Agents*, Academic Press, 1981, pp 159
- 19 W A MacCrehan and R A Durst, *Anal Chem* , **50** (1978) 2108
- 20 K Bratin, Ph D Dissertation, Purdue University, West Lafayette, IN, 1981

- 21 K Bratin, R C Briner, P T Kissinger, and C S Bruntlett, *Anal Chim Acta*, **130** (1981) 295
- 22 K Bratin and R C Briner, *Current Separations*, **2** (1980) 1
- 23 K Bratin and P T Kissinger, *Current Separations*, **4** (1982) 4
- 24 W A Jacobs, Ph D Dissertation, Purdue University, West Lafayette, IN, 1983
- 25 W A Jacobs and P T Kissinger, *J Liq Chromatogr* , **5** (1982) 881
- 26 W A Jacobs and P T Kissinger, *J Liq Chromatogr* , **5** (1982) 669
- 27 S M Rappaport, Z L Jin and X B Xu, *J Chromatogr* , **240** (1982) 145
- 28 U R Tjaden, J P Langenberg, K Ensing, W P Van Bennekom, E A De Bruijn and A T Van Oosterom, *J Chromatogr* , **232** (1982) 355
- 29 M Treskes, J De Long, O R Leeuwenkamp and W J F Van der Vijgh, *J Liq. Chromatogr* , **13** (1990) 1321
- 30 D A Joyce, and D N Wade, *J Chromatogr* , **430** (1988) 319
- 31 J B F Lloyd and D A Parry, *J Chromatogr* , **449** (1988) 281
- 32 M T Smith, D S Fluck, D A Eastmond and S M Rappaport, *Life Chemistry Reports*, **3** (1985) 250
- 33 P Maitoza and D C Johnson, *Anal Chim Acta*, **118** (1980) 233
- 34 D A Roston, R E Shoup and P T Kissinger, *Anal Chem* , **54** (1982) 1417A
- 35 D M Radzik, J S Brodbelt and P T Kissinger, *Anal Chem* , **56** (1984) 2927
- 36 A Bergens, *J Chromatogr* , **410** (1987) 437
- 37 Y Haroon, C A W Schubert and P V Hauschka, *J Chromatogr Sci* , **22** (1984) 89
- 38 R A Wallingford and A G Ewing, *Anal Chem* , **61** (1989) 98
- 39 P D Curry, C E Engstrom-Silverman and A G Ewing, *Electroanalysis*, **3** (1991) 358
- 40 T J O'Shea and S M Lunte, *Anal Chem* , **65** (1993) 247
- 41 W Lu and R M Cassidy, *Anal Chem* , **65** (1993) 1649
- 42 W Lu, R M Cassidy and A S Baranski, *J Chromatogr* , **640** (1993) 433

- 43 T J O'Shea, R D Greenhagen, S M Lunte, C E Lunte, M R Smyth, D M Radzik and N Watanabe, *J Chromatogr* , **593** (1992) 305
- 44 S J Williams, D M Goodall and K P Evans, *J Chromatogr* , **629** (1993) 379
- 45 R Tait, D J Skanchy, D P Thompson, N C Chetwyn, D A Dunshee, R A Rajewski, V J Stella and J F Stobaugh, *J Pharmaceut Biomed Anal* , **10** (1992) 615
- 46 T J O'Shea, P L Weber, B P Bammell, M R Smyth, C E Lunte, and S M Lunte, *J Chromatogr* , **608** (1992) 189
- 47 T J O'Shea, M Telting-Diaz, C E Lunte and S M Lunte, *Electroanalysis*, **4** (1992) 463
- 48 B L Hogan and E S Yeung, *Anal Chem* , **64** (1992) 2841
- 49 A G Ewing, *J Neurosci Meth* , **48** (1993) 215
- 50 R A Wallingford and A G Ewing, *Anal Chem* , **61** (1989) 98
- 51 P D Curry, G E Engstrom-Silverman and A G Ewing, *Electroanalysis*, **3** (1991) 358
- 52 M A Malone, P L Weber, M R Smyth and S M Lunte, *Anal Chem* , in press
- 53 A G Ewing, J M Mesaros and P F Gavin, *Anal Chem* , **66** (1994) 527A
- 54 T E Robinson and J B Justice (Eds), *Microdialysis in the Neurosciences*, Elsevier, Amsterdam, 1992
- 55 C E Lunte, D O Scott and P T Kissinger, *Anal Chem* , **63** (1991) 773A
- 56 S E Gartside, P J Cowen and T Sharp, *Neuropharmacology*, **31** (1992) 9
- 57 M J During, A Freese, M P Heyes, K J Swartz, S P Markey, R H Roth and J B Martin, *FEBS Letters*, **247** (1989) 438
- 58 P Russi, M Alesiani, G Lombardi, P Davolio, R Pellicciari and F Moroni, *J Neurochemistry*, **59** (1992) 2076
- 59 K J Swartz, M J During, A Freese and M F Beal, *J Neuroscience*, **10** (1990) 2965
- 60 M P Heyes and B J Quearry, *J Chromatogr* , **530** (1990) 108
- 61 H Q Wu, U Ungerstedt and R Swarcz, *European J Pharmacology*, **213** (1992) 375

- 62 F Moroni, P Russi, M A Gallo-Mezo, G Moneti and R Pellicciari, J Neurochemistry, **57** (1991) 1630
- 63 T Sharp, S R Brammell and D G Grahme-Smith, Life Sciences, **50** (1992) 1215
- 64 H Hashiguti, D Nakahara, W Maruyama, M Naoi and T Ikela, J Neural Transm (Gen Sect), **93** (1993) 213
- 65 A J Elderfield, R J W Truscott, I E T Ganon and G M Schier, J Chromatogr Biomed Applic , **495** (1989) 71
- 66 Anna-Karin Collin and Urban Ungerstedt, in ‘ Microdialysis, users guide, 4th edition’, Carnegie Medicin, 1988

CHAPTER 3

Development of a Mercury Thin Film Carbon Fibre

Ultramicroelectrode for the Adsorptive Stripping Voltammetric

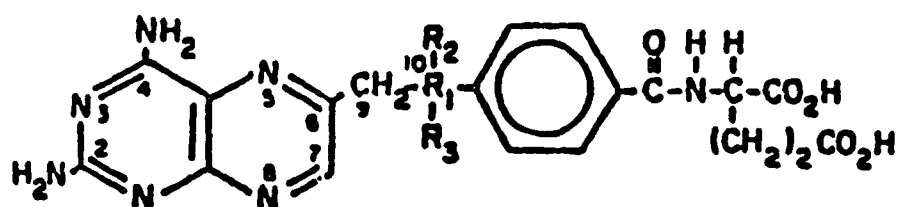
Determination of Selected Pteridines

3.1 Introduction

In this work a mercury thin film carbon fibre ultramicroelectrode was developed and applied to the adsorptive stripping voltammetry of selected pteridines, namely aminopterin, methotrexate and edatrexate. After optimisation of the conditions for mercury film deposition, the mercury thin film ultramicroelectrode was evaluated in terms of its analytical characteristics. The electrode was then applied to the analysis of these compounds in biological fluids and the results were compared to those obtained using a hanging mercury drop electrode.

3.1.1 *Clinical Importance of the Selected Pteridines*

Antimetabolites are chemically similar to endogenous cofactors and metabolic precursors that have an important function in the biosynthesis of nucleic acids and use similar cellular uptake processes and metabolic pathways as these endogenous metabolites. The compounds studied here are antifolates and act primarily by inhibiting the enzyme dihydrofolate reductase (DHFR) of the neoplastic cells. Dihydrofolate reductase functions in maintaining a cellular pool of reduced folate (tetrahydrofolate, FH_4), which serves as a cofactor in the *de novo* synthesis of purine nucleotides and thymidylate (dTMP). In the thymidylate synthetase (Ts) reaction (Figure 3.1B), 5,10-methylene tetrahydrofolate ($\text{CH}_2\text{-FH}_4$) is oxidised to inactive dihydrofolate (FH_2) during the reductive methylation of 2'-deoxyuridylate (dUMP). Dihydrofolate is usually reduced back to tetrahydrofolate by DHFR. Inhibition of DHFR by these antifolates, however, prevents the reduction of dihydrofolate, leading to a depletion of reduced folate and an impairment of the dTMP synthesis, which is an important mechanism of tumour cell toxicity. The



	R_1	R_2	R_3
Aminopterin (AMT)	N	H	—
Methotrexate (MTX)	N	CH ₃	—
Edatrexate (10-edam)	C	CH ₂ CH ₃	H

Figure 3.1A

Chemical structure of the selected pteridines

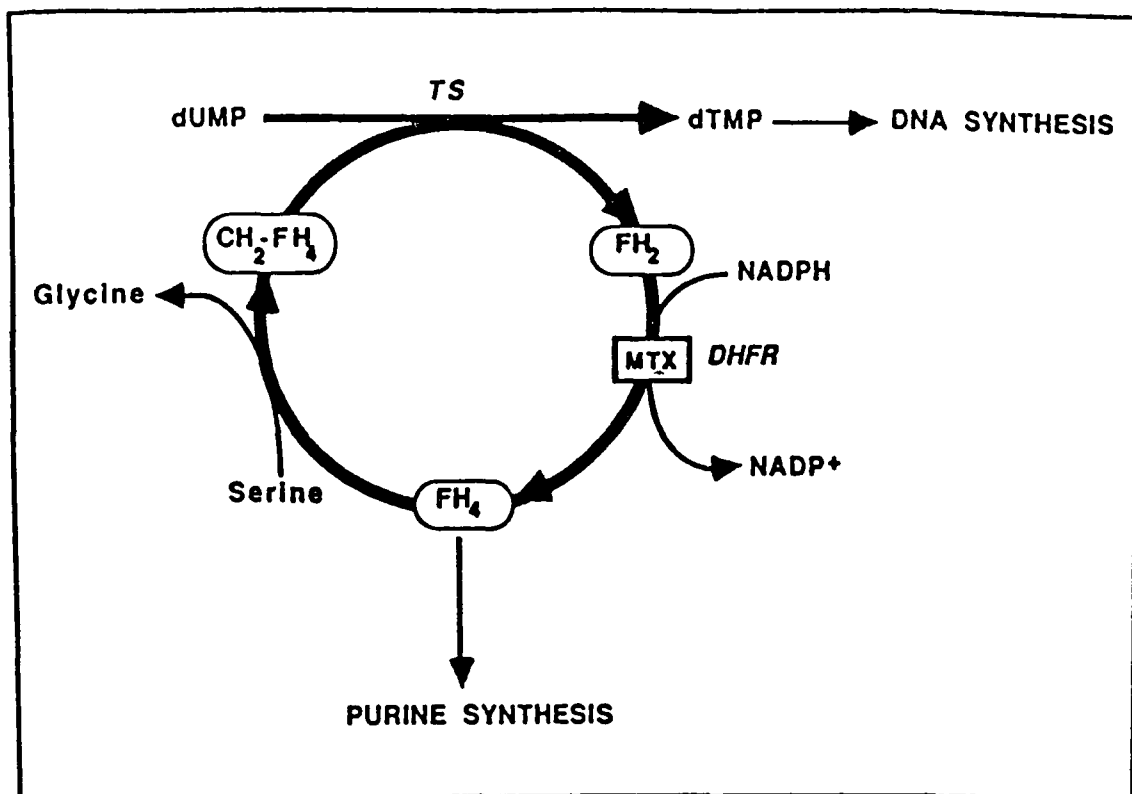


Figure 3.1B

Schematic of folate use in synthesis of thymidylate. Reduced folates (FH_4) serve as methyl donors ($\text{CH}_2\text{-FH}_4$) in the reductive methylation of 2'-deoxyuridyate (dUMP) to thymidylate (dTMP), a reaction catalysed by thymidylate synthase (TS). Use of $\text{CH}_2\text{-FH}_4$ leads to the formation of the inactive dihydrofolate (FH_2), which is normally reduced back to FH_4 by dihydrofolate reductase (DHFR). Inhibition of DHFR by MTX (or other antifolates) prevents the reduction to FH_2 , leading to the depletion of FH_4 and the inhibition of dTMP and DNA synthesis (Copied from reference 1)

prototypic anti-fol is a 4-amino-substituted pterin compound (Figure 3 1A) The substitution of the 4-hydroxyl group of folic acid with an amino moiety results in a folate analogue which has several thousand-fold increase in affinity for the intracellular target, dihydrofolate reductase Aminopterin (4-amino-4-deoxy) pteroylglutamic acid) was synthesised in 1947 by Seeger et al [2], and became the first antifolate compound to receive a clinical trial when Farber et al [3] showed it to be capable of inducing temporary remissions in acute leukaemia in children These studies provided the stimulus for the development of other antimetabolites as possible antitumour agents During the 1950's, aminopterin (AMT) was replaced by methotrexate (4-amino-4-deoxy-10-methyl-pteroylglutamic acid) in clinical usage because its toxicity was more predictable and because of studies showing a superior efficacy of methotrexate (MTX) over AMT in certain types of leukaemia The newer anti-folates are rationally designed analogues of folates or MTX, which have been synthesised in attempts to either overcome cellular resistance to MTX or to develop compounds of lower toxicity, maintaining the potency of MTX

MTX continues to be the drug of choice in the treatment of choriocarcinoma where approximately 50 % of the patients appear to be cured with the use of MTX alone In addition, good to excellent anti-tumour response has been found in patients with acute lymphoma, carcinoma of the breast, mycosis fungicides, epidermoid cancer of the head and neck area and osteogenic sarcoma MTX, the prototype folate antagonist, has probably been studied as intensively as any drug employed in present-day clinical medicine [4]

Antifolates are administered clinically by a number of routes, including oral, intravenous (IV), and intrathecal. For high dose anti-folate therapy, as is used in some cancer chemotherapy regimens, the IV route is usually used. The plasma pharmacokinetics of MTX following IV administration is characterised by three phases with the terminal half-life being approximately 8 to 10 hr. Greater than 90 % of the administered dose is eliminated unchanged through the kidney. However, a fraction of the dose undergoes polyglutamylation in both normal and malignant tissue. The MTX-polyglutamates are active in inhibiting DHFR and the intracellular persistence of these polyglutamates may account for the long duration of DHFR inhibition. MTX can also be metabolised in the liver by aldehyde oxidase to its 7-hydroxy derivative, and the plasma concentration of 7-hydroxy-MTX usually exceeds those of the parent compound 24 hr after administration of a moderate dose of MTX. The 7-hydroxy-MTX, however, is a poor inhibitor of DHFR. Figure 3.1C demonstrates typical plasma levels of MTX over a three day period after infusion of 10 mg/Kg of MTX for 6 hr to patients diagnosed as having acute lymphocytic leukaemia.

Although antifolates have been shown to be highly effective chemotherapeutic drugs, they also exhibit undesirable, sometimes fatal, side effects. The most frequent toxicity associated with MTX are observed in normal tissues that undergo rapid cell division (e.g., gastrointestinal mucosa and bone marrow). These toxicities include, gastrointestinal toxicity, renal toxicity, progressive hepatotoxicity and neurotoxicity. The production of these toxicities does not result solely from the total dose of antifolate administered, but results as a consequence of the persistence (>48 hr) of antifolate in plasma above a threshold level of 1×10^{-8} M.

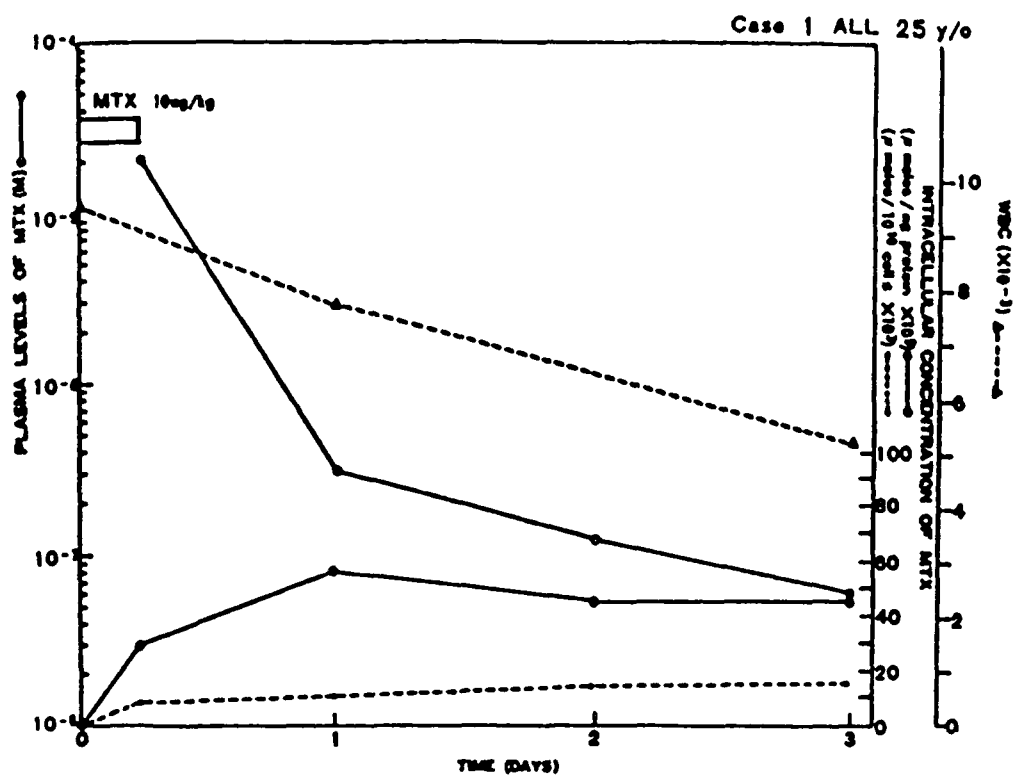


Figure 3.1C

MTX levels in plasma and leukemic cells after infusion of 10 mg/Kg of MTX for 6 hr to patients diagnosed as having acute lymphocytic leukemia.

Therefore, careful monitoring of the plasma concentration of these compounds is essential. Leucovorin (5-formyl-tetrahydrofolate) is frequently used to reduce the gastrointestinal and bone marrow toxicity associated with MTX therapy. The most important mechanism by which leucovorin reduces these toxicities is by replenishing the cellular pool of reduced folates (tetrahydrofolates), essential for the propagation of normal cells. Because of the high urinary concentration of MTX (1.7 to 11×10^{-3} M) that result during high dose MTX therapy and the limited solubility of MTX and its 7-hydroxy metabolite, renal precipitation of these compounds is avoided by alkalinisation of the urine and vigorous hydration. For more details regarding the pharmacokinetics and toxicity of these compounds the reader is referred to the references cited here [1-7]. Current research is aimed towards the development of more potent and less toxic antifolate drugs. Edatrexate (10-ethyl-10-deaza-aminopterin) is one of the new promising drugs and is currently undergoing phase 2 clinical trials [6,7]. Figure 3 1A illustrates the chemical structures of the selected pteridines.

Few methods have been reported for the analysis of AMT and edatrexate (10-edam) in biological fluids. A promising approach was reported, however, by Telling et al [8] using high performance liquid chromatography (HPLC) with fluorimetric detection for the analysis of 10-edam. The analysis of MTX in biological fluids has, however, been extensively reported using HPLC with both UV [9] and fluorescence detection [10]. Analyses of MTX in biological fluids have also been reported using adsorptive stripping voltammetry [11] and polarography [12], but to date nothing has been reported regarding the behaviour of these compounds on mercury thin film ultramicroelectrodes.

Much of the work to date relating to mercury thin film electrodes has been carried out using conventional sized graphite or glassy carbon electrodes [13-15] due to their inertness and simplicity of use. It has been found that the deposition of mercury occurs at sites of varying activity and that the deposition of larger amounts leads to the formation of mercury droplets, the size and distribution of which depends on the deposition potential. More recently, the popularity of microelectrodes has grown rapidly due to the recognition that many of the undesirable aspects of electrochemical and electroanalytical techniques can be reduced or eliminated by virtue of their use. Thus, much work has been directed toward the formation and characterisation of mercury films on microelectrodes using various substrates. Several workers have studied the possibility of using iridium as a substrate [16-20] and found that it was suitable for application to the adsorptive stripping analysis of several metals without problems of intermetallic compound formation. Platinum has also been widely studied as a substrate [21-23] and a mercury thin film platinum microelectrode was applied to the flow injection anodic stripping voltammetry of various heavy metal ions [24]. Silver has also been used to support mercury deposits [25,26] and was reported to yield a coherent surface of the entire mercury deposit. Numerous studies and applications of mercury thin film carbon fibre electrodes to the anodic stripping voltammetric [27-31] and potentiometric stripping analyses [32] of heavy metals have appeared in the literature. Carbon fibres have been reported to be suitable inert substrates and yield mercury films in the form of mercury micro-droplets. Despite the numerous reports regarding the use of mercury thin film microelectrodes for the analysis of

metals and inorganic compounds, no reports have appeared to date relating to their use in cathodic stripping voltammetry of organic compounds

3.1.3 Phase-Selective Alternating Current Voltammetry

Alternating current (AC) techniques involve superimposing an alternating potential waveform on top of a slowly increasing DC potential ramp. Figure 3.2 outlines some of the waveforms used in alternating current voltammetry. By far the most common waveform and the form used throughout this thesis, is sinusoidal AC voltammetry in which a small-amplitude sinusoidal alternating potential is superimposed onto the normal potential ramp used in DC voltammetry.

After filtering out the DC component of the experiment, a plot of alternating current versus direct potential yields a peak-shaped response, as shown in Figure 3.3. For a reversible system the peak position of the curve equals the half-wave potential ($E_{1/2}$) and the current amplitude is given by

$$i_p = \frac{n^2 F^2 A \omega^{\frac{1}{2}} D_o^{\frac{1}{2}} C_o^* \Delta E}{4RT}$$

where ω is the angular frequency of the applied wave

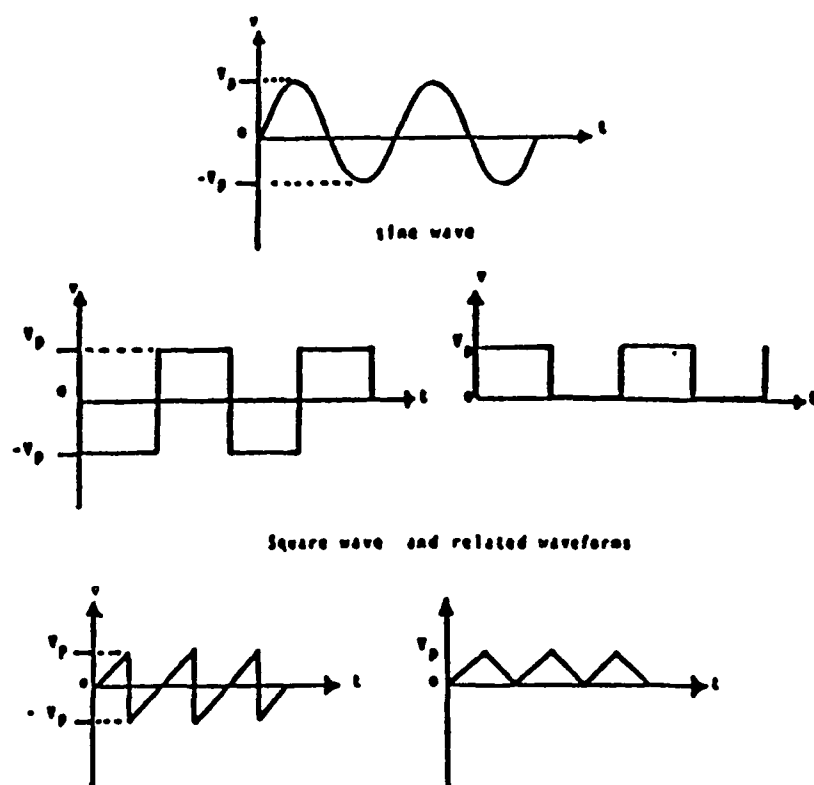


Figure 3.2

Some periodic waveforms available for use in alternating current voltammetry
(from reference 38)

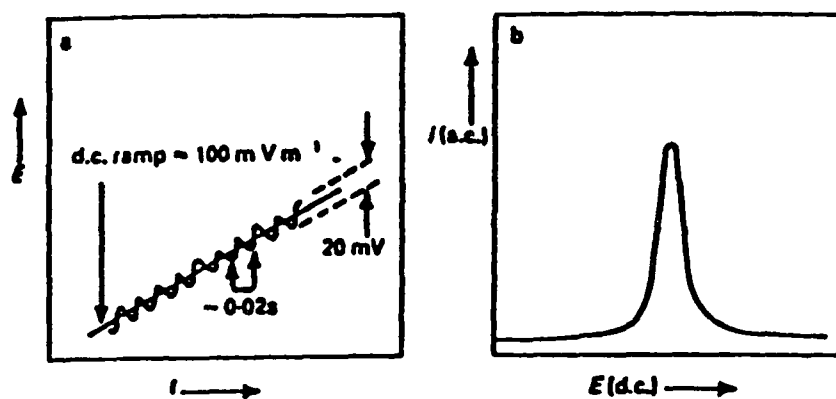


Figure 3.3

(a) Excitation waveform and (b) response obtained in AC voltammetry (from reference 39)

The general shape of the reversible wave is described by the following equation

$$E_{dc} = E_{\frac{1}{2}} + \frac{2RT}{nF} \ln \left[\left(\frac{i_p}{i} \right)^{\frac{1}{2}} - \left(\frac{i_p - i}{i} \right)^{\frac{1}{2}} \right]$$

The faradaic current that arises from an irreversible process is much smaller than that obtained for a reversible process in which the number of electrons transferred is the same. This is because for a reversible process the rate at which the oxidised form is reconverted to the reduced form and vice-versa is fast compared to the frequency of the applied potential and therefore the resultant alternating current signal will be large. In phase-selective AC voltammetry, careful selection of the detector phase angle allows for discrimination against the capacity current. The faradaic current shows an angle of 45° for a diffusion-controlled process, while capacity current shows a phase angle of 90° relative to the applied sinusoidal potential. Therefore, by careful selection of the detection phase angle, one effectively rejects the capacity current and measures only faradaic current. These factors make AC voltammetry a very sensitive technique for reversible processes. Since the reduction process of analytical significance of the selected pteridines is reversible in nature, the use of phase-selective AC voltammetry was, therefore, examined for their analytical determination.

3.2 Experimental

3.2.1 *Reagents and Materials*

Aminopterin was purchased from Sigma. Methotrexate was supplied by Cyanamid Iberica (as the disodium salt). Edatrexate (10-ethyl-10-deaza-aminopterin) was kindly supplied by Ciba-Geigy (Basle, Switzerland). All compounds were used without further purification. Stock solutions of 1×10^{-3} M of all compounds were prepared in 1×10^{-2} M sodium carbonate daily and stored at 4°C in the dark. 0.1 M ammonium acetate buffer (pH 5) was prepared by adjusting 0.1 M acetic acid to pH 5.0 using ammonium hydroxide solution and was used as the background electrolyte throughout the study. Initial pH studies were carried out using Britton-Robinson buffer of varying pH in the range of pH 2-9. All reagents were of analytical grade, including $\text{Hg}(\text{NO}_3)_2$ (Merck, Germany), hydrochloric acid (Panreac) and acetic acid (Panreac). All solutions were prepared using deionised water obtained by passing distilled water through a Milli-Q water purification system (Millipore). All deaerations were carried out using purified nitrogen (<1 ppm O_2), obtained from Sociedad Española de Oxígeno. The biological material examined consisted of pools of human urine and serum, respectively, obtained from healthy individuals. Samples consisted of 1 ml aliquots of the biological fluid spiked with appropriate amounts of analyte to achieve the desired final concentration.

3.2.2 *Instrumentation*

A Metrohm (Herisau) E-506 Polarecord was used for all voltammetric measurements. Linear sweep and cyclic voltammograms were recorded using a

Metrohm VA-scanner (E-612) linked to a Linseis XY-recorder (LY-1600) and a Metrohm EA-290 (Kemula) hanging mercury drop electrode (HMDE) of drop areas 2.2 mm^2 . Solutions were stirred using a constant speed magnetic stirrer (300 rpm) when adsorptive stripping analyses were carried out using the hanging mercury drop electrode. All potentials were referred to a Ag/AgCl/KCl, (3M) reference electrode and a platinum wire was used as the counter electrode. A 20 ml electrochemical cell was used which allowed the working electrode, reference electrode, counter electrode and nitrogen delivery tube to be fixed in position through a plexiglass cover. Two types of carbon fibres were used during the study, fibres supplied by Donnay having a nominal diameter of $7.5 \text{ }\mu\text{m}$, and fibres obtained from AVCO, having a nominal diameter of $14 \text{ }\mu\text{m}$. All pH measurements were made using a Crison micropH model 2001 pH meter.

3.2.3 *Procedures*

3.2.3.1 *Microelectrode preparation*

As outlined in the experimental section, two different types of fibres were employed during these studies. The same preparation and activation procedures were employed for both fibres. Initially the fibres were washed in methanol for 15 minutes and then washed with distilled water. The electrodes were then prepared by microscopically inserting a single fibre in the eye of a $100 \text{ }\mu\text{L}$ plastic micropipette. The eye was then sealed using low viscosity resin, Kit TK4 (A.R. Spurr, California). The resin was polymerised by placing in an oven overnight at 70°C . Following polymerisation the electrode was backfilled with mercury and the electrical contact was made using a copper rod which had been filed to remove

surface oxides. The electrode was then sealed using the low viscosity resin and polymerised as before. The fibres were then cut to desired lengths. In the case of the 7.5 μm fibres a length of 3.0 mm was used whereas in the case of the 14 μm fibres a length of 0.5 mm was employed. Figure 3.4 shows a schematic diagram of the ultramicroelectrodes used in these investigations.

3.2.3.2 *Carbon fibre activation*

As outlined previously any resins and organic materials present on the fibre surface were removed by washing with methanol prior to the ultramicroelectrode construction. Activation of the fibre surface was previously attempted [33] using both electrochemical and chemical techniques. Chemical techniques yielded the most satisfactory results. Consequently the fibres were activated by dipping in concentrated chromic acid for 5 minutes after which time they were washed carefully with distilled water. They were then dipped in concentrated nitric acid for 2 minutes and washed again with distilled water. At this stage the fibres were ready for mercury film deposition.

3.2.3.3 *General Methodology*

All compounds were found to precipitate in the presence of mercury nitrate salt due to the formation of insoluble mercury salts. Therefore two separate cells had to be employed. After prior activation of the carbon fibre, the mercury film was generated using the optimum conditions described later. Once formed, the mercury thin film microelectrode was quickly transferred to the analytical cell containing the 0.1 M ammonium acetate (pH 5.0) electrolyte. The optimum transfer procedure

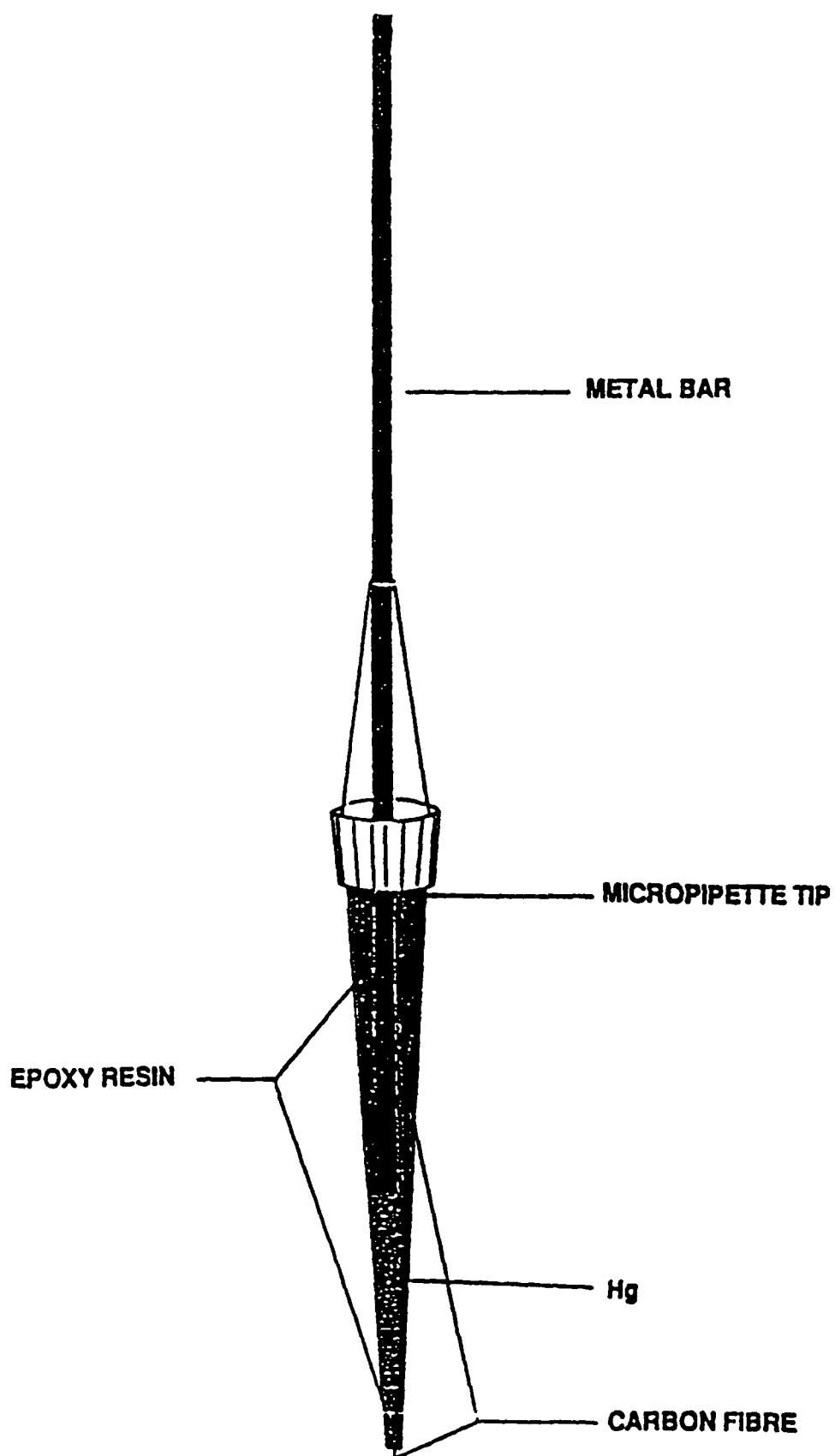


Figure 3.4

Schematic diagram of the cylindrical carbon fibre ultramicroelectrode used.

involved the careful removal of the first cell in a downward direction, followed by careful cleaning of the reference and counter electrodes and the subsequent placement of the analytical cell in an upward direction making sure to minimise vibrations of the fibre which is a potential cause of mercury film loss. This transfer procedure lasted approximately 10 seconds in total. Throughout the procedure a closed circuit was maintained with the potential set at the optimum film deposition potential. Once the analytical cell was in place the potential was scanned between this potential and -1.4 V to ensure that a stable film was produced for subsequent analyses. Prior to each measurement a negative potential (described later) was applied for 30 seconds to clean the mercury film of products of the previous reduction. Both solutions were deaerated for 10 minutes prior to film formation and analysis, respectively, and a nitrogen blanket was employed over the electrolyte throughout the analysis.

3.2.3.4 *Analysis of biological fluids*

The direct analysis of spiked urine was carried out by direct injection of appropriate volumes to the analytical cell. Following measurement of the response, standard additions were made and the original analyte concentration was determined by extrapolation. Alternatively solid-phase extraction (SPE) was used as a clean-up procedure for both urine and serum analyses [34]. The analysis of human serum using a HMDE was also carried out for comparison purposes using the same SPE procedure. In all cases 1 ml aliquots of biological fluid were fortified with appropriate amounts of analyte to achieve the final desired concentration. The 1 ml aliquot was then diluted to 10 ml with acetate buffer (pH 5.0) and mixed gently.

The resulting solution was passed through a reversed-phase C₁₈ cartridge (Sep-Pak, Waters) previously conditioned with 10 ml of pure methanol and 20 ml of water. The eluent was discarded, the cartridge washed with 20 ml of water and the retained materials eluted with 2 ml of pure methanol. The solvent was evaporated to dryness at 60°C under a stream of inert gas. The dry extract was reconstituted in a suitable volume (between 1 and 10 ml) of background electrolyte (0.1 M ammonium acetate, pH 5.0) by shaking for 2 minutes. Appropriate volumes of this solution were injected into the analytical cell and standard additions were used for analyte quantification using the optimum phase-selective AC voltammetric conditions described later. Blank biological samples were obtained by following the same procedure outlined above using non-spiked aliquots.

3.3 Results and Discussion

3.3.1 *Electrochemical behaviour of the Selected Pteridines*

Prior to the development of the mercury thin film ultramicroelectrode a hanging mercury drop electrode was used to study the electrochemical behaviour of the selected pteridines in terms of their electrode processes, pH dependence and adsorption behaviour on mercury. Using direct current adsorptive stripping voltammetry, the pH dependence of the first reduction process, the process of analytical importance was studied. The peak potential varied linearly with the pH in the range 2-9 following the equation $E_p(\text{mV}) = -60.82\text{pH} - 242.43$ for a 1×10^{-6} M aminopterin (AMT) solution. A pH of 5.0 provided the best analytical signals in all cases, and was therefore used in further studies. At this pH both aminopterin (AMT) and methotrexate (MTX) showed three reduction processes, the first of which is reversible. Figure 3.5 illustrates the cyclic voltammograms of the three compounds studied at various concentrations. It has been proposed [35] that the first process is a $2e^-/2H^+$ reduction of the pteridine ring to yield the 5,8-dihydro derivative. The smaller current of the anodic response is due to the subsequent tautomerisation of the 5,8-derivative to yield the 7,8-dihydro derivative, which cannot be re-oxidised back to the parent pteridine. The second and third reduction processes are under kinetic control because they are dependent on the chemical rearrangement outlined above. The second process is due to the $2e^-/2H^+$ reductive cleavage of the dihydro derivative, produced during the first reduction process, between the C-9 and N-10 positions to yield $R-NH_2$ and the 7,8-dihydro derivative. The third reduction process is then the subsequent $2e^-/2H^+$ reduction of this 7,8-

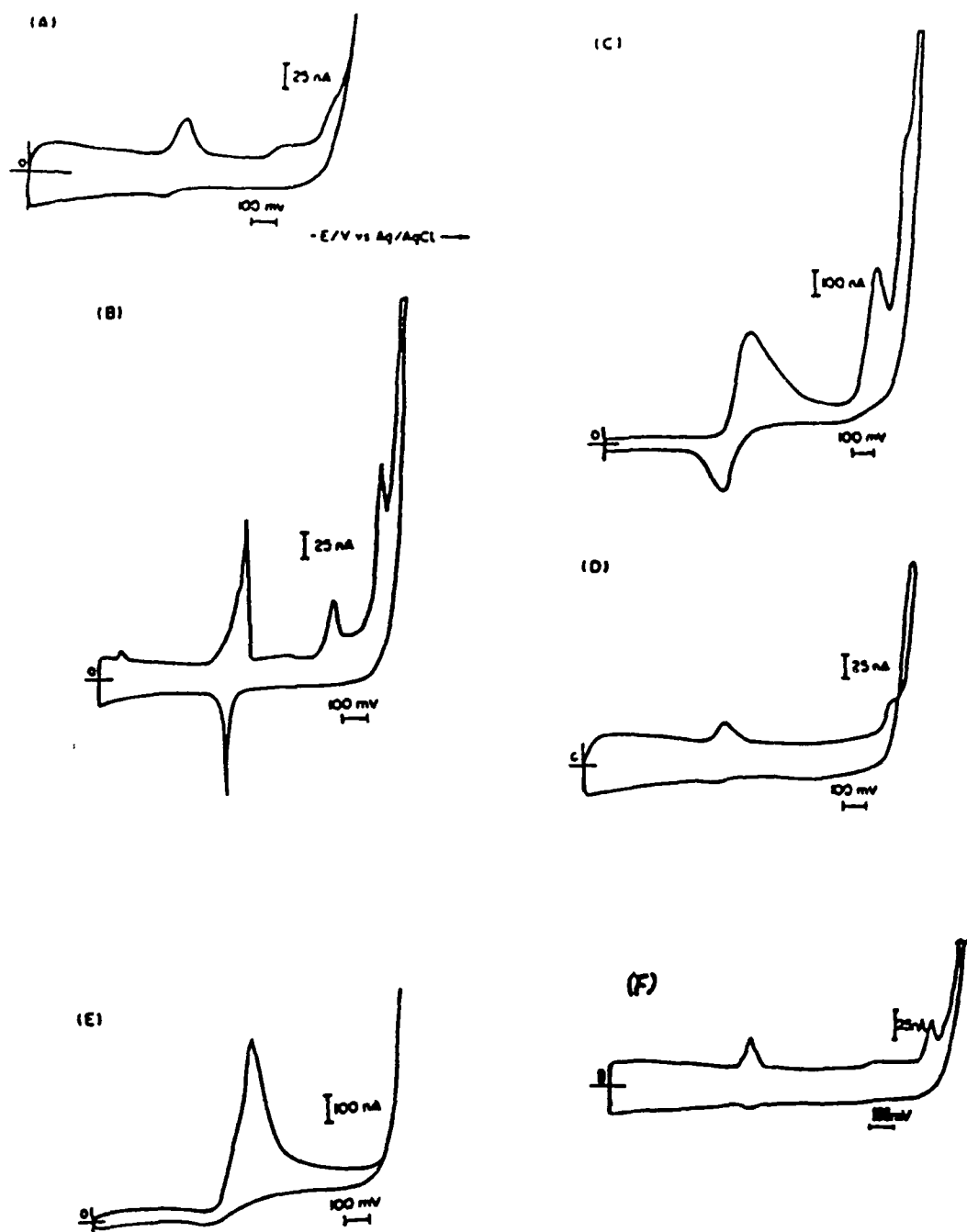


Figure 3.5

Cyclic voltammograms of aminopterin (AMT), edatrexate (10-edam), and methotrexate (MTX) in aqueous solutions at different concentrations (A) 1×10^{-6} M AMT, (B) 1×10^{-5} M AMT, (C) 2×10^{-4} M AMT, (D) 1×10^{-6} M 10-edam, (E) 2×10^{-4} M 10-edam; and (F) 1×10^{-6} M MTX. Electrolyte = 0.1 M ammonium acetate (pH 5.0), scan rate = 100 mVs^{-1} .

dihydro derivative to the 5,6,7,8-tetrahydro derivative. If the direction of the potential scan is switched immediately after the first reduction process, the anodic response increases because the majority of the 5,8-dihydro derivative has not yet been tautomerised to the 7,8-dihydro form. In the case of edatrexate (10-edam), the second reduction process exhibited by AMT and MTX is not seen since the nitrogen group at position 10 is replaced by a carbon group in 10-edam. Table 3.1 summarises the peak potentials of the electrochemical processes for each compound. It was evident from the cyclic voltammetric studies carried out at various concentrations that not only the pteridines, but also their successive reduction products, adsorb on the mercury surface.

Direct current accumulation curves of AMT and 10-edam were therefore carried out using a hanging mercury drop electrode at various concentrations ranging from 1×10^{-9} M to 2×10^{-7} M to study the effect of accumulation time on the cathodic stripping current of the first reduction process. Figure 3.6 outlines the results obtained. In the case of both compounds an initial linear increase in stripping current is followed by a decrease in slope to a point at which the current appears to be practically independent of time. This surface coverage appears to be the point at which a monolayer of adsorbed compound is present on the electrode surface.

	Half-wave Potentials, mV			
	1c	2c	3c	1a
<i>Amonopterin</i>	-620	-1030	-1210	-530
<i>Edatrexate</i>	-530	-----	-1250	-520
<i>Methotrexate</i>	-510	-975	-1210	-510

Table 3.1
Half-wave potentials vs Ag/AgCl of the electrochemical processes of the selected ptendines

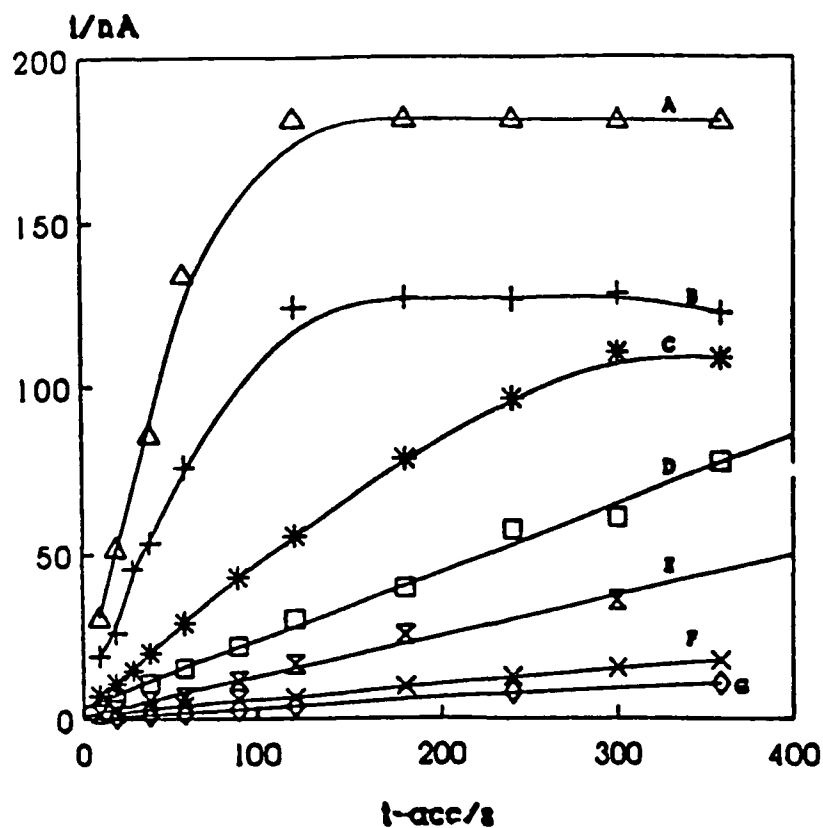


Figure 3.6

Direct current accumulation curves from agitated, aqueous solutions of various concentrations of aminopterin and edatrexate using a hanging mercury drop electrode (A) 2×10^{-7} M 10-edam, (B) 2×10^{-7} M AMT, (C) 8×10^{-8} M AMT, (D) 4×10^{-8} M AMT, (E) 2×10^{-8} M 10-edam, (F) 1×10^{-8} M AMT, (G) 1×10^{-9} M AMT Accumulation potential = -200 mV, scan rate = 100 mV s^{-1}

3 3 2 *Optimisation of the Conditions for Mercury Film Formation on the Carbon Fibre Electrodes*

The formation of the optimum mercury thin film is a critical factor in the development of a sensitive and reproducible electrode. Mercury deposition on carbon fibres can be in the form of a thin film or can be increased to an almost spherical shape. The deposition of larger amount of mercury for adsorptive stripping voltammetric applications might seem to be advantageous, facilitating the adsorption of more analyte. However, in this study it was seen that larger amounts of mercury produced unstable films and it seemed that the physical structure of the film was more important than the actual quantity of mercury present. Following a study of the literature, mercury nitrate in hydrochloric acid was selected as the mercury salt solution to be employed for the film formation. Therefore, the optimum concentrations of these had to be studied.

3 3 2 1 *Influence of solution composition*

A series of experiments were carried out to find the optimum concentrations of both the mercury salt and the hydrochloric acid. The mercury salt concentration was varied between 1×10^{-1} and 1×10^{-4} M, and a film was formed at each concentration by applying a deposition potential of -1200 mV for 30 seconds. After formation, the film was anodically stripped and the stripping peak was studied as an indication of the morphology of the film. At high concentrations of the mercury salt (1×10^{-1} M) the anodic stripping peak was broad and short. As the concentration was decreased to 1×10^{-3} M the stripping peak became sharper and the peak height

increased dramatically. At this concentration the mercury is thought to exist as numerous micro-droplets of high surface area. Below 1×10^{-3} M the peak height decreases as there is a decrease in the number of the mercury droplets on the fibre surface. Using the same experimental criteria the molarity of the HCl was studied in the range 1-6 M. The peak height of the mercury stripping peak increased up to 5 M HCl and then began to decrease. Thus, it is thought that at a concentration of 1×10^{-3} M $\text{Hg}(\text{NO}_3)_2$ in 5 M HCl the mercury exists in the form of numerous micro-droplets on the fibre surface. At different concentrations the quality of the film deteriorates in terms of a decrease in the number of droplets or a growth in the size of the droplets with an overall effect of a decrease in the surface area of mercury. Following this, two important parameters, namely, the electrodeposition potential (E_{film}) and the deposition time (t_{film}) were studied for two different types and dimensions of carbon fibres as described in the experimental section. In all cases a solution of 1×10^{-3} M $\text{Hg}(\text{NO}_3)_2$ in 5 M HCl was employed.

3.3.2.2 *Influence of deposition potential*

In the case of the 7.5 μm fibre, the E_{film} was optimised by sequentially forming a series of films at various deposition potentials ranging between -100 mV and -1200 mV while employing a t_{film} of 60 seconds. Each film was subsequently stripped anodically and the peak current was measured. Figure 3.7A shows a plot of the results obtained. Following a similar procedure the optimum E_{film} for the 14 μm was studied and the results obtained are represented in Figure 3.7B. Figure 3.8 shows the responses obtained during the E_{film} study for the 14 μm fibre. In the

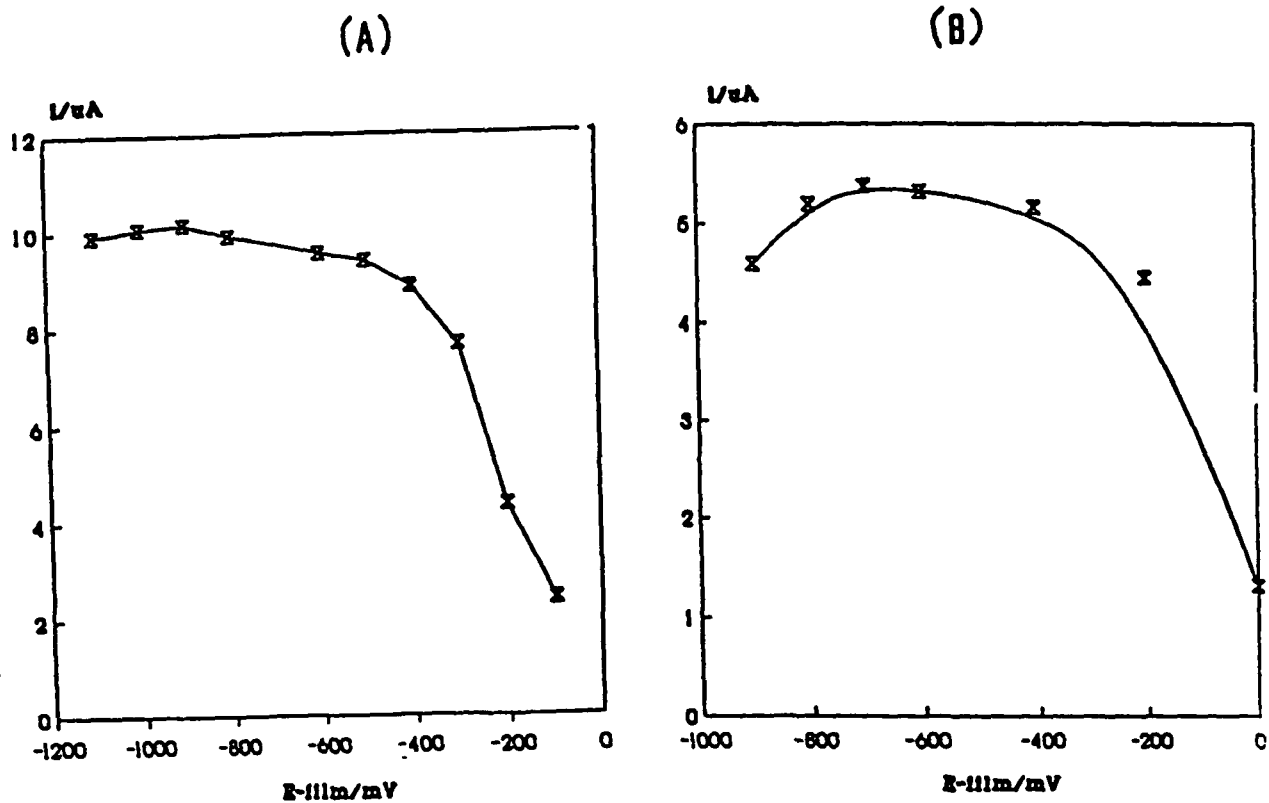


Figure 3.7

(A) Optimisation of the mercury thin film formation on a $7.5 \mu\text{m}$ carbon fibre in terms of the applied deposition potential (E_{film}) using direct current anodic stripping voltammetry. Mercury salt solution = $1 \times 10^{-3} \text{ M Hg}(\text{NO}_3)_2$ in 5 M HCl , $t_{\text{film}} = 60$ seconds, films were stripped anodically at 100 mV s^{-1} .

(B) Same as part (A) for a $14 \mu\text{m}$ carbon fibre. The films were stripped anodically at 50 mV s^{-1} .

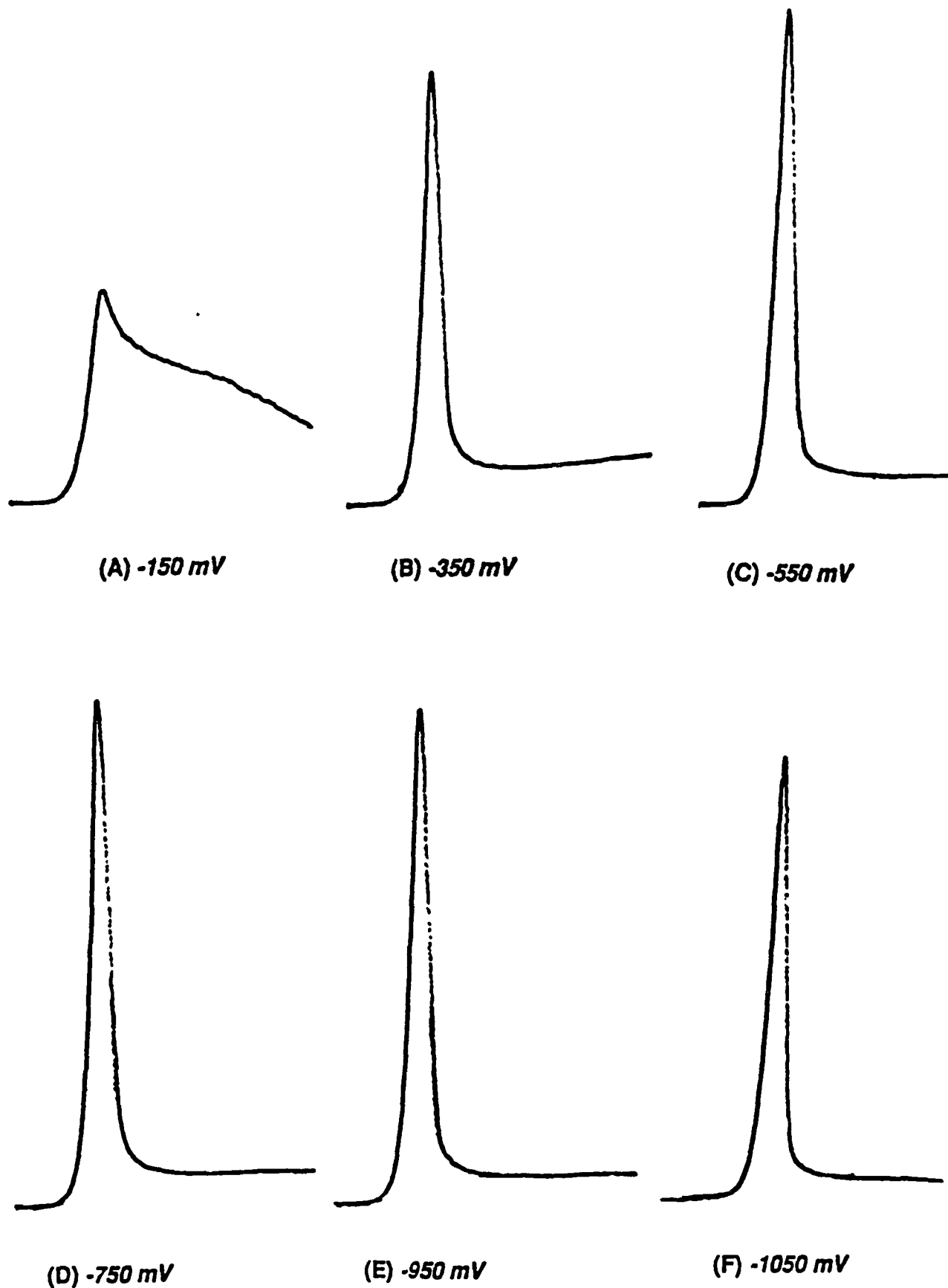


Figure 3.8

Anodic stripping voltammograms of the mercury film obtained during the optimisation of the deposition potential (E_{film}) for a $14\mu\text{m}$ carbon fibre Mercury salt solution = $1 \times 10^{-3} \text{ M Hg(NO}_3)_2$ in 5 M HCl , $t_{\text{film}} = 60 \text{ seconds}$, films were stripped anodically at 50 mV s^{-1}

case of both types of fibres the stripping current increased as the E_{film} became more negative until the potential at which hydrogen evolution occurs was reached. This potential was -950 mV and -850 mV in the case of the 14 μm and 7.5 μm fibres, respectively. Thus the optimum E_{film} values chosen were -800 mV and -750 mV, respectively. This trend can be explained by the fact that as more negative potentials are applied, the number of active sites on the carbon fibre surface becomes increasingly larger and hence the number of mercury droplets increase. However, at very negative potentials the evolution of hydrogen gas destabilises the film causing droplet detachment.

3.3.2.3 *Influence of deposition time*

Using the same criteria, the deposition time (t_{film}) was studied for both types of fibre, employing the respective optimum E_{film} values. Figure 3.9A and B represent the results obtained for the 7.5 μm and the 14 μm fibres, respectively. In both cases the anodic stripping current increased with increasing t_{film} up to a certain point after which it decreased again. It seems that the number of mercury micro-droplets increase up to a certain time (90 seconds for the 7.5 μm fibre, and 60 seconds for the 14 μm fibre). At longer times the size rather than the number of droplets increase leading to an overall decrease in surface area and a diminution in film stability. Therefore, employment of the optimum t_{film} value would provide the highest surface area film allowing for the most efficient compound adsorption. This theory was proven by studying the effect of t_{film} on the aminopterin phase-selective AC cathodic stripping response for a 7.5 μm fibre. This was studied by increasing

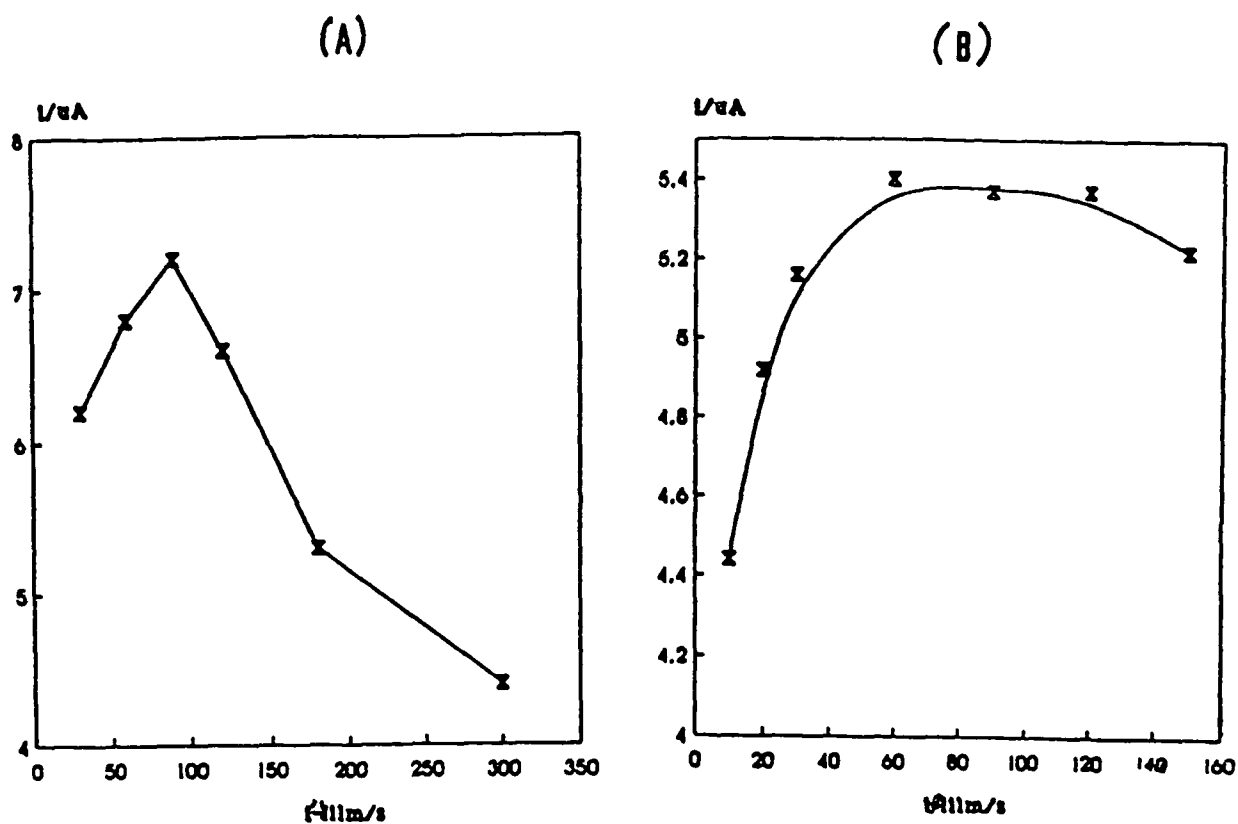


Figure 3.9

(A) Optimisation of the mercury thin film formation on a 7.5 μm carbon fibre in terms of deposition time (t_{film}) using direct current anodic stripping voltammetry. Mercury salt solution = 1×10^{-3} M $Hg(NO_3)_2$ in 5 M HCl, $E_{film} = -800$ mV. Films were stripped anodically at 100 mV s^{-1} . (B) Same as (A) for a 14 μm carbon fibre. $E_{film} = -750$ mV. Films were stripped anodically at 50 mV s^{-1} .

the t_{film} sequentially between 0 and 240 seconds and for each t_{film} the electrode was transferred to a 5×10^{-9} M AMT solution in 0.1 M ammonium acetate, pH 5, the AMT was accumulated for 60 seconds at an applied potential of 0 V and then cathodically stripped. The results obtained are graphically presented in Figure 3.10. A mercury deposition time of 90 seconds was found to be optimum, in close agreement with the initial part of the study. This proves the correlation between the quality of the mercury film and the cathodic stripping response of the compound.

3.3.2.4 *Reproducibility of film formation*

Between each film formation the fibre had to be regenerated producing a clean surface, free of mercury, this contributed to the reproducibility of the film. The optimum conditions for this regeneration were found to be the application of a potential of +790 mV for 40 seconds in the case of the 7.5 μm fibre and the application of a potential +1050 mV for 60 seconds in the case of the 14 μm fibre. This oxidised all the Hg(0) present on the fibre surface. Figure 3.11A and B show typical mercury anodic stripping peaks from the surface of the 7.5 μm and 14 μm fibres, respectively. The reproducibility of film formation employing these conditions was studied by forming and subsequently anodically stripping six consecutive films from a 7.5 μm fibre. Measurement of the peak current (i_p) of the stripping peaks yielded a relative standard deviation (% RSD) of 1.11 % ($n=6$). To study the reproducibility of the medium exchange of the film, 6 consecutive film coated electrodes were rapidly transferred to a blank 5 M HCl solution and stripped anodically. This transfer procedure yielded a % RSD of 13.3 % ($n=6$). Therefore,

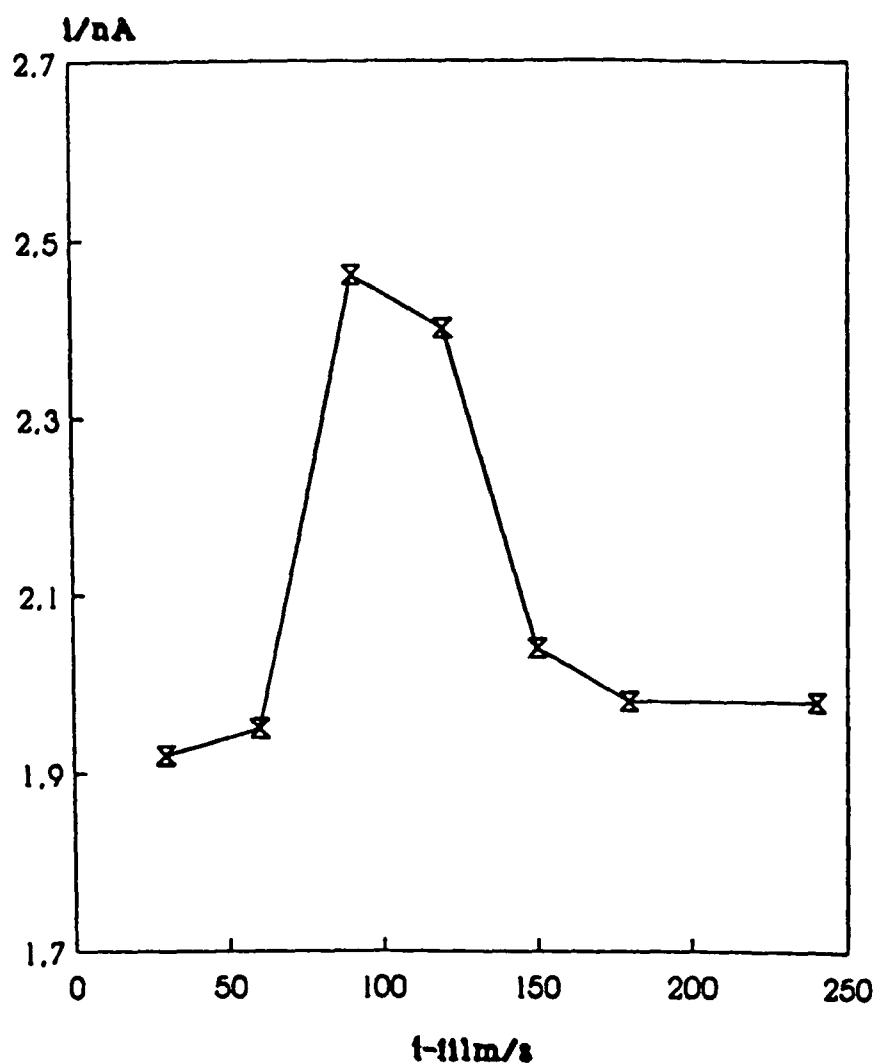


Figure 3.10

Optimisation of the mercury thin film formation on a $7.5\ \mu\text{m}$ carbon fibre in terms of t_{film} versus the aminopterin cathodic stripping response using phase-selective alternating current adsorptive stripping voltammetry. Mercury salt solution = $1 \times 10^{-3}\ \text{M Hg}(\text{NO}_3)_2$ in $5\ \text{M HCl}$, $E_{\text{film}} = -800\ \text{mV}$. Analytical cell contains $5 \times 10^{-9}\ \text{M AMT}$ in $0.1\ \text{M ammonium acetate (pH 5)}$ electrolyte, AMT accumulation time = 60 seconds at an applied potential of $0\ \text{V}$. See text for procedures and AC voltammetric conditions.

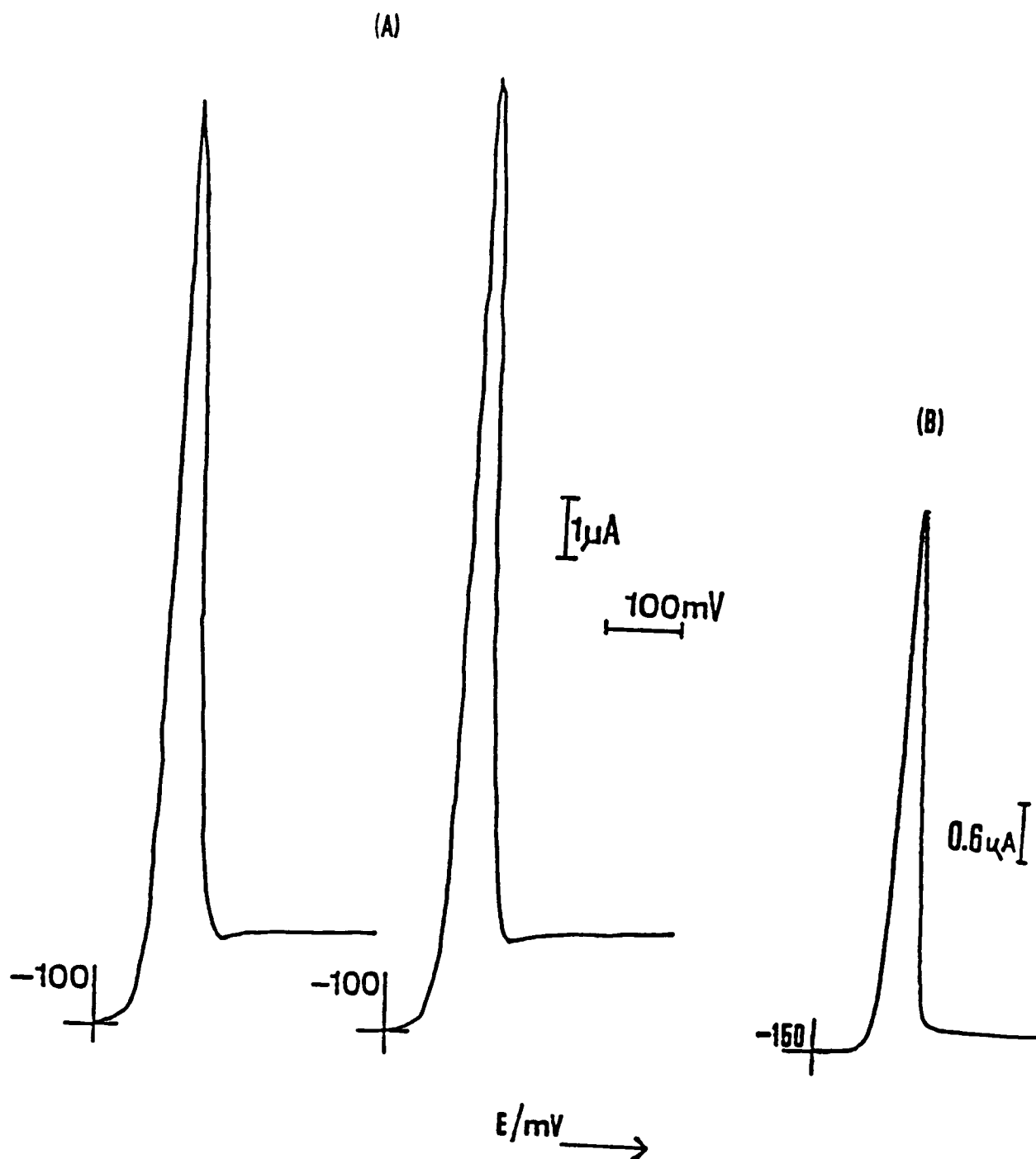


Figure 3.11

(A) Two typical anodic stripping peaks of the mercury film from a 7.5 μm carbon fibre electrode using direct current anodic stripping voltammetry. Mercury salt solution = 1×10^{-3} M $\text{Hg}(\text{NO}_3)_2$ in 5 M HCl, $t_{\text{film}} = 90$ seconds, $E_{\text{film}} = -800$ mV, scan rate = 100 mV s^{-1}

(B) A typical anodic stripping peak of the mercury film from a 14 μm carbon fibre. $t_{\text{film}} = 60$ seconds, $E_{\text{film}} = -750$ mV, scan rate = 50 mV s^{-1} . Other conditions as in (A)

this dictated the necessity to use the same film throughout the whole analysis run, cleaning the film surface between each measurement

3 3 3 *Optimisation of the Phase-Selective AC Voltammetric Parameters*

The three compounds studied exhibit reversible first processes with both reactant and product adsorption on the electrode surface. According to predictions by Laviron [36,37], sensitivity enhancement may be achieved by employing the AC voltammetric mode for these types of processes. Therefore, the phase selective AC voltammetric conditions were optimised for each compound in order to achieve the best analytical signal. Throughout these studies AMT was studied using a 7.5 μm fibre whilst 10-edam and MTX were studied using a 14 μm fibre.

3 3 3 1 *Effect of phase angle*

The effect of phase angle was studied in each case by measuring the signal characteristics of a 5×10^{-9} M solution of the compound over the complete range of the angles. Figure 3.12 represents graphically the influence of phase angle on the cathodic stripping peak intensity of 10-edam. Similar behaviour was also observed for AMT and MTX. It was found that at angles closer to 90° the current was essentially the charging current component, whereas angles closer to 0° produced the best signals. Optimum detection angles of 18° , 10° and 12° were chosen for AMT, 10-edam and MTX, respectively, since under the experimental conditions employed they were seen to produce the best discrimination of the faradaic current against the capacitive current, allowing easier measurement of the analytical signal. As the phase angle was increased to angles approaching 90° , a dramatic increase in

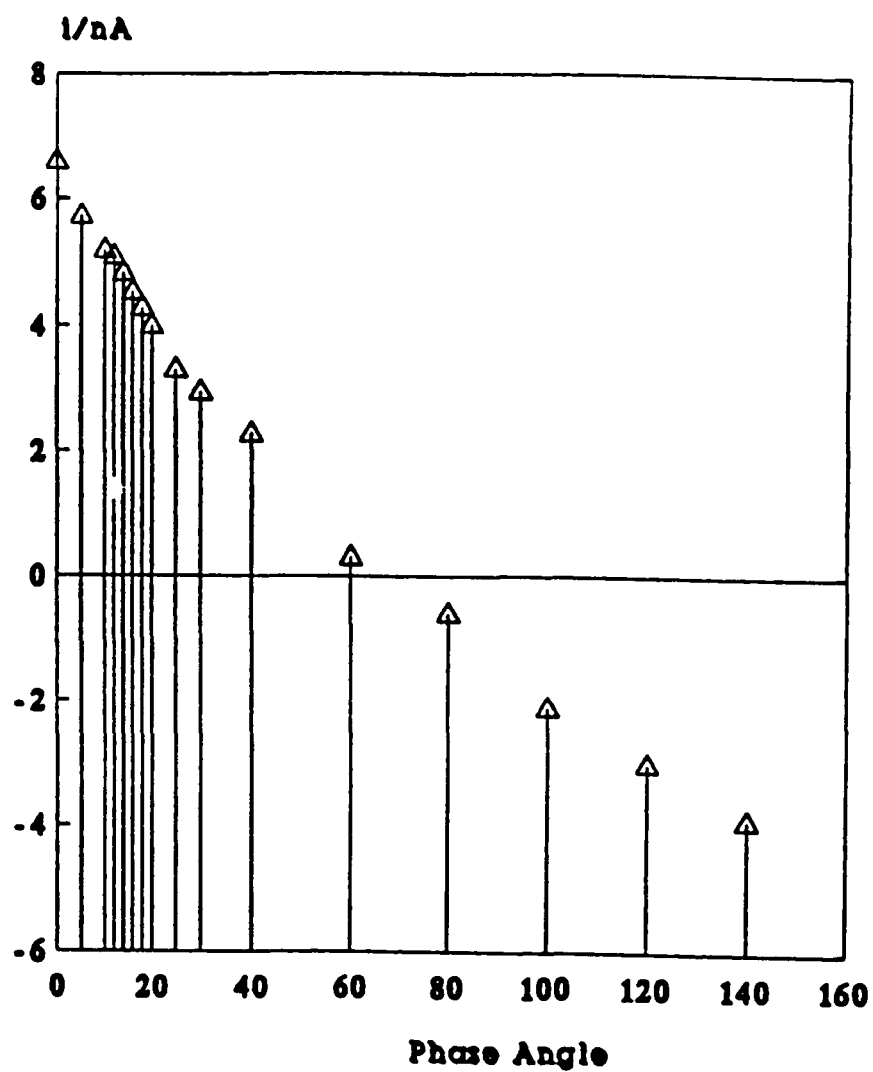


Figure 3.12

Influence of the phase angle on the cathodic stripping response of a 1×10^{-8} M 10-edam solution. Electrolyte = 0.1 M ammonium acetate (pH 5), $t_{acc} = 60$ seconds, $E_{acc} = -150$ mV. See text for procedures and AC voltammetric conditions.

the background current was observed in all cases resulting in an increasingly poor analytical signal

3.3.3.2 *Effect of the superimposed alternating current amplitude*

The AC voltage amplitude was studied by measuring the cathodic stripping peak current for a 5×10^{-9} M AMT solution and a 1×10^{-8} M 10-edam solution, respectively, for a range of pulse amplitudes. In the case of AMT a linear relationship was observed between the cathodic stripping current and the applied amplitude up to a value of 20 mV according to the following equation

$$i(\text{nA}) = 0.127 E(\text{mV}) - 0.015 \quad (r=0.9998)$$

Figure 3.13 represents the results obtained from a 1×10^{-8} M 10-edam solution showing a linear relationship up to 20 mV according to the following equation

$$i(\text{nA}) = 0.123 E(\text{mV}) + 0.078 \quad (r=0.9990)$$

A pulse amplitude of 20 mV was employed for further studies

3.3.3.3 *Effect of scan speed*

A scan speed of 10 mVs^{-1} was employed throughout since in AC voltammetry the scan speed does not significantly affect the signal. The slow scan speed of 10 mVs^{-1} provided a better peak shape than higher scan speeds would

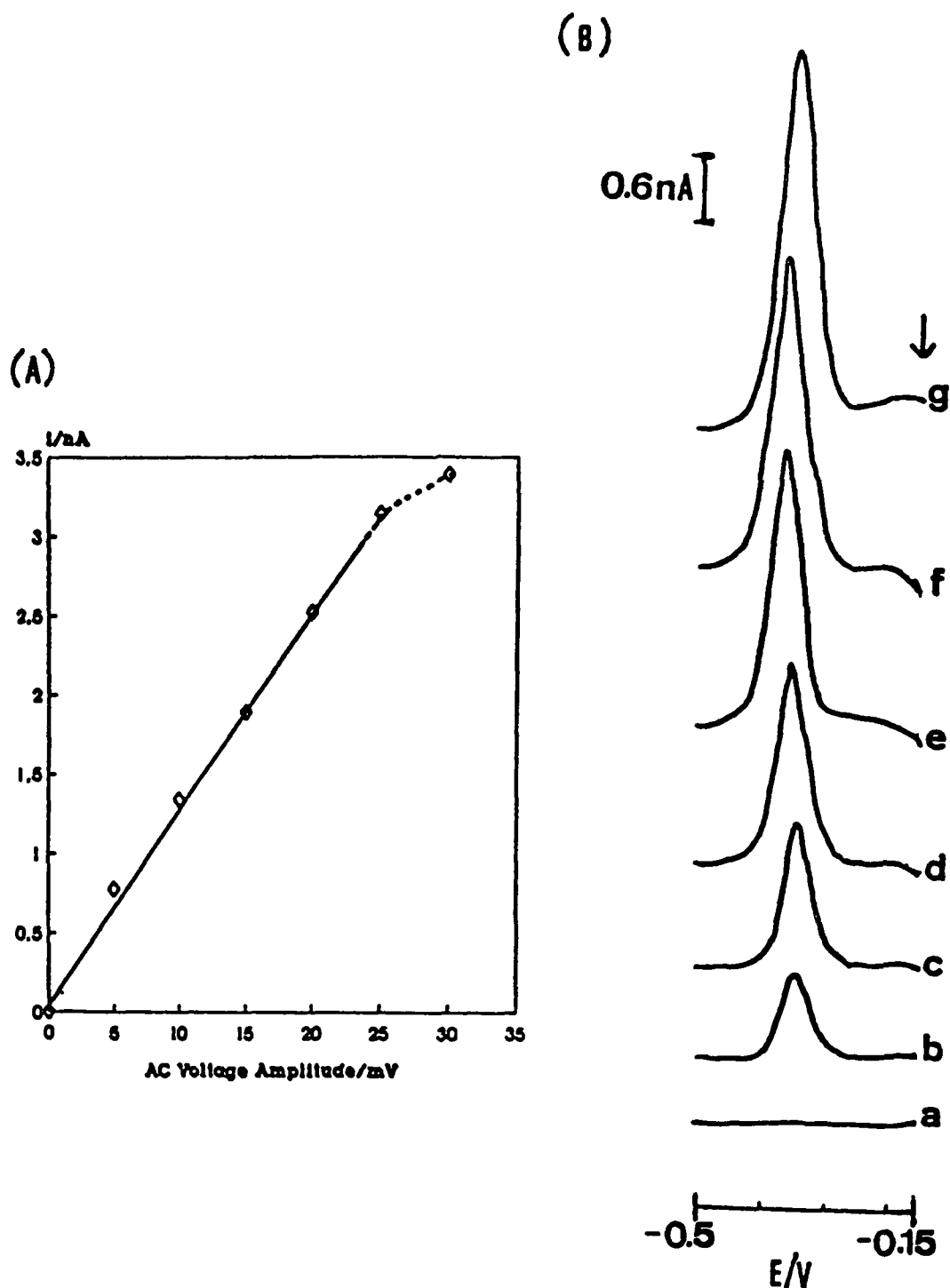


Figure 3.13

(A) Influence of the superimposed alternating current amplitude on a 1×10^{-8} M 10-edam solution. Electrolyte = 0.1 M ammonium acetate (pH 5.0); $t_{acc} = 0$ seconds; $E_{acc} = -150$ mV. See text for procedures and AC voltammetric conditions.

(B) 10-edam cathodic stripping responses used to produce graph (A) above. All conditions as above in (A).

3.3.3.4 *Effect of frequency of the superimposed current*

The instrument used operated at a fixed frequency of 75 Hz and didn't permit any frequency variation. The employment of the appropriate optimised conditions for the respective compounds produced very sensitive methods of analysis.

3.3.4 *Accumulation Behaviour on the Mercury Thin Film*

Ultramicroelectrode

As a prerequisite to the development of an efficient adsorptive stripping analytical procedure, parameters such as accumulation time and accumulation potential were studied. The effect of accumulation potential (E_{acc}) was studied for each compound by accumulating for 60 seconds from a 5×10^{-9} M solution of the respective compounds at different applied potentials ranging from -350 mV to +50 mV at 100 mV intervals. Following accumulation, the adsorbed species was stripped cathodically and the reduction peak intensity was measured. Figure 3.14 presents a plot of the peak current against E_{acc} for both 10-edam and MTX. At E_{acc} values more positive than -150 mV a large increase in the cathodic stripping current was observed, particularly for MTX. Obviously the employment of more positive accumulation potentials introduces the risk of oxidation of the mercury film. Therefore when using the mercury thin film ultramicroelectrode, as a compromise between higher current and the stability of the mercury film accumulation potentials of 0 mV, -150 mV and -250 mV were employed for AMT, 10-edam and MTX, respectively.

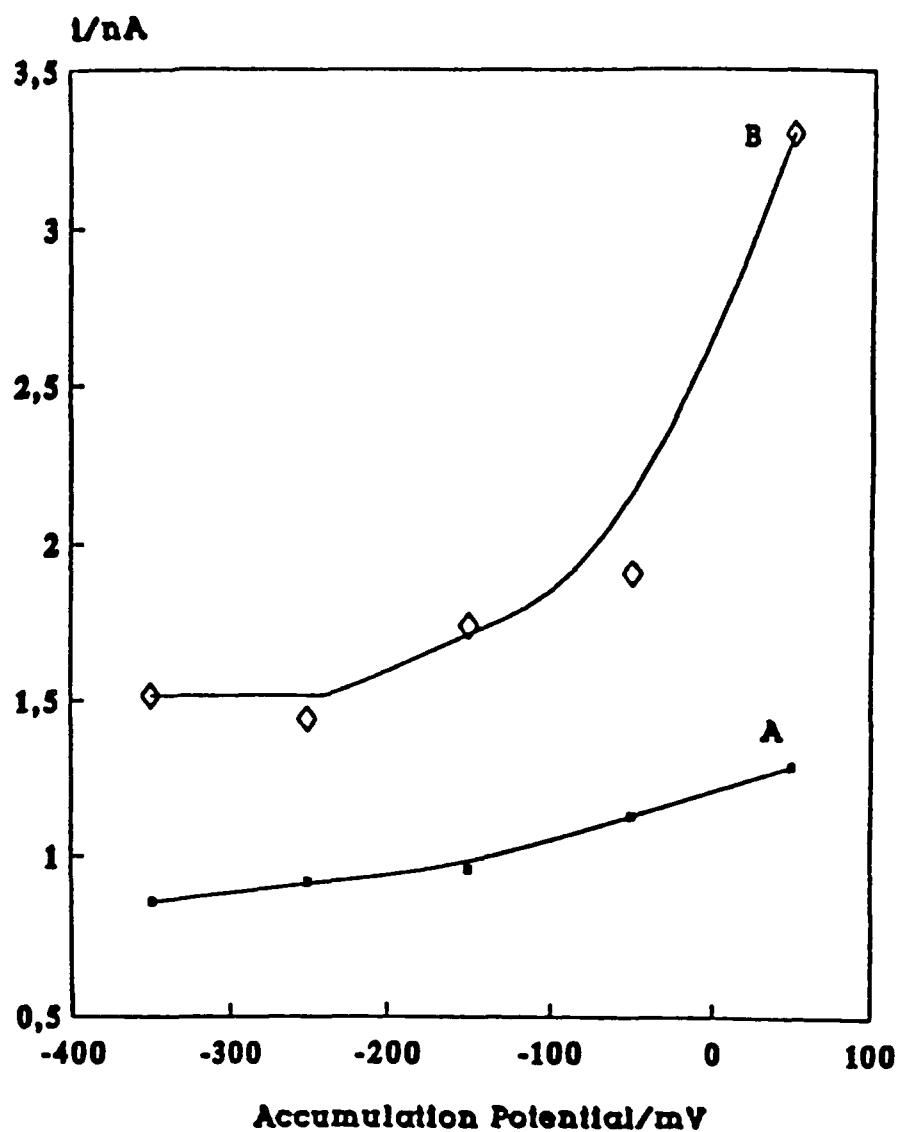


Figure 3.14

Effect of accumulation potential (E_{acc}) on the cathodic stripping current of (A) 5×10^{-9} M 10-edam and (B) 5×10^{-9} M MTX solutions using phase-selective AC stripping voltammetry. Electrolyte = 0.1 M ammonium acetate (pH 5.0), $t_{acc} = 60$ seconds. See text for procedures and AC voltammetric conditions.

Employing these accumulation potentials, accumulation curves were carried out at various concentrations of the compounds using the mercury thin film ultramicroelectrode. Due to the excellent mass transport characteristics of ultramicroelectrodes, accumulations were carried out from quiescent solutions without the need for convective mass transport. In each case the accumulation time was increased in small increments and the peak current of the resultant cathodic stripping peak measured. Figure 3.15 represents a plot of peak current against accumulation time for various concentrations of AMT ranging from 5×10^{-10} M to 5×10^{-8} M. Figure 3.16 represents the accumulation curves for both 10-edam and MTX in the concentration range 5×10^{-10} M to 1×10^{-8} M. Since the same film is used continuously, without renewal, a procedure for activation/cleaning of the electrode between each measurement had to be developed. The purpose of this procedure was to ensure that the electrode surface was free of compounds and their reduction products before each new measurement. In the case of the AMT studies (using a $7.5 \mu\text{m}$ fibre), the application of a potential of -1.4 V for 30 seconds gave the best results. The accumulation curves presented were carried out using these criteria. All the pteridine compounds studied showed similar accumulation behaviour on the ultramicroelectrode, starting with an initial linear increase of the peak current with time. As expected, the current also increased with increasing concentration. It was also evident that each concentration showed a similar trend in that the initial linear portion of the graph was followed by a decrease in slope after which the current increased again in a linear fashion at this lower slope. For example, this slope change occurred at a t_{acc} of 15 seconds for 5×10^{-8} M AMT.

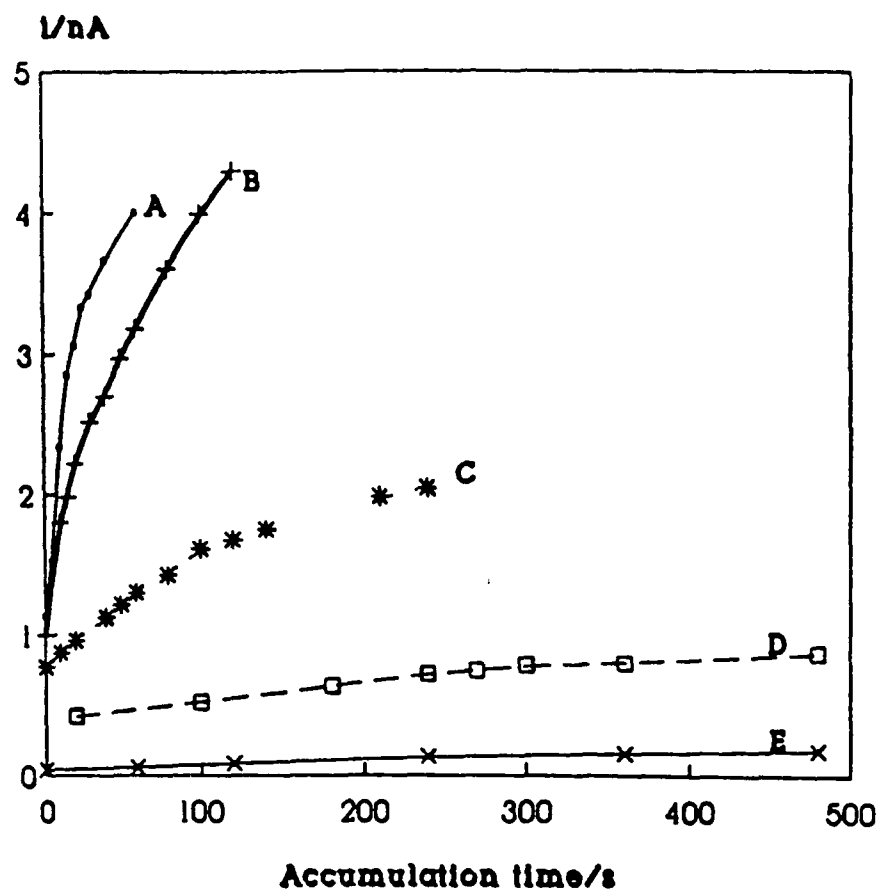


Figure 3.15

Aminopterin accumulation curves on a 7.5 μm mercury thin film carbon fibre electrode using phase-selective AC adsorptive stripping voltammetry $E_{\text{acc}} = 0\text{V}$ A, $5 \times 10^{-8}\text{ M}$ AMT, B, $1 \times 10^{-8}\text{ M}$ AMT, C, $5 \times 10^{-9}\text{ M}$ AMT, D, $1 \times 10^{-9}\text{ M}$ AMT, and E, $5 \times 10^{-10}\text{ M}$ AMT. See text for procedures and AC voltammetric conditions.

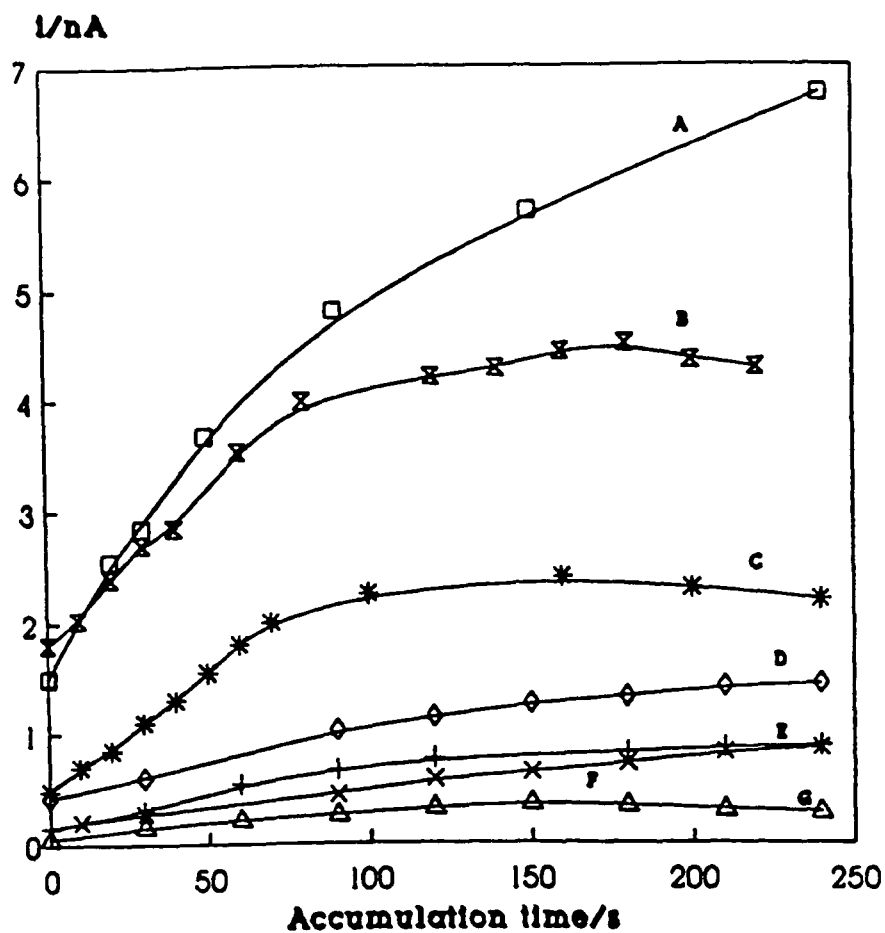


Figure 3.16

Edatrexate and methotrexate accumulation curves on a 14 μm mercury thin film ultramicroelectrode using phase-selective AC adsorptive stripping voltammetry E_{acc} for 10-edam = -150 mV, E_{acc} for MTX = -250 mV A, 1×10^{-8} M 10-edam, B, 5×10^{-9} M 10-edam, C, 5×10^{-9} M MTX, D, 1×10^{-9} M 10-edam, E, 1×10^{-9} M MTX, F, 5×10^{-10} M 10-edam; and G, 5×10^{-10} M MTX. See text for procedures and AC voltammetric conditions.

and a t_{acc} of 360 seconds for 5×10^{-10} M AMT. In all cases, at longer accumulation times, the second linear portion of the curve was followed by another decrease in slope to a point at which the response was virtually independent of accumulation time. This region of the curves might be interpreted as saturation of the electrode surface. However, the current continues to increase with increasing concentration. Therefore, the change in slope may be due to modification of the mercury film at higher surface coverages of the compound, since at higher surface coverages the peak potential also shifted a few millivolts more negative. Careful examination of the accumulation curves facilitated the selection of appropriate accumulation times for further studies.

3.3.5 *Analytical Characterisation of the Mercury Thin Film*

Ultramicroelectrode

In the development of an analytically useful electrode certain analytical characteristics must be evaluated. These include the useful analytical range of the electrode, the limit of detection, reproducibility of the signal and the stability of the electrode. These electrode parameters were studied in full before the system was applied to the analysis of real samples.

3.3.5.1 *Analytical range/Limit of detection*

As outlined earlier, two different types of fibres were studied. The AMT studies were carried out using the 7.5 μm fibres and the 10- μm and MTX studies were carried out using the 14 μm fibres respectively. As before, all accumulations were carried from quiescent solutions. By carefully selecting appropriate accumulation

times, different concentration ranges of the compounds could be studied, with excellent precision and linearity. Again, due to the superior diffusional mass transport characteristics of ultramicroelectrodes, relatively low accumulation times were required. Obviously, at high accumulation times lower concentrations could be studied, but the linear dynamic range was shortened. Thus, a compromise between limit of detection and linear range must be made to suit the analysis of interest. For example, by using an accumulation time of 180 seconds a linear calibration plot was yielded between 2×10^{-10} M and 8×10^{-9} M AMT in aqueous solution according to the following equation

$$i(nA) = 2.88 \times 10^{-8} C_{AMT}(M) + 0.360 \quad (r=0.9994)$$

However, the employment of the very short accumulation time of 10 seconds facilitated the study of higher concentration ranges yielding a linear calibration plot between 1×10^{-8} M and 1×10^{-7} M AMT according to the following equation

$$i(nA) = 5.74 \times 10^{-7} C_{AMT}(M) + 0.525 \quad (r=0.9991)$$

Similarly, using a 14 μ m fibre varying concentration ranges of 10-edam and MTX could be studied. For example, employment of a 240 seconds accumulation time allowed for a linear calibration plot between 1×10^{-10} M and 5×10^{-9} M 10-edam according to the following equation

$$i(nA) = 9.95 \times 10^8 C_{10\text{-edam}}(M) + 0.140 \quad (r=0.9999, n=11)$$

The peak shape obtained from the 14 μ m electrodes was far superior to that of the 7.5 μ m electrodes. Figure 3.17 A and B demonstrates this showing calibration

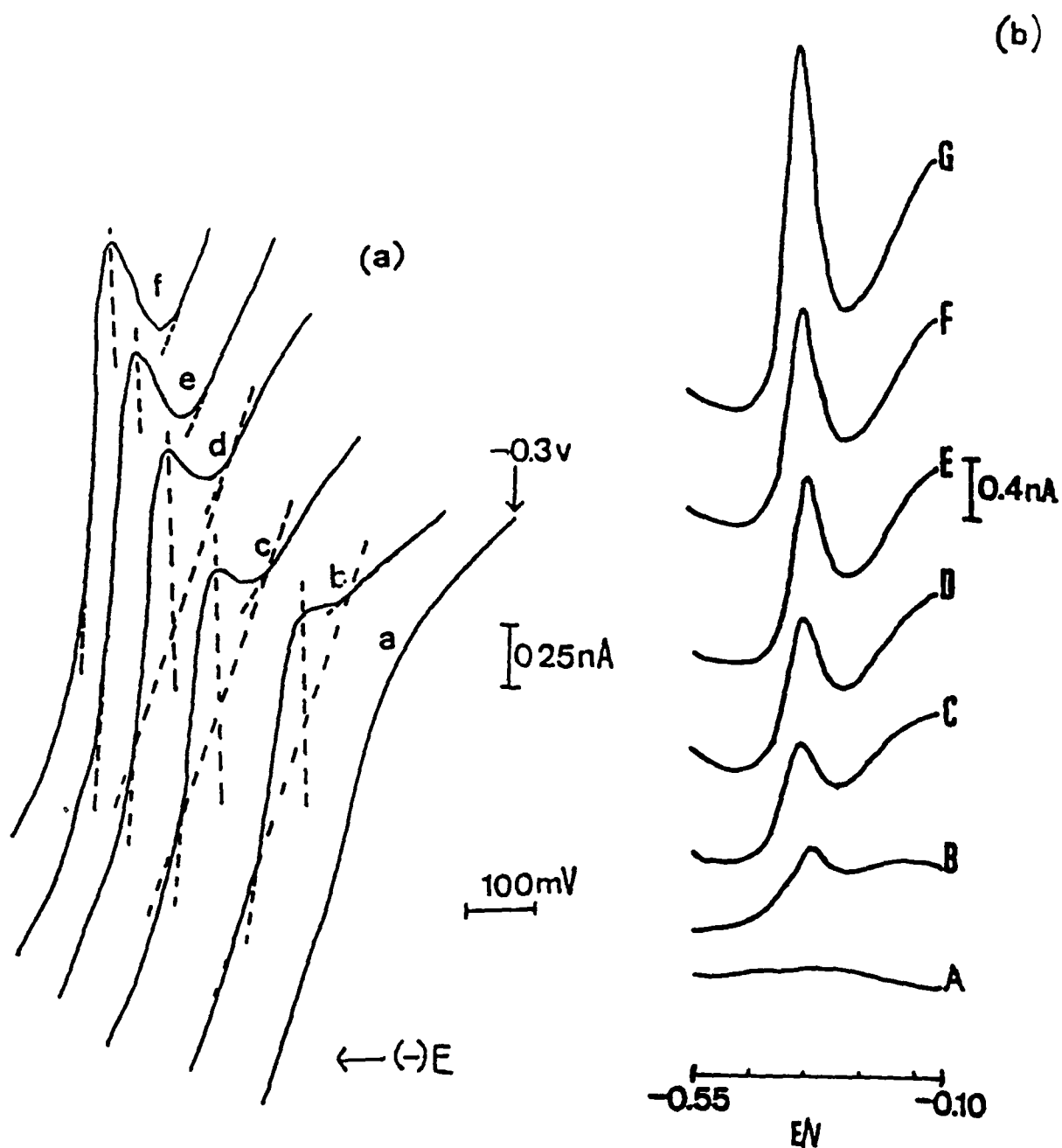


Figure 3.17

(A) Phase-selective AC adsorptive stripping voltammograms of AMT in aqueous solution using a 7.5 μm mercury thin film carbon fibre ultramicroelectrode. $E_{\text{acc}} = 0 \text{ V}$; $t_{\text{acc}} = 180 \text{ seconds}$. A, Blank electrolyte; B, $2 \times 10^{-10} \text{ M}$; C, $4 \times 10^{-10} \text{ M}$; D, $6 \times 10^{-10} \text{ M}$; E, $8 \times 10^{-10} \text{ M}$; and F, $1 \times 10^{-9} \text{ M}$ AMT.

(B) Phase-selective AC adsorptive stripping voltammograms of 10-edam in aqueous solution using a 14 μm mercury thin film ultramicroelectrode. $E_{\text{acc}} = -150 \text{ mV}$; $t_{\text{acc}} = 240 \text{ seconds}$. A, Blank electrolyte; B, $2 \times 10^{-10} \text{ M}$; C, $4 \times 10^{-10} \text{ M}$; D, $6 \times 10^{-10} \text{ M}$; E, $8 \times 10^{-10} \text{ M}$; F, $1 \times 10^{-9} \text{ M}$; and G, $2 \times 10^{-9} \text{ M}$ 10-edam. See text for procedures and AC voltammetric conditions.

responses in the same concentration ranges for (A) 7.5 μm and (B) 14 μm electrodes. The superior response is most likely related to the greater stability of the mercury film on the 14 μm fibre. The shorter length (0.5 mm) of the 14 μm fibres compared to that of the 7.5 μm fibres (3.0 mm) may lead to greater film stability during the medium exchange procedure. Employment of an accumulation time of 15 seconds yielded an MTX calibration plot in the range of 1×10^{-9} M to 2×10^{-8} M following the equation:

$$i(\text{nA}) = 1.18 \times 10^8 C_{\text{MTX}}(\text{M}) + 0.280 \quad (r=0.9995, n=8)$$

The superior performance of the 14 μm electrode provided extremely low limits of detection compared to the 7.5 μm electrode. Using the 7.5 μm mercury thin film ultramicroelectrode employment of a 180 second accumulation time yielded a limit of detection of 1×10^{-10} M AMT (S/N=3). However, using the 14 μm ultramicroelectrode, a 300 second accumulation time yielded a very low limits of detection of 5×10^{-14} M 10-edam and 5×10^{-13} M MTX (S/N=2), respectively. Figure 3.18 A and B shows the responses obtained at these limiting concentrations for (A) 10-edam and (B) MTX. In each case a higher concentration of the compound was added after the limit of detection to prove that the response was due to the compound of interest. These additions are also shown in Figure 3.18.

[It should be noted that different electrodes were used in Figures 3.17 and 3.18 which may explain the slight discrepancy in the magnitude of currents in terms of differences in surface area and and/or activity of the electrodes.]

3.3.5.2 *Reproducibility and stability*

The precision of the analytical signal was evaluated at three different concentrations ranging from low to high for both types of fibres. The results obtained are summarised in Table 3.2. The study was carried out by accumulating the given

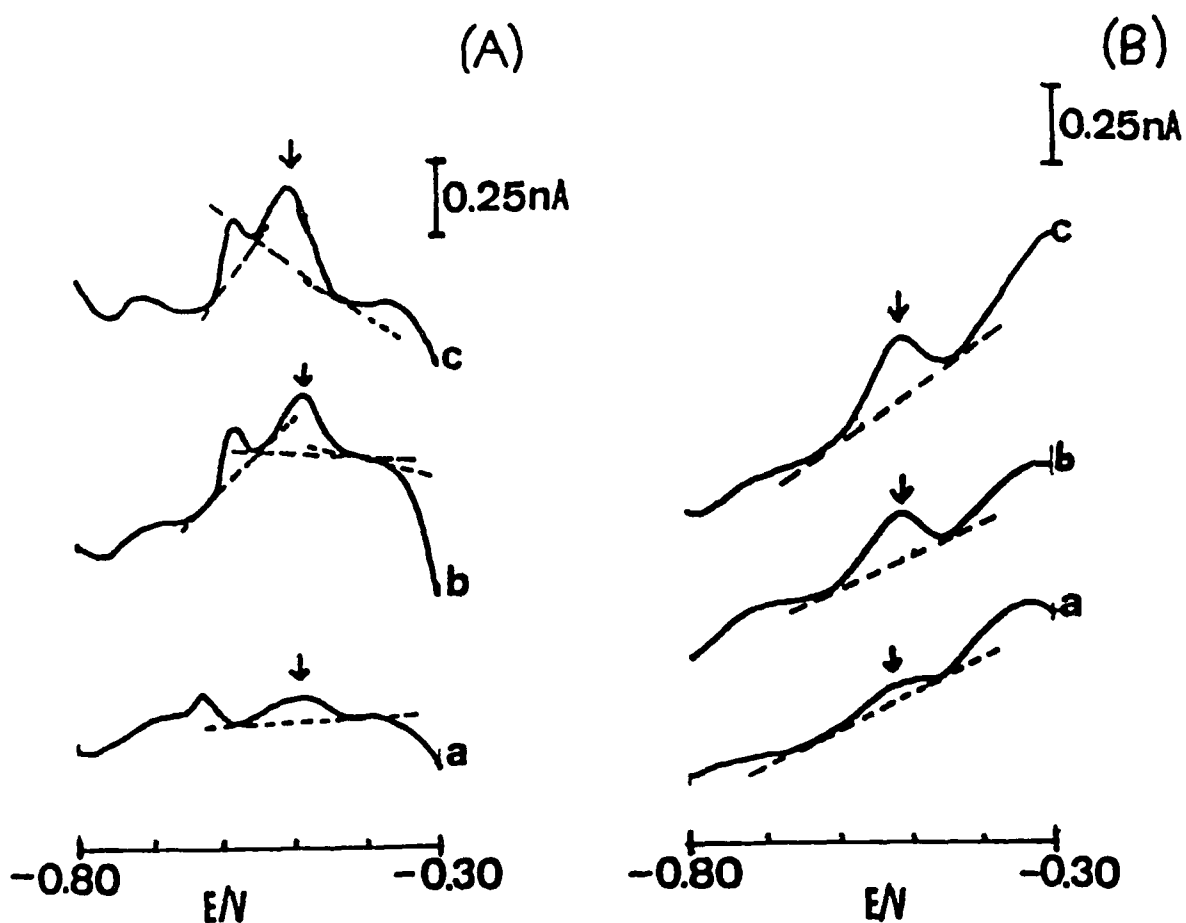


Figure 3.18

(A) Limit of detection for 10-edam using a 14 μm mercury thin film ultramicroelectrode $E_{\text{acc}} = -150$ mV; $t_{\text{acc}} = 300$ seconds (a), Blank electrolyte, (b), 5×10^{-14} M 10-edam (limit of detection), and (C), 1×10^{-13} M 10-edam.

(B) Limit of detection for MTX using a 14 μm mercury thin film ultramicroelectrode $E_{\text{acc}} = -250$ mV, $t_{\text{acc}} = 300$ seconds (a), Blank electrolyte; (b), 5×10^{-13} M MTX (limit of detection), and (C) 7.5×10^{-13} M MTX. See text for procedures and AC voltammetric conditions

<i>Concentration/Compound</i>	<i>t_{occ} (s)</i>	<i>Fibre diameter</i>	<i>% RSD</i>	<i>n</i>
1x10 ⁻⁴ M AMT	20	7.5 µM	2.49 %	10
1x10 ⁻⁹ M AMT	60	7.5 µM	2.79 %	10
5x10 ⁻¹⁰ M AMT	120	7.5 µM	3.57 %	10
1x10 ⁻⁷ M 10-edam	10	14 µM	2.03 %	10
1x10 ⁻⁸ M 10-edam	10	14 µM	1.39 %	10
5x10 ⁻¹⁰ M 10-edam	90	14 µM	2.63 %	10

Table 3.2

Reproducibility of the signal using 7.5 µM and 14 µM fibres, respectively, at various concentrations of aminopterin (AMT) and edatrexate (10-edam)

concentration for a certain accumulation time and then cathodically stripping the adsorbed compound. The peak current of ten consecutive runs was used to calculate the precision of the response in each case. As is evident from Table 3.2 the relative standard deviation values are very low in all cases proving the high precision of the system developed. The 14 μm electrode again gave superior results compared to the 7.5 μm electrode. Figure 3.19 presents 5 consecutive voltammograms of a 1×10^{-8} M 10-EDAM solution using a 10 second accumulation time. The high precision of the electrodes is a good indicator of the short term stability of the mercury film. The long term stability of the electrodes was also monitored and proved to be very dependent on the quality of the mercury film present. It was found that the 7.5 μm electrode could be used for at least a period of 4-6 weeks and the 14 μm electrode for a period in excess of 8 weeks without any significant diminution in performance. Compound adsorption directly onto the fibre surface is the main cause of electrode deactivation. However, the presence of a good mercury film minimised this adsorption. The shape of the anodic stripping peak of the mercury film was a good indicator of the condition of the fibre surface. When this peak was seen to broaden and decrease in height, the surface of the fibre was regenerated by dipping in concentrated chromic acid for 30 seconds. In this way the chromic acid re-oxidised any reduction products adsorbed on the surface of the carbon fibre, thus providing a clean surface. This procedure would normally not be carried out more than approximately ten times for any given fibre since excessive exposure to chromic acid can, in itself, be detrimental to the nature of the carbon fibre surface.

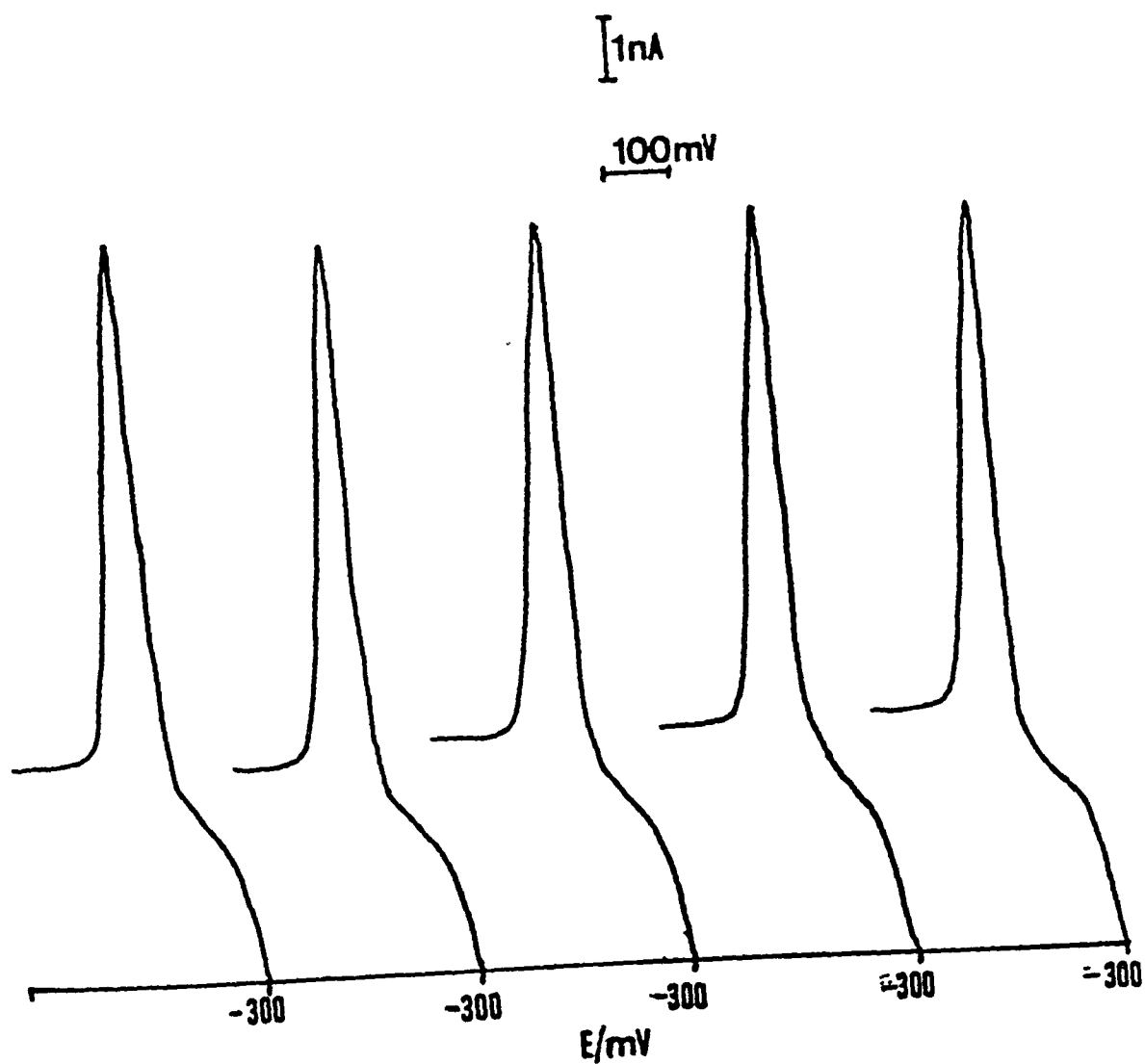


Figure 3.19

Five consecutive cathodic stripping responses of a 1×10^{-8} M 10-edam solution using a $14\text{ }\mu\text{m}$ mercury thin film ultramicroelectrode $E_{\text{acc}} = -150\text{ mV}$, $t_{\text{acc}} = 10\text{ seconds}$ See text for procedures and AC voltammetric conditions.

When the analytical performance of this electrode is compared to previous reports using classical mercury electrodes several advantages of the ultramicroelectrode are evident. Primarily, the charging current related to ultramicroelectrodes is minimal compared to that of conventional size electrodes. The low charging currents exhibited by these mercury thin film ultramicroelectrodes is evident in the voltammograms presented in this chapter. This fact, combined with the greater diffusional mass transport characteristics of ultramicroelectrodes, allowed for the use of much lower accumulation times, and accumulation from quiescent solutions without the necessity for convective mass transport. These factors are particularly advantageous for the analysis of biological fluids since longer accumulation times and agitation of the analyte solution enhance the mass transport of large interfering compounds which otherwise have relatively low diffusion coefficient. Also much lower limits of detection were achieved using the mercury thin film ultramicroelectrode and the precision of the signal compared favourably with that of the classical electrodes. Bearing in mind the numerous advantageous features of this ultramicroelectrode its application to the analysis of real biological samples was the next logical step.

3.3.6 *Analysis of the Selected Pteridines in Biological Fluids*

To evaluate its true potential as an analytical tool the mercury thin film carbon fibre ultramicroelectrode was applied to the analysis of the selected pteridines in human urine and serum. The direct analysis of these compounds was carried out and compared to results obtained for their analysis following solid-phase extraction.

The results obtained were also compared to the analysis of these compounds in serum using a hanging mercury drop electrode.

3.3.6.1 *Direct analysis of urine using the mercury thin film ultramicroelectrode*

Taking advantage of the high sensitivity of the ultramicroelectrode the direct analysis of these compounds in human urine was attempted using both types of fibres. The high sensitivity available allowed for high dilutions of the urine thus reducing the effects of extraneous compounds naturally present in urine and eliminating the need for a prior extraction procedure. Due to the superior mass transport characteristics of ultramicroelectrodes, accumulation was carried out from quiescent solution. Following the procedure outlined earlier, 1 ml aliquots of urine were spiked with appropriate amount of the respective compound to achieve the final desired concentration in urine. Direct injections of suitable quantities of these samples were subsequently made to the analytical cell. Again due to the superior mass transport characteristics of ultramicroelectrodes, short accumulation times were used to take full advantage of the greater diffusion rate of the analyte compared to the extraneous compounds present in urine. After injection of the sample a standard addition method was followed and the initial concentration of the analyte in urine was calculated by extrapolation. The direct analysis of aminopterin in urine was carried out using a 7.5 μm fibre. Pooled urine samples were spiked with appropriate amounts of an AMT stock solution to achieve final concentrations of 5×10^{-6} M, 1×10^{-6} M, and 5×10^{-7} M AMT in urine. At the higher concentration an overall dilution of 1:800 was employed and an accumulation time of 90 seconds yielded reproducible results with a relative standard deviation (% RSD) of 1.75 %. However, at the lower concentration of 5×10^{-7} M larger dilutions could not be

made since the final concentration in the cell would approach the limit of detection of the electrode. At this concentration a 1 200 dilution had to be used and a relatively high accumulation time of 120 seconds resulting in a high %RSD value of 16.5%. This is due to the modification of the electrode surface by naturally occurring compounds in urine. Figure 3.20 shows a typical urine analysis run using the 7.5 μm electrode and demonstrates the gradual adsorption of extraneous compounds onto the electrode surface throughout the analysis run. An obvious way to reduce the effect of these extraneous compounds would be to employ higher dilutions and lower accumulation times. However, under these conditions it was difficult to see the response using the 7.5 μm electrode. However, employment of the 14 μm fibre yielded more satisfactory results. The superior sensitivity of this electrode allowed for higher dilutions and lower accumulation times, thus reducing the effect of extraneous compounds. The electrode was successfully applied to the direct analysis of 10-edam in human urine. For example, when analysing urine containing 5×10^{-6} M 10-edam an injection volume of 20 μl was used (overall 1 1000 dilution) and a very short accumulation time of 15 seconds was employed. Very reproducible results with a low relative error were yielded. For lower concentration of 1×10^{-6} M and 5×10^{-7} M in urine an injection volume of 40 μl was used and accumulation times of 20 seconds and 25 seconds, respectively, were employed. When high dilutions were not used, extraneous peaks at -345 mV and -650 mV respectively interfered with the analysis. However, under the experimental conditions outlined above those responses were minimised and satisfactory results were obtained with no interference problems at the reduction potential of the

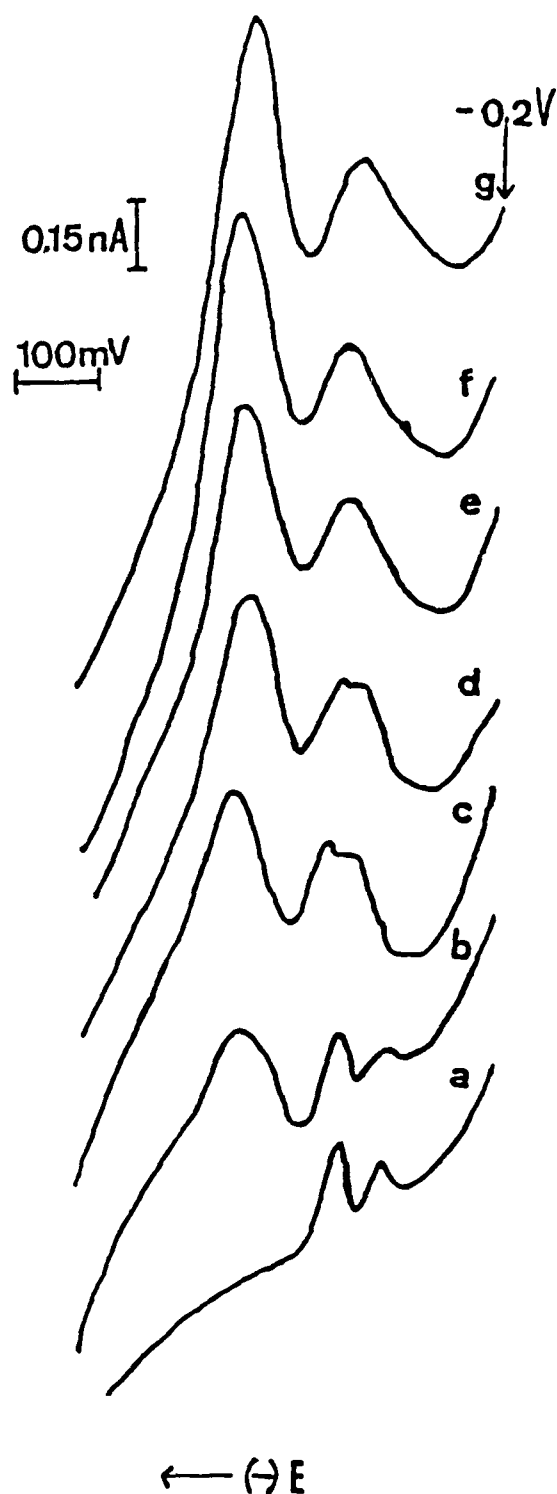


Figure 3.20

Standard additions for the direct analysis of urine spiked with 5×10^{-6} M AMT using phase-selective AC adsorptive stripping voltammetry. Electrode = $7.5 \mu\text{m}$ mercury thin film ultramicroelectrode, $E_{\text{acc}} = 0\text{V}$, $t_{\text{acc}} = 40$ seconds. A, Blank urine; B, 0.5 ml sample; C, $2 \mu\text{l}$; D, $4 \mu\text{l}$; E, $6 \mu\text{l}$; F, $10 \mu\text{l}$; and G, $14 \mu\text{l}$ of a 1×10^{-4} M AMT standard solution. See text for procedures and AC voltammetric conditions.

analyte Table 3 3 summarises the results obtained for various concentrations of 10-edam in urine Figure 3 21 shows a typical urine blank, sample injection and standard additions for the direct analysis of a urine sample containing 1×10^{-6} M 10-edam When this is compared to the previous figure showing the analysis of AMT using a 7 5 μm electrode it is evident that the effect of extraneous compounds is significantly lower and the peak shape in turn is far superior The superiority of the response is related to the use of higher dilutions and lower accumulation times which are made possible by the higher sensitivity of the 14 μm electrode Analysis of the results presented in Table 3 3 indicates that the relative error increases at lower analyte concentrations since higher dilutions cannot be employed This is due to the positive effect of the matrix resulting in some modification of the mercury film and gradual passivation of the carbon fibre surface by extraneous urine compounds This, in turn, lowers the slope of the standard addition plot leading to slightly positive results A limit of detection of 1×10^{-8} M edatrexate in urine was recorded under these conditions

3 3 6 2 *Analysis of human urine following solid-phase extraction using the mercury thin film ultramicroelectrode*

The presumption was made that the slight positive error exhibited during the direct analysis of urine was due to the modification of the mercury film and slight electrode passivation by compounds naturally present in urine To prove that this was the case a solid phase extraction method was employed prior to the electroanalysis procedure for comparison purposes Urine samples were spiked with 1×10^{-6} M edatrexate and subjected to the solid-phase extraction procedure

<i>True Concentration</i>	<i>n=3</i>		
	<i>Concentration Determined</i>	<i>Relative Error</i>	<i>% RSD</i>
5×10^{-4} M	5.26×10^{-4} M	5.09 %	1.48 %
1×10^{-4} M	1.04×10^{-4} M	7.24 %	7.07 %
5×10^{-7} M	5.65×10^{-7} M	12.87 %	4.17 %

Table 3.3
Direct analysis of 10-*edam* in urine using a 14 μ M mercury thin film ultramicroelectrode

<i>True Concentration</i>	<i>Concentration determined</i>	<i>Relative error</i>	<i>Average Relative error (n=3)</i>
1×10^{-4} M	9.62×10^{-7} M	3.85 %	_____
1×10^{-6} M	9.74×10^{-7} M	2.57 %	_____
1×10^{-6} M	1.06×10^{-6} M	5.62 %	4.01 %

Table 3.4
10-*edam* analysis in urine following solid-phase extraction using a 14 μ M mercury thin film ultramicroelectrode

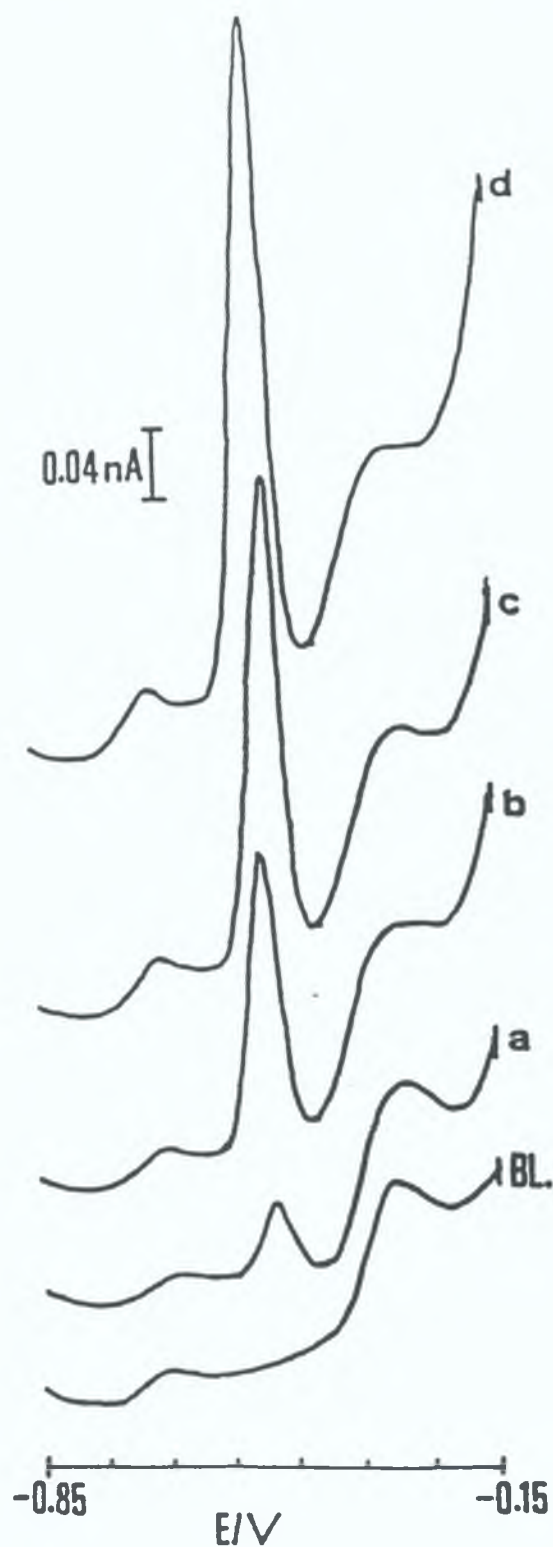


Figure 3.21

Phase-selective AC stripping voltammograms of : (BL) blank urine; (a), direct injection of 40 μl of urine sample $1 \times 10^{-6} \text{ M}$ in 10-edam; followed by; (b), 10 μl ; (c), 20 μl ; and (d), 30 μl of a $1 \times 10^{-5} \text{ M}$ 10-edam standard solution. Electrode = 14 μm mercury thin film ultramicroelectrode; $E_{\text{acc}} = -150 \text{ mV}$; $t_{\text{acc}} = 20 \text{ seconds}$. See text for procedures and AC voltammetric conditions.

outlined in the experimental section. After drying down at 60°C the dry extract residue was reconstituted in 10 ml of electrolyte and 200 µl of this was injected to the analytical cell. A standard addition method was employed as before for quantification of the analyte. The results obtained are summarised in Table 3.4. It can be seen that the results obtained exhibited a lower average relative error (4.01 %, n=3) than those obtained using direct analysis of urine containing the same concentration of 10-edam. More importantly, the results show a negative average error rather than a positive one obtained using direct analysis. Figure 3.22 shows a typical standard addition run following solid-phase extraction for a urine sample containing 1×10^{-6} M 10-edam. Comparison with the voltammograms of the direct analysis of 10-edam in urine demonstrates that the effect of the responses at -345 mV and -650 mV were minimised using solid-phase extraction. Thus, as expected, the employment of solid phase extraction reduced the concentration of extraneous compounds and therefore reduces the positive matrix effect. The percent recovery achieved using this extraction method was calculated to be 99.7 ± 5.1 % indicating almost complete recovery of the compound from urine.

Therefore, the use of a prior clean-up step may be advantageous for the analysis of very low concentrations of the compound in urine. However, the results obtained using direct analysis are acceptable for normal therapeutic levels. The life of the electrode was lowered by gradual passivation of the fibre by compounds present in urine. However, the presence of a good quality mercury film and employment of high urine dilutions and short accumulation times minimised this effect. Surface fouling was alleviated by regenerating the carbon fibre surface for 60 seconds in

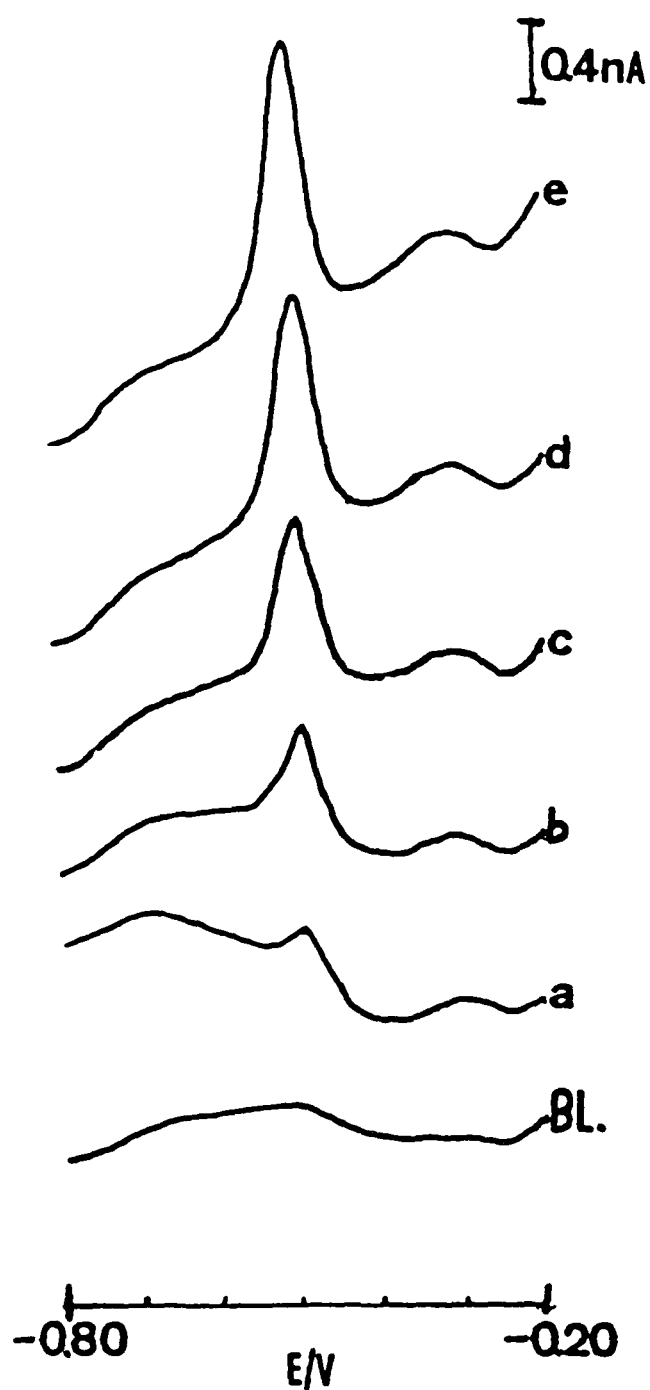


Figure 3.22

Phase-selective AC stripping voltammograms of 10-edam analysis in urine following solid phase extraction. Electrode = 14 μ m mercury thin film ultramicroelectrode, $E_{acc} = -150$ mV, $t_{acc} = 30$ seconds. BL, urine blank, a, 200 μ l injection of urine extract (1×10^{-6} M in 10-edam), b, 25 μ l, c, 50 μ l, d, 75 μ l, and e, 100 μ l of a 1×10^{-6} M 10-edam standard solution. See text for procedures and AC voltammetric conditions.

concentrated chromic acid. The same electrode could normally be used for up to 5 different analysis runs involving approximately 35 measurements before it had to be replaced.

3.3.6.3 *Analysis of human serum following solid-phase extraction using the mercury thin film ultramicroelectrode*

The analysis of human serum was attempted using the same procedures and extraction methods outlined above. Volumes of between 20 and 40 μl of the serum extracts containing between 1×10^{-6} M and 5×10^{-6} M edatrexate were injected into the analytical cell and low preconcentration times of between 20 and 50 seconds were employed. Under these conditions good signals were obtained for the edatrexate present in the serum. However, the slope of the subsequent standard addition plot was strongly influenced by surface effects of extraneous compounds present in the serum. These compounds caused distortion of the mercury film and eventual passivation of the carbon fibre. Larger dilutions and lower preconcentration periods were introduced but did not alleviate the problem. The passivation caused a significant decrease in the slope of the standard addition plot resulting in high positive errors. As expected, the error was lower when serum containing higher concentrations of the compound were analysed. Reactivation of the fibres was attempted as before using chromic acid. The reactivation allowed the electrode to be used for another analytical run but with inferior performance to originally. After two analyses of serum the fibre usually could not be reactivated and had to be replaced.

3 3 6 4 *Analysis of human serum using a hanging mercury drop electrode*

A hanging mercury drop electrode was used for the analysis of 10-edam and aminopterin respectively in human serum as a comparison method for the mercury thin film ultramicroelectrode results. Serum aliquots spiked with varying amounts of AMT ranging from 5×10^{-6} M to 1×10^{-8} M were analysed. Initial studies showed that serum compounds produced two reduction processes at -550 mV and -970 mV, respectively, the first of which was a broad peak and competed with the analytical signal of interest. Therefore investigation of various combinations of open circuit versus applied potential and agitated solution versus quiescent solution accumulation conditions was carried out. It was found that accumulation from a quiescent solution with an applied potential of -200 mV produced the best results and totally avoided the interference problem from serum compounds at -550 mV. The employment of relatively short accumulation times was also advantageous in that it discriminated against the large serum compounds which diffuse at a slower rate than the analyte towards the electrode surface. The employment of these conditions yielded a sensitive and reproducible method. Using a standard addition method the overall assay recovery was determined at a concentration of 5×10^{-7} M AMT in serum. Table 3 5 summarises the results obtained. The average percentage recovery at this concentration was calculated to be 73.57 % (n=5). Figure 3 23 illustrates a typical standard addition analysis at this concentration and it clearly demonstrates that no interferences are presented by the serum compounds under the conditions employed. At the lower concentration of 1×10^{-7} M AMT an average percentage recovery of 65.03 % (n=2) was calculated and at 5×10^{-8} M AMT a

Assay Recovery

<i>Sample</i>	<i>Added concentration (ngml⁻¹)</i>	<i>Assay result (ngml⁻¹)</i>	<i>% Recovery</i>
<i>1</i>	229.2	171.62	74.88 %
<i>2</i>	229.2	160.92	70.21 %
<i>3</i>	229.2	165.65	72.27 %
<i>4</i>	229.2	174.02	75.92 %
<i>5</i>	229.2	170.92	74.58 %

Table 3.5

Assay recovery results for the analysis of aminopterin in human serum using solid phase extraction and a hanging mercury drop electrode

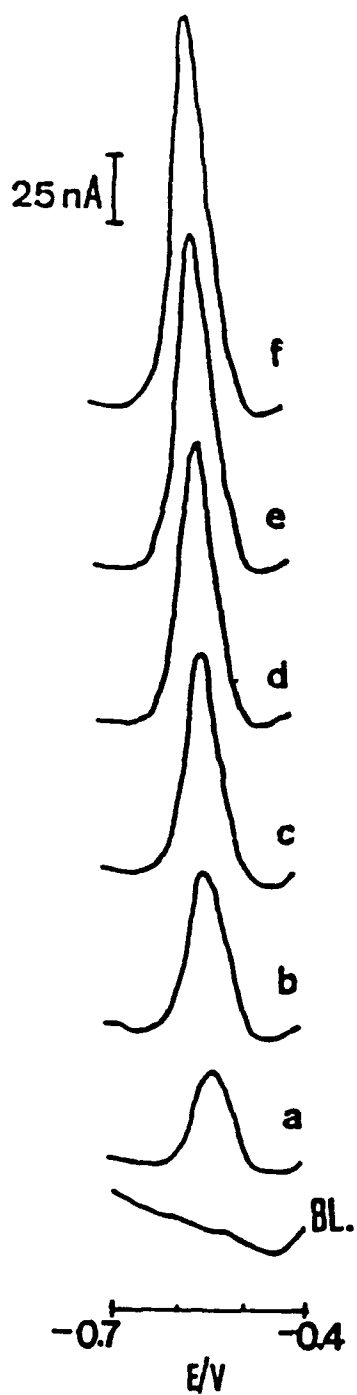


Figure 3.23

Phase-selective AC stripping voltammograms of a serum blank (BL) and (a), a serum sample extract (5×10^{-7} M AMT), followed by standard additions of (b), 20 μ l, (c), 40 μ l, (d), 60 μ l, (e), 80 μ l, and (f), 100 μ l of a 1×10^{-5} M AMT standard solution using a hanging mercury drop electrode $E_{\text{occ}} = -200$ mV, $t_{\text{occ}} = 10$ seconds. See text for procedures and AC voltammetric conditions.

percentage recovery of 62.94 % (n=2) was yielded. At a concentration of 1×10^{-8} M a signal was yielded which corresponded to the limit of detection (S/N=3) of the method. This method was also applied to the analysis of 10-edam in human serum. The percentage recovery was again evaluated at a concentration of 5×10^{-7} M in serum and yielded an average of 94.46 % (n=3) which is superior to the result yielded for AMT and may be attributed to the greater retention of 10-edam on the reversed-phase cartridges. This method is sensitive enough for application to the analysis of clinical samples of patients undergoing chemotherapy with these compounds. The main reason for the success of the mercury drop electrode is the facility of renewing the electrode surface after each measurement. This is not possible with the ultramicroelectrode and it therefore suffers gradual passivation by the compounds, particularly proteins, present in serum. Several attempts, with varying degrees of success, to alleviate the problem of passivation of solid electrodes have appeared in the literature. Some examples were reviewed in Chapter 1 of this thesis.

3.4 Conclusions

A mercury thin film ultramicroelectrode has been developed and applied to the analysis of selected pteridines in biological fluids with and without the incorporation of a prior extraction method. The employment of optimum conditions for activation of the fibre and formation of the mercury film provided an ultramicroelectrode that compared very favourably with the performance of classical mercury electrodes. The limits of detection exhibited by the mercury thin film ultramicroelectrodes were lower than those reported previously using classical mercury electrodes. The employment of an electrochemical cleaning procedure between each measurement to remove reduction products from the surface of the electrode provided a very reproducible signal and facilitated the use of the same electrode for long periods of time. Of the many conclusions that can be drawn from this work perhaps the most important one is that it was proven for the first time that the cathodic stripping analysis of organic compounds is possible using mercury thin film ultramicroelectrodes even under limited conditions where the compounds are insoluble in the presence of mercury salts. The electrode developed was applied to the analysis of selected pteridines but the analysis of other reducible organic compounds may be possible employing a variant of the system developed.

3.5 References

- 1 G Powis, D Phil and M P Hacker, Eds , The Toxicity of Anticancer Drugs, Pergamon Press, 1991
- 2 D R Seeger, J M Smith and M E Hultquist, J Am Chem Soc , **69** (1947) 2567
- 3 S Farber, L K Diamond, R D Mercer, R F Sylvester and J A Wolff New Engl J Med , **283** (1948) 787
- 4 D G Johns and J R Bertino in, J F Holland and E Frei, Eds , Cancer Medicine, LEA-Frebigier, 1982
- 5 K Kimura, and Y-Ming Wang, Eds , Methotrexate in cancer Therapy, Raven Press, 1986
- 6 R F Souhami, R M Rudd, S G Spiro, R Allen, P Lamond and P G Harper, Cancer Chemother Pharmacol , **30** (1992) 465
- 7 M D Green, P Sherman and J Zalcborg, Investigational New Drugs, **10** (1992) 31
- 8 O V Tellingén, J H Beijnen, H R Van der Woude, P F Bruning and W F Nooyen, J Chrom Biomed Applic , **529** (1990) 135
- 9 T P Assadullahi, E Daglı and J O Warner, J of Chrom Biomed Applic , **565**, (1991), 349
- 10 H Kubo, Y Umiguchi, M Fukumoto, T Kinoshita, Analytical Sciences, **8** (1992) 789
- 11 T R I Cataldi, A Guerrieri, F Palmisano and P G Zamboni, Analyst, **113** (1988) 869
- 12 A J Miranda Ordieres, A Costa Garcia, J M Fernandez Alvarez and P Tunon Blanco, Anal Chim Acta, **233** (1990) 281
- 13 M Stulikova, J Electroanal Chem Interfacial Electrochem , **48** (1973) 33
- 14 S H Lieberman and A Zirino, Anal Chem , **46** (1974) 20
- 15 L Loung and F Vydra, J Electroanal, Chem Interfacial Chem , **50** (1974) 379
- 16 J Golas, Z Galus and J Osteryoung, Anal Chem , **59** (1987) 389
- 17 J Golas and Z Kowalski, Anal Chim Acta , **221** (1989) 305
- 18 S P Kounaves and W Deng, J Electroanal Chem , **301** (1991) 77

- 19 S P Kounaves and J Buffle, *J Electroanal Chem* , **216** (1987) 53
- 20 S P Kounaves and J Buffle, *J Electroanal Chem* , **239** (1988) 113
- 21 G Gunawardena, G Hills and B Scharifker, *J Electroanal Chem* , **130** (1981) 99
- 22 R K Wehmeyer and R M Wightman, *Anal Chem* , **57** (1985) 1989
- 23 Z Stojek and J Osteryoung, *Anal Chem* , **60** (1988) 131
- 24 E B T-Tay, S B-Khoo, and S W Loh, *Analyst*, **114** (1989) 1039
- 25 Z Stojek and J Osteryoung, *Anal Chem* , **61** (1989) 1305
- 26 M Ciszowska, M Penczek, and Z Stojek, *Electroanalysis*, **2** (1990) 203
- 27 G Schulze and W Frenzel, *Anal Chim Acta*, **159** (1984) 95
- 28 J Golas and J Osteryoung, *Anal Chim Acta*, **181** (1986) 211
- 29 V J Jennings and J E Morgan, *Analyst*, **110** (1985) 121
- 30 J P Sottery and C W Anderson, *Anal Chem* , **59** (1987) 140
- 31 A S Baranski, *Anal Chem* , **59** (1987) 662
- 32 C Hua, D Jagner and L Renman, *Talanta*, **35** (1988) 597
- 33 J Amez del Pozo, Doctoral Thesis, University of Oviedo, 1993
- 34 A J Miranda Ordieres, A Costa Garcia, J M Fernandez Alvarez and P Tunon Blanco, *Anal Chim Acta*, **233** (1990) 281
- 35 G Dryhurst, in *Electrochemistry of Biological Molecules*, Academic Press, New York, 1977, pp 324-357
- 36 E Laviron, *J Electroanal Chem* , **97** (1979) 135
- 37 E Laviron, *J Electroanal Chem* , **52** (1974) 395
- 38 A M Bond, Ed , *Modern Polarographic Methods in Analytical Chemistry*, Marcel Dekker , 1980
- 39 J P Hart, Ed , *Electroanalysis of Biologically Important Compounds*, Ellis Harwood Limited, 1990

CHAPTER 4

Flow Injection Amperometric Determination of Nitrite Using a Carbon Fibre Ultramicroelectrode Modified with the Polymer [Os(bipy)₂(PVP)₂₀Cl]Cl

4.1 Introduction

The potential hazard of nitrite to human health has been well documented [1] Nitrite is a common additive in processed meats and it is known that it can be converted to potentially carcinogenic nitrosamines in the presence of primary amines in the stomach Conventional techniques for nitrite determination are based upon spectrophotometric determination of an azo dye formed by coupling diazotized sulfanilamide with N-(1-naphthyl-) ethylenediamine dihydrochloride (Greiss reaction), the absorbance of which is proportional to the amount of nitrite present [2] These methods have limited sensitivity and dynamic range, and frequently suffer from interferences such as ascorbic acid

Several polarographic methods for the sensitive determination of the nitrite ion have been reported in the literature Harrington et al [3] introduced a method employing differential pulse polarography with a detection limit of 0.3 ppb NO_2^- This method depended on a quantitative reaction between nitrite ion and diphenylamine at low pH with thiocyanate ion as a catalyst Zhao and Cai [4] investigated trace nitrite determination by catalytic polarography in iron (II) thiocyanate medium, achieving a limit of detection of 0.46 ppb NO_2^- Recently, various workers have studied nitrite determination using both complexation [5] and coordinating [6] agents in conjunction with polarographic detection

However, polarographic methods have obvious disadvantages for sensing and flow applications, and in recent years more emphasis has been placed on the use of solid electrodes for such applications A large number of methods have been developed for the voltammetric determination of nitrite by oxidation at solid electrodes Cox

and Kulesza [7] modified a platinum electrode by chemisorption of iodine, which was found to improve the reproducibility and decrease the peak width in the oxidation of nitrite by linear scan voltammetry. Nitrite oxidation at a bare glassy carbon electrode was reported by Newbury and Lopez de Haddad [8], but this method suffered from both ascorbate and chloride ion interferences. The determination of nitrite following oxidation at both electrochemically pre-treated [9] and polymer modified [10-12] glassy carbon electrodes at lower operational potentials has therefore been investigated. With the ruthenium polymer modified electrodes reported by Barisci et al [11] and Wallace et al. [12], the major problem associated with the electrodes was their long term stability. These workers improved the stability to some extent by treatment with UV light or by coating with other polymer layers. More recently, the modification of a carbon paste electrode with a similar ruthenium polymer was reported [13] to exhibit greater stability than the glassy carbon equivalent. The long term stability of the modified electrode showed only an 8 % diminution in response, for the oxidation of nitrite, over a 5 day period, in contrast to the previous report of a 50 % response reduction after only 8 hours using the glassy carbon based modified electrode [11].

Reduction of nitrite at Au, Pt and carbon electrodes is known to cause severe surface fouling [14]. Reductive techniques are also limited by the negative potentials that are required for detection where metal cations, hydrogen peroxide and oxygen interferences may be problematic. A modified electrode for the reduction of nitrite at moderate potentials based on modification of glassy carbon macro-electrodes with the electrocatalytic polymer $[\text{Os}(\text{bipy})_2(\text{PVP})_{10}\text{Cl}]\text{Cl}$ has

recently been reported [15] Such modification offered several advantages over existing electrochemical and spectrophotometric procedures

In recent years there has been much interest in the application of microelectrodes These electrodes have several advantageous features when compared with macroelectrodes For example, they enable time-independent currents to be monitored, are virtually non-destructive of the analyte and can be used in solutions of very high resistance [16]

This work describes the flow detection of nitrite in meat samples using a carbon fibre microelectrode that has been modified by chemisorption of the electrocatalytic polymer $[\text{Os}(\text{bipy})_2(\text{PVP})_{20}\text{Cl}]\text{Cl}$, where $\text{bipy}=2,2'$ -bipyridyl and $\text{PVP}=\text{poly}-(4\text{-vinylpyridine})$ Cyclic voltammetry was used to study the voltammetric behaviour of the polymer modified carbon fibre and its response to nitrite reduction Subsequently, the modified electrode was applied to the determination of nitrite in processed meat and the results were compared with those obtained using a standard spectrophotometric method [17]

Electroanalytical techniques have progressively gained in interest in recent years, particularly in the area of amperometric detection following various types of chromatographic techniques. Traditionally, one of the limiting factors was the narrow range of electrode substances available. The traditional reliance on mercury electrodes and solid metal and carbon electrodes often lead to practical limitations in terms of lack of stability and selectivity, as well as low sensitivity for the analyte of interest. Solid electrodes possess major advantages over mercury electrodes in flowing systems in terms of stability. However, these solid electrodes often suffer from fouling and low sensitivity and selectivity. Thus, in an effort to improve the sensitivity and selectivity of these electrodes, various modifications of the electrode substrate have been investigated. Electrochemically activated electrodes may be considered modified electrodes in the broader sense of the definition. However, one usually refers to chemically modified electrodes (CMEs) when discussing this field.

The present day applications of modified electrodes include (a) immobilised electron-transfer mediators; (b) preconcentrating films, and (c) permselective films for selectivity enhancement and protection of the electrode surface, or a combination of the above. Several methods are used to modify electrode surfaces according to the nature of the modification and the desired subsequent application of the modified electrode. These methods include adsorption, covalent attachment and polymeric coatings. Polymeric coatings have become the most widely used method mainly due to greater stability and definition of the resultant

CME Simple adsorption of the modifier generally leads to instability due to slow desorption, whereas covalent bonding techniques are often complex and laborious. Therefore adsorption of polymers, either inherently electroactive or with incorporated electroactive (mediating) groups onto the electrode surface, has become one of the areas of greatest interest in the field of CMEs.

Polymeric modifications involve the use of preformed polymers or the application of an inert polymer to the electrode surface prior to the incorporation of the active centre. Examples of the latter include the use of polymeric materials such as polyvinylpyridines and Nafion, which have the ability to electrostatically bind charged species such as ferricyanates, iridates and ruthenium complexes. Preformed polymers can be deposited on the electrode surface by a variety of techniques, including polymer solution casting (of which dip coating is a variation), electrodeposition and photodeposition, and electropolymerisation.

The modification of electrodes for analytical purposes must fulfill certain criteria. Stability of the CME is of major importance, particularly for flow-through detectors. Monolayer-coated electrodes (usually formed by covalent bonding or direct adsorption) are usually not sufficiently stable for flow analyses, since the small amount of modifying material gets easily passivated or dissolved by the carrier electrolyte. Polymer films generally tend to be more stable but still suffer from stability problems due to solubility problems in either aqueous or non-aqueous media depending on their structure. Many problems associated with polymeric films can be circumvented by careful attention to film thickness. Very thin films are more prone to stability problems, whereas unnecessarily thick films

inhibit mass transport of the analyte resulting in lower signals and larger response times. Another potential problem associated with this type of CME is the ability of the redox centre to be repeatedly cycled. Repeated redox cycling and the related ingress and egress of charge compensating counterions can cause film rupture and mechanical failure. The reproducibility of the CME response, a factor of obvious analytical importance, may suffer drastically as a result of even minor instability problems. Another desirable, but not essential, characteristic of CMEs is their ability to accommodate synthetic variation leading to a broader analytical application of the particular electrode.

Once a CME is produced, it must be characterised under the foreseen analytical operating conditions. The various characteristics of the modifier, including atomic, molecular and morphological properties are generally the interest of the theoretical electrochemist. The electroanalytical chemist generally concentrates on characterisation of the operational CME, usually employing electrochemical techniques. Cyclic voltammetry is widely used to determine the nature of the modifying layer in terms of its redox potential, peak intensity, peak-to-peak separation, and sweep rate dependence of peak currents. In the case of electropolymerisation of monomers, cyclic voltammetry can be used very effectively to follow the electropolymerisation process. The area under the cyclic voltammogram is normally taken as a measure of the amount of electroactive material present on the electrode. This can be used to estimate layer thickness and can also be used to monitor electrode stability during, for example, repetitive scans. Chronocoulometry has also been used to calculate layer thickness. For a

solution reaction the peak height of the cyclic voltammogram is proportional to the square root of the scan rate. However, for a surface-bound redox couple, the peak current is directly proportional to the scan rate. Therefore, a plot of peak current versus scan rate at low scan rates (usually $<10 \text{ mVs}^{-1}$) can provide information about the charge transfer process within the modifier layer. The CME should always be characterised under the same conditions (pH, ionic strength etc.) that their subsequent analytical application dictates.

Once the electrode is characterised using the above criteria, it is further investigated in the analytical system of interest which may be a batch or flowing system. Several analytical characteristics including stability, reproducibility, dynamic range, and limit of detection must be carefully evaluated to validate the electrode before it can be applied to the analysis of real samples.

In this thesis (chapter 3), a mercury thin film ultramicroelectrode was developed by the electrodeposition of mercury. This electrode may be considered as a modified electrode and was fully evaluated using various criteria, as outlined in detail in chapter 3, before its application to the determination of selected pteridines in biological fluids.

Also in this thesis (present chapter) a carbon fibre ultramicroelectrode was modified by polymer solution casting (dip coating) with the preformed polymer $[\text{Os}(\text{bipy})_2(\text{PVP})_{20} \text{Cl}]\text{Cl}$. This electrode was characterised and subsequently applied to the flow amperometric determination of nitrite as outlined later.

4.2 Experimental

4.2.1 Reagents and Materials

All reagents were of analytical grade. All aqueous solutions were prepared using deionised water obtained by passing distilled water through a "Milli-Q" water purification system. The electrolyte used throughout was 0.1 M H_2SO_4 . Nitrite standard solutions were prepared daily using sodium nitrite [BDH(now Merck)], by appropriate dilutions in 0.1 M Na_2SO_4 (Riedel-de Haen), since nitrite solutions are known to be unstable at low pH [17]. The synthesis of the polymer has been reported elsewhere [18,19]. Carbon fibres (14 μm diameter) were obtained from Avco. The surface of these fibres had no external coating. The meat sample analysed was Denny processed ham.

4.2.2 Instrumentation

Cyclic voltammetry was performed using an EG&G Princeton Applied Research (PAR) polarographic analyser/stripping voltammeter in conjunction with a "JJ-Instruments" X-Y recorder Model PL4). A 20 mL laboratory-built three-electrode cell was employed for batch studies incorporating the modified electrode, a Ag/AgCl reference electrode and a platinum counter electrode. The working electrode used for the batch studies was prepared by inserting a carbon fibre in the narrow end of a plastic micropipette tip and heat sealing it. The electrical connection was made by back filling with mercury and dipping in a copper wire.

The flow injection apparatus consisted of a Gilson Minipuls-3 peristaltic pump, a 6 port rheodyne injector with a 20 μl fixed volume sample loop which was connected

to a 3-electrode system described below. The electrode terminals were connected to an EG&G PAR Model 400 EC-detector which was linked to a Philips PM8251 single pen recorder to record the amperometric signals. A Shimadzu ultraviolet/visible recording spectrophotometer (Model UV-240) was used in the comparison method for determination of nitrite in meat.

4.3 Procedures

4.3.1 *Construction of the Carbon Fibre Flow Cell*

The preparation of the carbon fibre working electrode was carried out using a method reported previously [20]. The Ag/AgCl reference electrode was prepared by firstly connecting a silver wire (0.1 mm i.d.) to the anode and a platinum electrode to the cathode of a 1.5 V battery, after which the assembly was immersed in a solution of 1 M HCl for 2 minutes. The wire was then inserted in a polyethylene tube (15 mm x 1 mm i.d.) one end of which was plugged with a ceramic porous rod (2 mm x 1 mm i.d.). The tube was then filled with the 1 M HCl internal reference solution and closed by heating. A 2 cm piece of stainless steel tubing (1 mm x 0.2 mm i.d.) served as a counter electrode. Throughout this chapter, potentials are quoted, after numerical conversion, versus the standard calomel electrode (SCE).

After modification of the working electrode (described below), the working, reference and counter electrodes were mounted in a T-tube arrangement reported previously [21], so that the electrolyte passed first through the working electrode and then via the counter electrode to waste. A schematic diagram of the flow cell is shown in Figure 4.1.

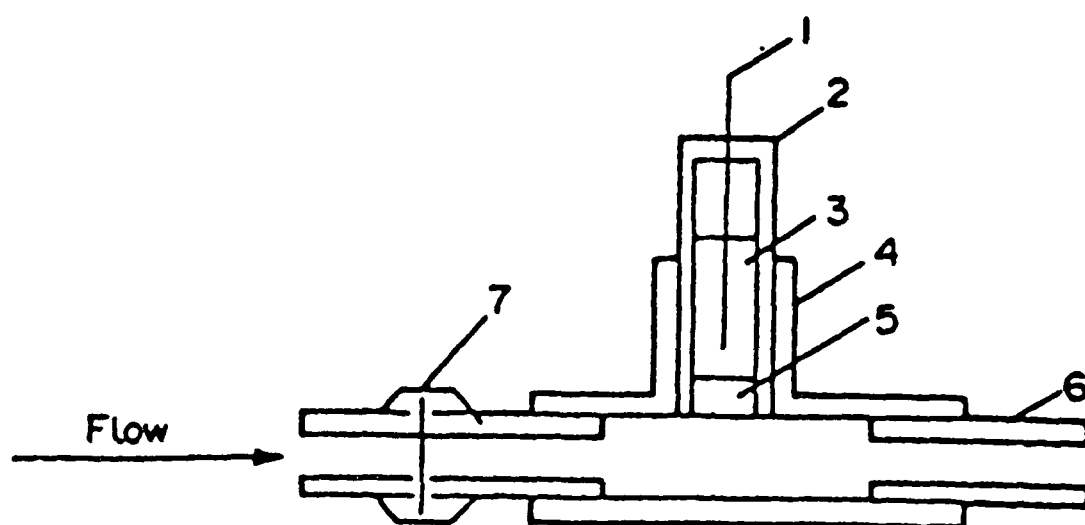


Figure 4 1

Schematic diagram of the ultramicroelectrode flow cell 1 Silver wire coated with silver chloride, 2 Reference electrode body 3 Internal reference solution, 4 T-tube, 5 Ceramic rod, 6 Stainless steel auxiliary electrode and 7 fibre electrode (from reference 20)

4 3 2 *Modification of the Working Electrode*

The electrode was connected to the tubing of a peristaltic pump via silicon tubing. The carbon fibre was cleaned by pumping 25 mL of 5 M HCl, 25 mL of deionised water and 25 mL of methanol respectively through the electrode at a rate of 1 mLmin⁻¹. The electrode was then air dried by pumping air through for a 1 hour period. When dry, the electrode was modified with the polymer solution of desired concentration in methanol. A 2 cm plug of polymer solution (0.1 % w/v) was first drawn into the peristaltic tubing, followed by air. The plug was pumped slowly toward the electrode. The pump was stopped for 40 seconds when the plug surrounded the electrode surface allowing the polymer to chemisorb onto the fibre surface, after which time the pump was restarted so that air flowed pass the electrode surface. In this way the electrode was dried for a 3 hour period before use.

4 3 3 *Meat Sample Analysis*

The analysis for nitrite in meat was carried out on a sample of processed ham (Denny). This involved the prior extraction of the nitrite from a 5 g sample of meat using a standard AOAC method [22]. The extract was, then filtered and made up to 50 mL in a volumetric flask. Prior to injection the extract was diluted with 0.2M Na₂SO₄ 1+1, so that samples and standards were 0.1 M in Na₂SO₄. 20 µL injections of standards and samples were made.

4.4 Results and Discussion

4.4.1 Cyclic Voltammetry

Preliminary studies were carried out to investigate the retention of the osmium polymer on the carbon fibre surface and its electrocatalytic activity toward nitrite reduction. Well defined oxidation and reduction responses associated with the surface bound Os(II)-Os(III) couple were observed in 0.1 M H₂SO₄. This supporting electrolyte had previously been shown to be optimum for a macro glassy carbon electrode using a similar polymer [15]. Figure 4.2 shows a typical cyclic voltammogram obtained from a modified electrode in 0.1 M H₂SO₄. The peak to peak separation (ΔE_p) of these waves was found to be 45 mV, indicating reasonably favourable kinetics associated with the Os(II)-Os(III) redox couple. A linear dependence of the cathodic and anodic peak currents on scan rate was observed at lower scan rates (less than 10 mVs⁻¹), indicating the predominantly surface behaviour of the modifier, as noted with some other polymer modified electrodes [23]. The modified microelectrode stabilized very rapidly and repetitive cycling over a 2 hour period produced no significant change in response, indicating strong adsorption of the polymer.

The effect of nitrite reduction on this redox couple is shown in Figure 4.3. On addition of nitrite to the solution, an electrocatalytic reduction occurred at the same potential as that observed for the reduction of Os(III) to Os(II). When the voltammogram obtained after nitrite addition (Fig. 4.3, B and C) is compared to that obtained from the same electrode in blank electrolyte solution (Figure 4.3, A) the nitrite response can clearly be seen. The cyclic voltammogram is significantly

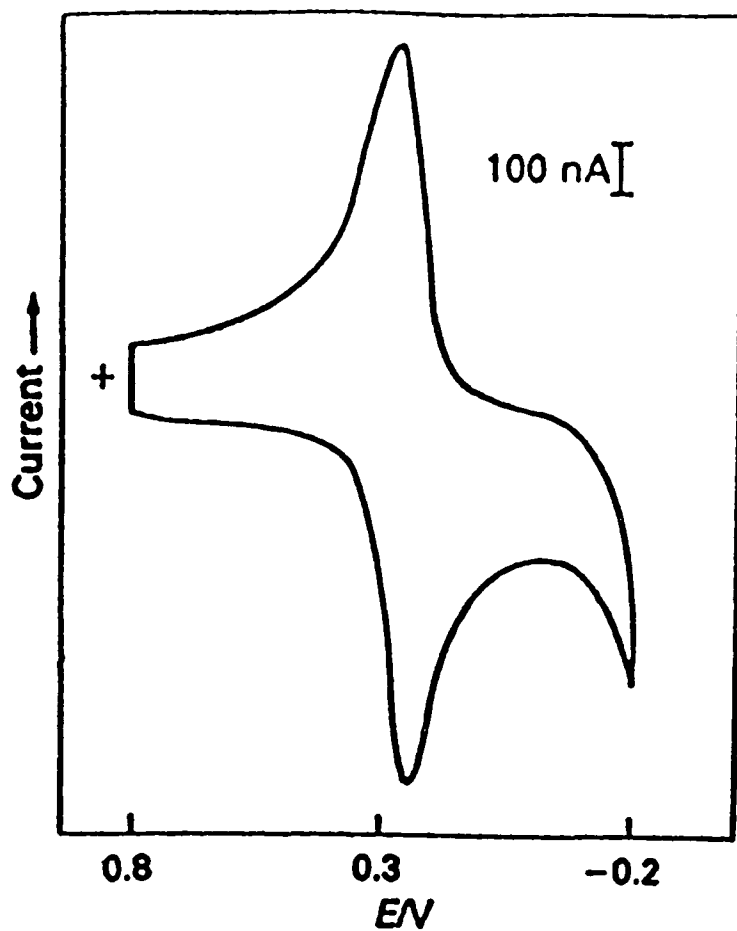


Figure 4.2

Typical cyclic voltammogram obtained for $[\text{Os}(\text{bipy})_2(\text{PVP})_{20}\text{Cl}]\text{Cl}$ Scan rate = 100 mVs^{-1} , Electrolyte = $0.1 \text{ M H}_2\text{SO}_4$.

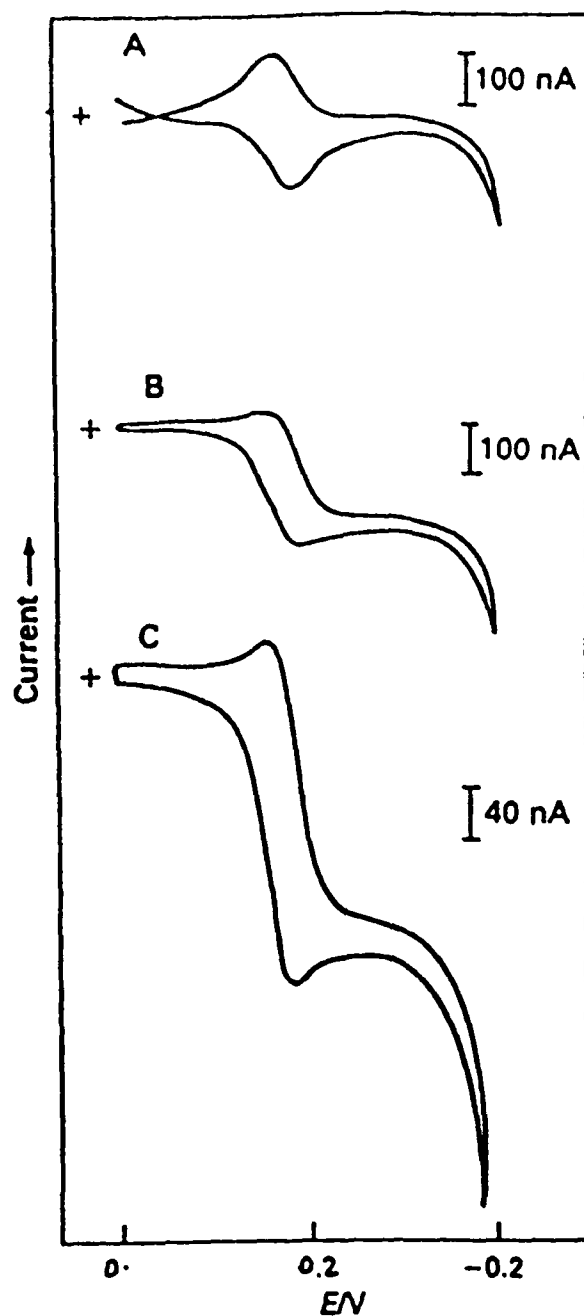


Figure 4.3

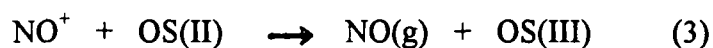
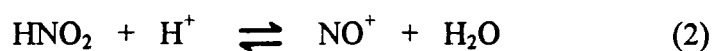
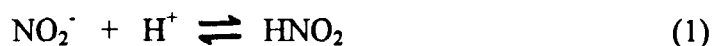
Cyclic voltammograms for A, Modified electrode in blank 0.1 M H_2SO_4 electrolyte, B, same electrode as A in 5 mM NO_2^- , and C, same as B at higher sensitivity outlining the typical electrocatalytic shaped curve obtained on addition of nitrite. Scan rate = 10 mVs^{-1} , electrolyte = 0.1 M H_2SO_4 .

elongated along the current axis, which is indicative of an electrocatalytic reaction. The electron transport kinetics at the bare carbon fibre surface were too slow to yield a useful analytical signal.

Cyclic voltammetry was used to determine the length of time needed for optimum coating of the microelectrode with the polymer. This was examined by dipping the fibres in a polymer solution (0.1 % w/v) for different lengths of time varying from 10 seconds to 360 seconds and performing cyclic voltammetry on the resulting modified electrodes. The cyclic voltammetric peak heights were then measured, and 40 seconds was found to be the optimum coating time giving rise to the best sensor response. At coating times above 40 seconds the methanol solvent appeared to redissolve the polymer from the electrode surface. The effect of the concentration of polymer used to modify the electrode was also investigated. It was found that thicker polymer films produced smaller responses to nitrite, which is probably a result of hindered analyte and counter ion mass transport within the film [24,25]. As the osmium response is always present, the response for nitrite must be recorded on top of a substantial background current. However, by using amperometric detection with flow injection, the background current can readily be offset, so that the subsequent responses will be due to addition of nitrite.

4.4.2 *Flow Injection*

When utilising the polymer modified carbon fibre electrode in flowing systems, the potential applied ensures that all the osmium is in the Os(II) form, so that when the analyte reaches the surface it is reduced at the osmium centres within the polymer according to the following proposed cross-exchange mechanism:



The potential was varied from +195 mV down to -250 mV in 50 mV increments, and injections of 20 μl of 50 μgml^{-1} NO_2^- standard solution were made at each potential. Decreasing the potential resulted in increased sensitivity for nitrite reduction, but below -150 mV the background noise also increased. Therefore, the detection potential was set at -150 mV. The flow rate of the 0.1 M H_2SO_4 electrolyte was kept low (0.2 mlmin^{-1}) since the kinetics of nitrite reduction are quite slow. In fact, a useful signal cannot be obtained using these conditions at a bare carbon fibre electrode. However, under the same conditions using the polymer modified electrode, well defined and reproducible responses were obtained.

The linearity of the method was determined by injecting a range of nitrite standards in the concentration range 0–400 μgml^{-1} and constructing a calibration curve. The method was linear over this range with a correlation coefficient, $r = 0.999$ and a regression equation as follows: $y \text{ (nA)} = 0.197x \text{ (}\mu\text{gml}^{-1}\text{)} - 1.9845$. The limit of detection was determined to be 0.1 μgml^{-1} using a signal-to-noise ratio of 3:1. The precision of the method was evaluated in terms of the variability between 20 replicate injections of various concentrations of NO_2^- solution. This resulted in a relative standard deviation of 2.15 % for the concentrations examined. Figure 4.4 shows some typical amperometric responses obtained from the modified fibre flow

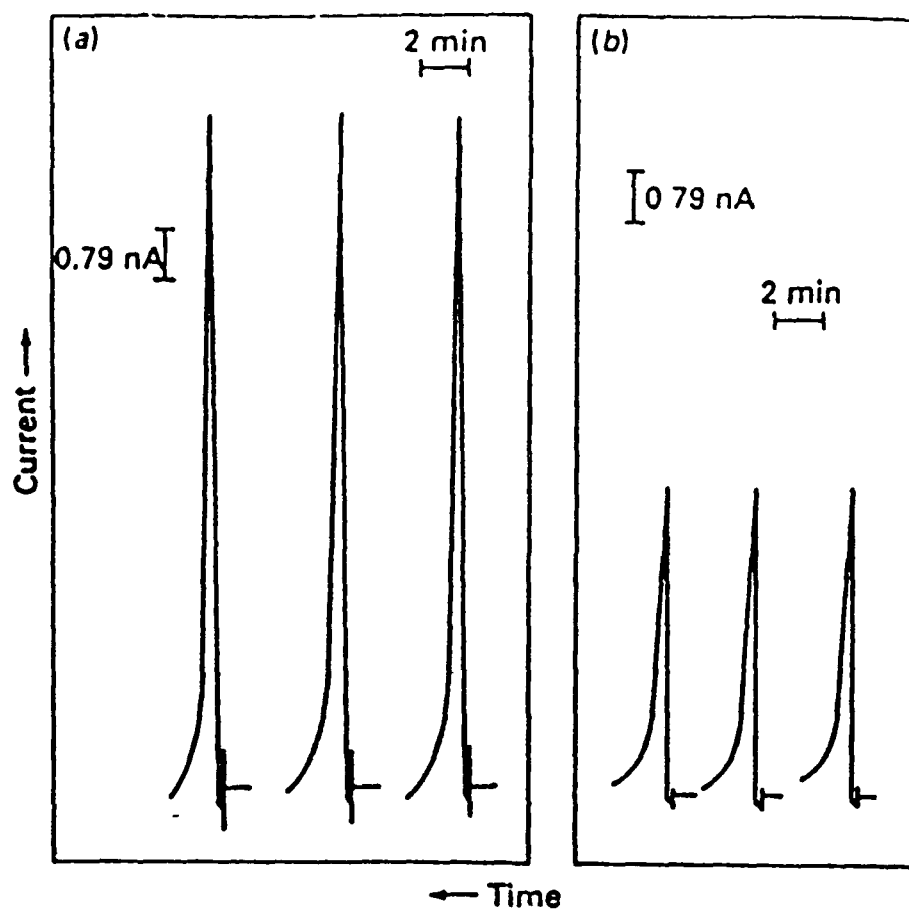


Figure 4.4

Flow amperometric responses of the osmium polymer modified electrode to consecutive injections of (a) 50 and (b) 25 μgml^{-1} of NO_2^- . Constant potential operation at -150 mV versus SCE, electrolyte = 0.1 M H_2SO_4 , flow rate = 0.2 mlmin^{-1}

cell at different nitrite concentrations, where the reproducibility of the response is clearly evident.

The long term stability of the electrode was monitored over a three week period. After three weeks of continuous use involving over 240 standard injections and 30 meat extract injections the electrode showed no appreciable change in sensitivity. No surface fouling effects were observed over this period of time. These results demonstrate the long-term stability of the modified microelectrode. This level of stability is rare for modified electrodes.

Similar work has also been carried out using a ruthenium polymer modified carbon fibre microelectrode as a continuation of studies of ruthenium polymer modified glassy carbon electrodes [11,12]. In this instance the oxidation of nitrite was investigated, which is a kinetically faster reaction than that of nitrite reduction. The use of the ruthenium polymer modifier lowered the overpotential for nitrite oxidation compared to that at a bare carbon fibre electrode. This method was approximately seven times more sensitive for nitrite determination with a slope of $1.41 \text{ nA}\mu\text{g}^{-1}$ compared to the method reported here. It had a shorter analysis time and comparable short term reproducibility. However, the main problem associated with this electrode was its long term stability. When monitored over a nine day period, a gradual decrease in response was observed owing to stripping of the polymer from the carbon fibre surface. Severe interference from ascorbic acid was also evident. The long term stability of the osmium polymer modified electrode reported here was shown to be far superior, and deemed to be of more analytical importance in the design of an operational sensor for nitrite.

4.4.3 *Determination of Nitrite in Meat*

For both the electrochemical method and the spectrophotometric reference method, the nitrite was extracted from the meat sample using a standard AOAC method [22]. For the analysis using the modified microelectrode the extract was diluted 1+1 with 0.2 M Na₂SO₄. Using a range of nitrite standards (0→12 µgml⁻¹ prepared from NaNO₂), a calibration curve was constructed, which had a correlation coefficient, $r = 0.999$ and a regression equation as follows; $y \text{ (nA)} = 0.098x \text{ (ugml}^{-1}) - 0.016$. Electrochemical analysis of the meat sample yielded a result of 86.6 +/- 1 µgml⁻¹ of NO₂⁻ (n=2), which compares favourably with the result of 84.0 +/- 1.2 µgml⁻¹ (n=2) obtained using the reference spectrophotometric method [17].

Thirty consecutive injections of the meat extract were made, without the need for pretreatment of the electrode, resulting in no deterioration of the response. Hence, in addition to exhibiting electrocatalytic properties, the polymer acts as a protective membrane by inhibition of adsorption of matrix compounds such as proteins, and thus preventing surface fouling. The polymer also prevented the severe surface fouling encountered at solid electrodes on nitrite reduction [14]. The method has a moderate analytical throughput and is capable of handling 30 samples per hour.

4.4.4 *Interferences*

For electrocatalysis at redox polymers such as those described here, the Gibbs free energy for the cross-exchange reaction must be negative. This requirement imposes certain limitations on the types of reaction that can occur at electrodes modified with these materials. By exploiting this thermodynamic limitation, the sensitivity and

selectivity of sensors constructed can be controlled by synthetic control of the $E_{1/2}$ of the electrocatalytic centre and by the manipulation of the formal potential of possible analytes and interferences. As the osmium polymer has an $E_{1/2}$ of 0.250V versus SCE [18], it therefore has wide scope for mediating reduction reactions. This provides a material that can be used in a range of analytical applications, with sensitivity and selectivity being controlled by the $E_{1/2}$ of the redox centre. The ascorbate anion is a common interferent when determining NO_2^- in processed meats as sodium ascorbate is frequently added as an anti-oxidant. This compound does not interfere using the osmium polymer modified electrode, as the ascorbate ion cannot undergo oxidation at the modified electrode when the sensor is operating in the Os(II) state. This can be seen in Figure 4.5A, when an injection of $500 \mu\text{gml}^{-1}$ ascorbic acid produces only a background response. In Figure 4.5B and C the response for $50 \mu\text{gml}^{-1}$ of nitrite and $50 \mu\text{gml}^{-1}$ of nitrite plus $500 \mu\text{gml}^{-1}$ of ascorbic acid solutions is shown. It can be seen that interference in the determination of nitrite does not occur even with a 10-fold excess of ascorbic acid. This feature is of considerable advantage for the determination of nitrite. Considering the limitations imposed by the thermodynamic requirements for cross-exchange reactions, then only reduction reactions are feasible with the electrocatalyst in the Os(II) redox state.

The thiocyanate anion, another potential interferent, was also found to be electroinactive at the redox polymer. This is because the formal potential for thiocyanate oxidation is more positive than the $E_{1/2}$ of the electrocatalytic centre, thus eliminating possible surface-fouling effects caused by the oxidation of this anion.

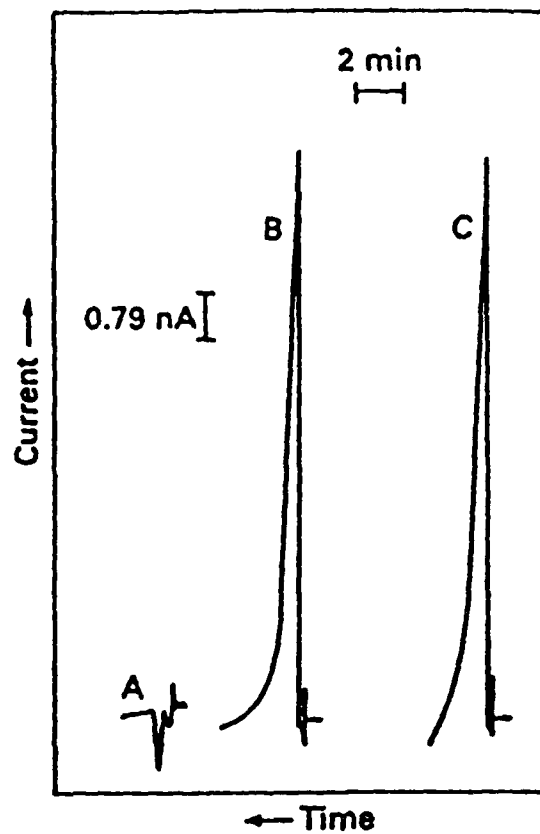


Figure 4.5

Effect of ascorbic acid on the response of the modified electrode to nitrite A, 500 μgml^{-1} ascorbic acid, B, 50 μgml^{-1} NO_2^- , and C, 500 μgml^{-1} ascorbic acid plus 50 $\mu\text{g ml}^{-1}$ NO_2^- Operational conditions as for Figure 4 3

The only major interferent in the electrochemical method was found to be iron(III). However, standard procedures are available to remove iron(III) prior to the determination of nitrite [17]. Interference from iron(III) can also be eliminated by the addition of ethylenediaminetetraacetic acid (EDTA) to the sample and carrier electrolyte. The $[\text{Fe}(\text{EDTA})]^-$ complex formed has a formal potential more negative than the $E_{1/2}$ of the osmium polymer and consequently is thermodynamically removed from the reaction at the modified electrode.

4.5 Conclusions

The osmium polymer modified carbon fibre flow electrode has been demonstrated to be sensitive, accurate and reproducible for the determination of the nitrite ion in a meat sample. The electrode was also shown to be stable over extended periods of use, and may be operated under conditions where common interferents such as ascorbic acid and thiocyanate are non-electroactive.

When compared to the common spectrophotometric techniques, the modified microelectrode has a comparable analysis time, however considerably wider linear ranges, increased sensitivity and lower limits of detection are characteristic of the modified microelectrode. Also, the proposed method does not require the use of potentially unstable complexing or colour-forming reactions. The microelectrode flow cell is also simple and inexpensive to produce and is easy to operate.

4.6 References

1. W Lijinsky and S S Epstein, *Nature*, **223** (1970) 21
2. H Barnes and A R Folkard, *Analyst*, **76** (1951) 599
3. S Chang, R Kozeniauskas and G W Harrington, *Anal Chem*, **49** (1977) 14
4. Z Zhao and X Cai, *J Electroanal Chem*, **252** (1988) 361
5. Z Gao, G Qing and Z Zhao, *Anal Chim Acta*, **230** (1990) 105
6. K Markusova and M Fedurco, *Anal Chim Acta*, **248** (1991) 109
7. J A Cox and P J Kulesza, *J Electroanal Chem*, **175** (1984) 105
8. J E Newbury and M P Lopez de Haddad, *Analyst*, **110** (1985) 81.
9. A Y Chamsi and A G Fogg, *Analyst*, **113** (1988) 1723.
10. J A Cox and K R Kulkarni, *Analyst*, **111** (1986) 1219
11. J N Barisci, G G Wallace, E A Wilke, M Meaney, M R Smyth and J G Vos, *Electroanalysis*, **1** (1989) 245
12. G G Wallace, M Meaney, M R Smyth and J G Vos, *Electroanalysis*, **1** (1989) 357
13. T J O' Shea, D Leech, M R Smyth and J G Vos, *Talanta*, **39** (1992) 443
14. G Mengoli and M M Musiani, *J Electroanal Chem*, **269** (1989) 99
15. A P Doherty, R J Forster, M R Smyth and J G Vos, *Anal Chim Acta*, **255** (1991) 45
16. S Pons and M Fleischmann, *Anal Chem*, **59** (1987) 1391A
17. *Vogels Textbook of Quantitative Inorganic Analysis*, Longmann, New York, 4th edn, 1978, pp 97, 158 and 755
18. R J Forster and J G Vos, *Macromolecules*, **23** (1990) 4372
19. J M Clear, J K Kelly, C M O' Connell and J G Vos, *J Chem Res*, march (1981) 3039
20. C Hua, W Yunping, J Chunghan and Z Tonghui, *Anal Chim Acta*, **235** (1990) 273

- 21 C Hua, K Sagar, K McLaughlin, M Jorge, M P Meaney and M R Smyth, *Analyst*, **116** (1991) 1117
- 22 *Official Methods of analysis of the association of Official Analytical Chemists*, AOAC, Washington, DC, 13th edn , 1980
- 23 R W Murray, in *Electroanalytical Chemistry*, A J Bard, Ed , Marcel Dekker, New York, 1984, vol 13, p 240
- 24 P Denisevich, H D Abruna, C R Leidner, T J Meyer and R W Murray, *Inorg Chem* , **21** (1982) 2153
- 25 T Ikeda, R Shmehl, P Denisevich, K Willman and R W Murray, *J Am Chem Soc* , **104** (1982) 2683
- 26 M Silvia, M Gallego and M Valcarel, *Anal Chim Acta*, **179** (1986) 341

Chapter 5

Conclusions

The main objectives of this doctoral thesis were to develop useful microelectrochemical detection systems and to apply them to selected biomedical and biopharmaceutical analyses. These objectives have been met and the systems developed have been shown to possess definite advantages over previously existing techniques.

In the area of capillary electrophoresis the utility of electrochemical detection using microelectrodes was demonstrated. The miniature dimensions of microelectrodes allows for their insertion in the end of the capillary, for 'off-column' detection, which leads to advantages, both in terms of higher sensitivity and reduced band broadening, compared to 'end-column' detection. A system was also developed for reductive electrochemical detection since up to now only easily oxidisable species have been detected following capillary electrophoretic separations. The instrumental set-up was shown to be much simpler than that of liquid chromatography with reductive electrochemical detection (LCEC), and system deoxygenation could be completed in 15 minutes compared to at least 8 hours for LCEC. The concentration detection limits achieved dinitrophenyl amino acid derivatives and selected anthraquinone compounds were comparable to those reported previously for LCEC. However, the mass detection limits, in the low fmol region, were several orders of magnitude lower than those reported for LCEC. The high selectivity of reductive electrochemical detection was demonstrated by the direct detection of mitomycin C in human serum without the use of any prior extraction procedures. CE possesses several advantages over LC techniques, particularly for sample volume limited analyses. The system developed here should be applied to many other compounds in the future, and this work has demonstrated that it possesses major advantages over currently existing techniques.

The ability to analyse ultrasmall volumes using CEEC systems is also very important for biomedical analyses since the sample volume is often very limited. One such sample volume limited technique is microdialysis. In this thesis, the utility

of CEEC for the analysis of tryptophan and its metabolites in microdialysate samples from the brain of an anaesthetised rats has been demonstrated. Microdialysis samples are always volume limited and require highly sensitive techniques capable of dealing with small volumes. Both these challenges were met using continuous microdialysis sampling over approximately 8 hour periods followed by capillary electrophoretic separations and 'off-column' electrochemical detection. Following various manipulatory experiments, including tryptophan and kynurenine loading respectively, the increase and decrease of tryptophan concentrations and subsequently its metabolites in the extracellular fluid of the rats brain, could be monitored. This field of research is one of the most challenging of analytical chemistry, since it requires the successful integration of several techniques each of which is being pushed to its limits. The future research in this field will undoubtedly focus on developing similar systems to the one described here with improvements in terms of automation and robustness. The ideal scenario would be the development of a robust system for the continuous on-line sampling, derivatisation (if necessary), separation and detection of microdialysates with a high analysis turnover rate so that the temporal resolution of the technique could be improved.

A major challenge for the analytical chemist is always to develop techniques that are increasingly sensitive. This is particularly true in the area of biomedical analysis since the analytes of interest are often found at trace levels in biological fluids. This challenge was addressed in this thesis through the development of a mercury thin film ultramicroelectrode that combined the adsorptive characteristics of mercury electrodes with the superior mass transport characteristics of ultramicroelectrodes. This modification of the carbon fibre electrode by electrodeposition of mercury on its surface yielded a sensitive and reproducible electrode. It was shown that by employing phase-selective AC voltammetry, the system discriminated against non-reversible processes which increased the overall selectivity and sensitivity of the technique for reversible processes. The technique was successfully applied to the

analysis of selected pteridines in biological fluids. The monitoring of the concentration of these chemotherapeutic compounds in biological fluids of patients undergoing chemotherapy is of crucial importance, since insufficient clearance of the compounds leads to highly toxic side effects and sometimes death. Using cathodic stripping voltammetry it was demonstrated that this system was sensitive enough for clinical applications exhibiting limits of detection as low as 5×10^{-14} M for edatrexate. This was the first time that mercury thin film ultramicroelectrodes were used for the cathodic stripping analysis of organic compounds. An important advance for the future would be the successful employment of this technique in flowing systems so that its high sensitivity could be combined with the resolving power of chromatographic techniques. This would be the key to many new biomedical applications of the technique.

Modification of a carbon fibre electrode with the redox polymer $[\text{Os}(\text{bipy})_2(\text{PVP})_{20}\text{Cl}]\text{Cl}$ was then shown to greatly improve the characteristics of the microelectrodes for the flow amperometric determination of nitrite. The electrocatalytic effect of this modification for the reduction of the nitrite ion was demonstrated and shown to be far superior to the bare electrode characteristics. In fact, the electron transport kinetics at the bare electrode surface were too slow to yield a useful analytical signal. Conversely, modification of the microelectrode with the redox polymer yielded an analytically useful electrode that was used for the flow amperometric determination of the nitrite ion at very moderate potentials. By exploiting the thermodynamic limitations of the polymer modified electrode very good selectivity was achieved. This allowed for the determination of nitrite in meat samples without interferences from other commonly present ions. The electrode was shown to be stable over extended periods of use. When compared to standard spectrophotometric techniques, the modified electrode has a shorter analysis time, a wider linear range and does not suffer from interferences from other commonly present ions. Future research in this area would be well directed towards the

development of other redox polymers with different electrocatalytic centres and polymer characteristics that would be capable of functioning under a wider range of analytical conditions

Significantly different characteristics were observed for each type of microelectrode employed in this thesis, especially in terms of electrode passivation. For the analysis of biological fluids, adsorption of endogenous materials such as proteins to the electrode surface is frequently a problem. For the microdialysis experiments no significant passivation of the electrode surface occurred due to the molecular cut-off point of the microdialysis membrane used for sampling. The samples collected using microdialysis probes are essentially protein free and can generally be analysed directly without the necessity of any further clean-up procedures. The mediator polymer used to modify the carbon fibre electrodes for the analysis of the nitrite ion also helped to protect the electrode surface. The mercury thin film electrode, although prone to adsorption of various compounds was, electrochemically cleaned between each measurement which alleviated this problem to some extent. It was also observed that the employment of microelectrodes in flowing streams reduced the extent of surface passivation since the electrode surface only contacts the sample plug intermittently and is continuously washed by the flowing electrolyte.

Overall, the research carried out for this doctoral thesis has brought about several significant improvements in the area of electroanalytical chemistry, and has created a platform for future interesting and useful research projects with the ultimate goal of introducing new and improved systems to the field of biomedical and biopharmaceutical analysis.

Publications

Articles

- “Reductive Electrochemical Detection for Capillary Electrophoresis”, Michael A Malone, Paul L Weber, Susan M Lunte, and Malcolm R Smyth, *Analytical Chemistry*, in press
- “The Use of Capillary Electrophoresis with Electrochemical Detection for Monitoring Tryptophan Metabolites in *in vivo* Microdialysis Samples”, Michael A Malone, Hong Zhou, Susan M Lunte, and Malcolm R Smyth, *Journal of Chromatography*, in press
- “Phase-Selective Alternating Current Adsorptive Stripping Voltammetry of Aminopterin on a Mercury Thin Film Carbon Fibre Electrode”, Michael A Malone, Agustin Costa Garcia, Paulino Tunon Blanco, and Malcolm R Smyth, *Analyst*, 1993, **118**, 649-655
- “Phase Selective AC Adsorptive Stripping Voltammetric Assay for Aminopterin and 10-edam in Human Serum”, Michael A Malone, Agustin Costa Garcia, Paulino Tunon Blanco, and Malcolm R Smyth, *Journal of Pharmaceutical and Biomedical Analysis*, 1993, **10**, 939-946
- “Adsorptive Stripping Voltammetric Behaviour of Edatrexate and Methotrexate at a Mercury Thin Film Ultramicroelectrode and Application to Biopharmaceutical Analysis”, Michael A Malone, Agustin Costa Garcia, Paulino Tunon Blanco, and Malcolm R Smyth, *Analytical Methods and Instrumentation (AMI)*, 1993, **1**, 164-171
- “Flow Injection Amperometric Determination of Nitrite at a Carbon Fibre Ultramicroelectrode Modified with the Polymer [Os(bipy)₂(PVP)₂₀Cl]Cl”, Michael A Malone, Andrew P Doherty, Malcolm R Smyth, and Johannes G Vos, *Analyst*, 1992, **117**, 1259-1263

Book Chapters

- “Applications of Voltammetry in Bioanalysis” in “Bioanalytical Chemistry”, Editors, Malcolm R Smyth and Richard O’ Kennedy, Ellis Horwood, to be published, 1994